TAMPEREEN TEKNILLINEN YLIOPISTO
TAMPERE UNIVERSITY OF TECHNOLOGY

TUIRE MARIN

SELECTIVE LASER SINTERING OF POLYOLEFINS

Master of Science Thesis

Examiners: Asst. Prof. Essi Sarlin and Ilari Jönkkäri
Examiners and topic approved on 1st March 2017

ABSTRACT

TUIRE MARIN: Selective laser sintering of polyolefins
Tampere University of technology
Master of Science Thesis, 69 pages, 10 Appendix pages
September 2017
Master's Degree Programme in Materials Engineering
Major: Materials technology
Examiners: Assistant professor Essi Sarlin and Ilari Jönkkäri

Keywords: selective laser sintering, polypropylene, polyethylene, powder flowability, sintering window, energy density, tensile strength, sintering quality, porosity

Selective laser sintering (SLS) is a powder based additive manufacturing method especially equipped to produce small batch sizes of products with customized properties. However, the limited raw material availability restricts the production of functional parts with SLS. The purpose of this master's thesis is to investigate the usability of polyolefins, namely polypropylene and polyethylene, as possible materials to be used in the SLS.

The theoretical part of this thesis includes basic information about selective laser sintering and its requirements. In addition, possible powder production methods are investigated including mechanical and physiochemical methods. Furthermore, some general information about polyolefins is discussed. The experimental part investigates injection moulding grade polypropylene and polyethylene as well as two different commercial polypropylene powders. The material properties of these polyolefins were investigated to determine their suitability to be used in the SLS. Grinding was employed to pulverize materials in granulate form. Furthermore, the flowability of the powders was evaluated with a SLS machine and tensile specimens were produced with the SLS for the tensile testing. In addition, the fracture surfaces of the tensile specimens were investigated with SEM to evaluate the sintering quality and porosity of the specimens.

Thermal analysis showed that all the investigated polypropylenes had adequate thermal properties, however, the investigated polyethylene did not. Rheological properties were superior for the commercial polypropylene powders compared to the injection moulding grade. The commercial powders had a relatively spherical morphology and sufficient particle size. However, grinding did not lead to the desired extrinsic properties.

The flowability evaluation showed that the grinded polypropylene could not be spread evenly enough to be able to use it in the SLS. However, both of the commercial powders showed promising flowability and the tensile specimens could be manufactured with one of the commercial powders. The tensile specimens were produced with the different energy density levels to determine the optimal value for the specific material.

According to the tensile tests, increasing the energy density level increases the tensile strength. However, all the SLS specimens showed very brittle behavior and quite low tensile stress at break. The sintering quality evaluation with SEM showed that the powder particles were not completely coalescence and the individual powder particles could be seen quite clearly in the structure. Using higher energy density levels could lead to lower porosity and better tensile properties.

TIIVISTELMÄ

TUIRE MARIN: Polyolefiinien selektiivinen lasersintraus
Tampereen teknillinen yliopisto
Diplomityö, 69 sivua, 10 liitesivua
Syyskuu 2017
Materiaalitekniikan diplomi-insinöörin tutkinto-ohjelma
Pääaine: Materials technology
Tarkastajat: Assistant Professor Essi Sarlin ja Ilari Jönkkäri

Avainsanat: selektiivinen lasersintraus, polypropeeni, polyeteeni, jauheen levittyvyys, sintraus ikkuna, energiatiheys, vetolujuus, sintraus laatu, huokoisuus

Selektiivinen lasersintraus (SLS) on jauhepohjainen materiaalia lisäävän valmistuksen menetelmä, joka soveltuu erityisesti pienten kappale-erien tuotantoon. Suppea raaka-aineen saatavuus kuitenkin rajoittaa tekniikan hyödyntämistä funktionaalisten kappaleiden tuotannossa. Tämän opinnäytteen tarkoitus on tutkia polyolefiinien, erityisesti polypropeenin ja polyeteenin, käyttöä selektiivisessä lasersintrauksessa.

Kirjallisuustutkimusosa käsittelee selektiivisen lasersintrauksen perusperiaatteita ja vaatimuksia. Lisäksi esitellään mekaanisia ja kemiallisia jauheenvalmistusmenetelmiä ja käydään läpi polyolefiinien yleisiä ominaisuuksia, keskittyen polypropeeniin ja polyeteeniin. Kokeellisessa osuudessa tutkitaan ruiskuvaluun tarkoitettua polypropeenia ja polyeteeniä, sekä kahta kaupallista polypropeenijauhetta. Näiden polyolefiinien materiaaliominaisuuksien perusteella määritetään, kuinka hyvin ne soveltuvat selektiiviseen lasersintraukseen. Granulaattimuodossa olevat materiaalit jauhetaan pienempään partikkelikokoon. Jauheen levittyyttä testataan SLS laitteistolla ja vetosauvoja valmistetaan sintraamalla. Lisäksi kappaleiden sintrauslaatua ja huokoisuutta arvioidaan tutkimalla vetosauvojen murtopintoja pyyhkäisyelektronimikroskoopilla.

Tutkimuksissa tuli esille, että tutkittu polyeteeni ei omaa sopivia termisiä ominaisuuksia, jotta sitä voitaisiin käyttää lasersintrauksessa. Kaikilla tutkituilla polypropeeneilla sen sijaan oli riittävät termiset ominaisuudet. Kaupallisilla polypropeenijauheilla oli sovelluskohdetta ajatellen paremmat reologiset ominaisuudet, kuin ruiskuvaluun tarkoitetulla polypropeenilla. Kaupallisten jauheiden partikkelimuoto oli pallomainen ja raekoko oli sopiva. Itse jauhettu jauhe sen sijaan ei omannut haluttuja ulkoisia ominaisuuksia.

Jauheen levittyvyyskokeissa havaittiin, että itse jauhettua jauhetta ei ollut mahdollista levittää riittävän tasaisesti, jotta sen käyttäminen SLS:ssä olisi mahdollista. Kaupallisten jauheiden levittymisominaisuudet vaikuttivat lupaavilta ja toisesta jauheesta saatiin valmistettua vetosauvoja SLS:llä. Vetosauvojen valmistuksessa käytettiin eri energiatiheyksiä, jotta voitiin määrittää tutkitulle materiaalille optimaalinen energiatiheyden arvo.

Vetokokeiden perusteella havaittiin, että energiatiheyden kasvatus nostaa kappeleiden vetolujuutta. Kaikki valmistetut kappaleet käyttäytyivät kuitenkin hyvin hauraasti ja saavutetut vetolujuudet olivat melko matalia. Sintrauslaadun arviointi SEM kuvista osoitti, että jauhepartikkelit eivät olleet täysin sulautuneet yhteen ja yksittäisten jauhepartikkelien rajapinnat erottuivat sintratusta rakenteesta melko selkeästi. Suuremmilla energiatiheyksillä voisi olla mahdollista vähentää huokoisuutta ja kasvattaa vetolujuutta.

PREFACE

This study was carried out between January 2017 and August 2017 at the Department of Materials Science at Tampere University of Technology (TUT) in collaboration with Materflow Corporation and Aalto University.

I would like to thank my examiners Essi Sarlin and Ilari Jönkkäri for their guidance during this whole process. I would also like to thank the staff at Aalto University as well as at Materflow for providing some of the experimental results and for manufacturing the test specimens for this study. I am also grateful to my coworkers at TUT for their help and guidance for the experiments conducted at TUT.

Finally, my family and friends have my deepest gratitude for their support during this journey.

Tampere, 23.8.2017

Tuire Marin

CONTENTS

LIST OF SYMBOLS AND ABBREVIATIONS

AM	Additive Manufacturing
ASTM	American Society for Testing and Materials
C%	Degree of crystallinity (in %)
CAD	Computer aided design
CO_2	Carbon dioxide
DSC	Differential scanning calorimetry
EAB	Elongation at break
EDS	Energy-dispersive x-ray spectroscopy
HDPE	High-density polyethylene
H_R	Hausner ratio
ISO	International Organization for Standardization
LDPE	Low-density polyethylene
LLDPE	Linear low-density polyethylene
MDPE	Medium-density polyethylene
MFI	Melt flow index
MFR	Melt flow rate
N_2	Nitrogen gas
PA	Polyamide
PA11	Polyamide 11
PA12	Polyamide 12
PE	Polyethylene
PEEK	Polyether ether ketone
PP	Polypropylene
PS	Polystyrene
PSD	Particle size distribution
SEM	Scanning electron microscope
SiO_2	Silica
SLS	Selective laser sintering
T_c	Onset crystallisation temperature
TGA	Thermogravimetric analysis
T_m	Onset melting temperature
T_{onset}	Onset temperature for thermal degradation
UHMWPE	Ultra-high-molecular-weight polyethylene
UV	Ultraviolet
VLDPE	Very low-density polyethylene
wt%	Percentage by weight
ρ_{bulk}	Bulk density
ρ_{tap}	Tapped density
ΔH_c	Crystallisation enthalpy
ΔH_m	Melting enthalpy
ΔH_m^0	Melting enthalpy for 100% crystalline material

1. INTRODUCTION

Selective laser sintering (SLS) is a powder based additive manufacturing (AM) method. With this method a wide variety of different material types, such as polymers, metals and ceramics, can be used in commercial SLS production. However, when considering polymers, the production is mainly restricted to polyamide 12 (PA12) and polyamide 11 (PA11). The advantage of the AM methods compared to the traditional production methods, such as injection moulding, is that more complex and geometrically challenging parts can be produced without mould tooling. In addition, these techniques are especially equipped to produce low volumes of parts, enabling the production of smaller batch sizes with customized properties, with reasonable costs. (Hopkinson et al. 2006, p. 64; Goodridge et al. 2012)

Due to the advantages of AM techniques, they could be very useful for companies that manufacture customised low volume products. However, the limited raw material availability restricts the production of functional parts since many materials used in AM techniques do not have the required material properties. There have been studies to find and develop polymeric materials with sufficient material properties that could be used in the SLS. (Fiedler et al. 2007; Bai et al. 2016; Zhu et al. 2016) The aim of this master's thesis is to study the usability of polyolefins, namely polypropylene (PP) and polyethylene (PE), in the SLS applications. The investigation will be based on a theoretical review as well as on some experimental studies.

The SLS is a challenging technique due to its very specific material requirements. Material needs to be in a powder form with a specific particle size and particle morphology, to achieve a sufficient flowability of the powder in the SLS machine. In addition, the intrinsic properties, such as thermal and rheological properties, also have significant influence to the material processability in the SLS. Modifying the intrinsic properties is difficult since they are typically determined from the molecular structure of the material. However, extrinsic properties can be influenced with the powder production method, at least to some level. Thorough investigation of the material properties is necessary to determine its suitability to be used in the SLS applications. In addition to the rather specific material requirements, the SLS process itself is quite complicated and understanding the different processing parameters and their influence to each other and to the process is necessary to be able to successfully produce high quality parts. (Goodridge et al. 2012; Schmid et al. 2014; Gibson et al. 2015; Schmid & Wegener 2016)

PP and PE are widely used polymers for many kinds of applications and they occupy 50% of the total plastic production worldwide. (Al-Ali AlMa'adeed & Krupa 2016, p. 51) There have been attempts to use PP and PE in SLS with some positive results, but there are many difficulties to overcome as well. Some of the intrinsic material properties of PP and PE can cause some serious challenges to the SLS process. PP and PE typically have a quite high degree of crystallinity, which in turn results in a high degree of shrinkage during cooling. The shrinking behaviour can cause distortions to the SLS parts and decrease the accuracy and quality of the parts. Furthermore, some PP materials have been found to have insufficient rheological properties to be able to fully coalescence during the SLS and form dense parts with low porosity. However, some of the challenges can be resolved by altering the processing parameters of the SLS process. (Fiedler et al. 2007; Goodridge et al. 2012; Schmid & Wegener 2016)

Even though the extrinsic properties of the powder can be affected with the processing method, at least to some level, obtaining suitable PP and PE powders for SLS is difficult since traditional grinding is found to lead to insufficient morphology. (Goodridge et al. 2012; Schmid & Wegener 2016) On the other hand, the precipitation processes, used to obtain the suitable polyamide (PA) powders, do not work so well with the polyolefins due to their insoluble nature. (Al-Ali AlMa'adeed & Krupa 2016, p. 2) However, despite of these difficulties, there are at least two powder suppliers that offer PP powders for the SLS at the moment. Thus, producing PP powders with suitable extrinsic properties is possible (Advanc3d Materials 2017; Diamond Plastics 2017).

The goal of this study was to manufacture suitable polypropylene and polyethylene powders for the SLS by mechanical size reduction as well as to investigate the commercially available polypropylene SLS powders for their suitability in SLS for the production of functional parts. The aim was to investigate the significance of the different material properties to the produced parts and to try to recognise the main difficulties regarding the processing of polyolefins and to overcome them by altering the processing parameters of the SLS process.

The theoretical part of this study includes Chapters from 2 to 4, where Chapter 2 presents some basic information about the SLS technique and its requirements, Chapter 3 presents the evaluation of the suitable powder production methods and Chapter 4 presents some general information about polyolefins, focusing on PP and PE, as well as some previous studies regarding PP and PE in the SLS applications. The experimental part of this study starts in Chapter 5, which presents the experimental materials and methods that were used for this investigation. The experimental part includes powder characterisation measurements that were employed to estimate the suitability of different powders for the SLS and some flowability experiments with an SLS machine. Furthermore, tensile tests and porosity evaluations were employed to the parts produced with the SLS technique. Chapter 6 presents the results of the experiments and Chapter 7 offers some conclusions based on both the theoretical and experimental investigations.

2. SELECTIVE LASER SINTERING

Selective laser sintering was first invented and patented in 1979 by Ross Householder, but it was not commercialised until the late 1980s by Carl Deckard at the University of Texas at Austin. This led to the formation of the DTM Corporation. First commercial machine was developed by DTM Corporation in 1992 followed by an EOSINT machine by EOS GmbH in 1994. (Hopkinson et al. 2006, p. 64) 3D Systems acquired DTM Corporation in 2001 and with EOS they are still the major manufacturers in the field of selective laser sintering (Gibson et al. 2015, p. 132).

2.1 General principle

The selective laser sintering machine typically consist of a powder bed chamber, also called part bed, with a lowering piston, feed and overflow bins, a powder feed roller, CO_2 laser and laser scanning mirrors. In addition, the machine is usually equipped with infrared heaters to enable the pre- and post-heating of the powder. Controlled temperature is an important factor in the selective laser sintering process as will be discussed later on. Furthermore, the powder bed chamber is a closed system, usually filled with the nitrogen gas (N_2) to reduce the risk of oxidation and degradation of the powdered material. (Gibson et al. 2015) Figure 2.1 presents the schematic principle of the selective laser sintering equipment.

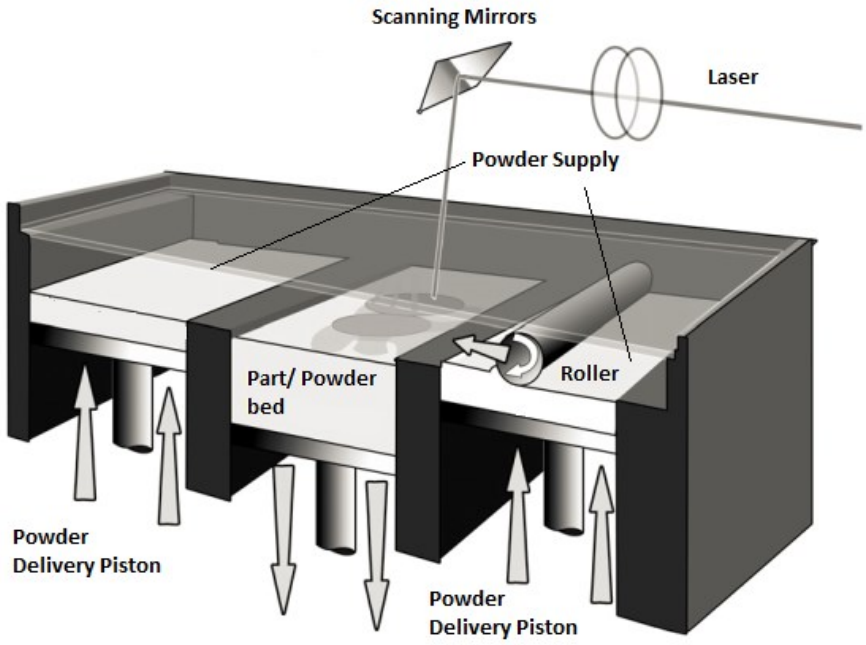

Figure 2.1. *Selective laser sintering equipment adapted from (Hopkinson et al. 2006, p. 65).*

In laser sintering process, a 3D object is built based on a computer aided design (CAD) file. This CAD file, in .stl format, is sliced into discrete layers where each slide represents the cross-sectional area of one sintering layer of the part. For each slide, a thin layer of powder is spread over the build area and the cross-section of the part, based on the CAD model, is selectively sintered using the CO_2 laser. The build platform is lowered between the layers, enabling the new layer of powder to be spread over the previously sintered layer. The lowering of the platform determines the layer thickness of the part, which typically ranges from 0.02 to 0.15 mm. The non-consolidated powder surrounding the sintered part remains in place during the sintering process. Thus, no additional support structures during sintering are required. These processing steps are repeated until the part is ready. Typically, a cooling down period is required to ensure uniform and accurate parts. The finished parts need to be cleaned from the loose powder and further finishing operations can be applied if necessary. (Hopkinson et al. 2006; Goodridge et al. 2012; Gibson et al. 2015)

The basic working principle for the laser sintering machines, produced by different manufactures, is the same, but there can be some variations in the way of depositing and the heating of the powder (Goodridge et al. 2012). Even though these differences are not the major concern for the processing, they are relevant and should be considered. Different working methods can affect the efficiency of the processing, and thus the final properties of the parts.

2.2 Material requirements

There are some general requirements that the polymer powders for the SLS should meet. Such requirements include no sintering during storage, a low melt viscosity at low shear stresses and a wide temperature range between melting and degradation temperatures. Furthermore, powder should have sufficient dry-flow characteristics, a low moisture sensitivity as well as no significant emission of volatiles during processing. In addition, for the SLS, it is essential that the powder has suitable thermal properties, particle size and morphology. (Khait et al. 2001; Schmid et al. 2014)

Since the majority of polymer materials are not directly produced in a powder form, the particle size need to be converted to a suitable range before sintering, generally around 20-80 μm (Schmid et al. 2014). Some material properties, such as toughness, brittleness and hardness, as well as the cohesiveness of the particles, particle shape and heat sensitivity, can highly influence the powder production process and it is relevant to consider them when choosing the method. (Khait et al. 2001) More information about the suitable polymer powder production methods is presented in Chapter 3.

Material properties can be categorized into intrinsic and extrinsic properties, where intrinsic properties contain thermal, optical and rheological properties and extrinsic properties include powder and particle properties. Intrinsic properties are typically

determined from the molecular structure, and thus influencing them is difficult. However, the intrinsic properties of the material need to be established to be able to determine the materials suitability for the SLS process. It is important to understand the relationship with different material properties, as well as the SLS process itself, in order to optimise the properties of the produced parts. The extrinsic properties of the material can be controlled with the production of the powder to some level. (Schmid et al. 2014; Schmid & Wegener 2016) Both the intrinsic and extrinsic properties are discussed in more detail in Subchapters 2.2.1 and 2.2.2.

2.2.1 Intrinsic properties

In the laser sintering system, the polymer powder is deposited to form a thin layer and the CO_2 laser beam is then used to selectively fuse or melt the polymer particles in a required shape. The top polymer layer needs to be fully coalescence and adhesion with the previously sintered layers is required as well. This means that for the semi-crystalline polymers, crystallisation should be prevented as long as possible but at least for several layers. (Schmid & Wegener 2016)

The processing temperature needs to be very precisely controlled in-between the melting and crystallisation temperature of the given polymer to prevent too early crystallisation (Schmid & Wegener 2016). However, with wide temperature range for processing, also called "sintering window", small variations to the optimum processing temperature can generally be accommodated. The processing temperature range for a polymer can be determined from its differential scanning calorimetry (DSC) curve. (Goodridge et al. 2012) The idealized DSC curve of SLS material is presented in Figure 2.2.

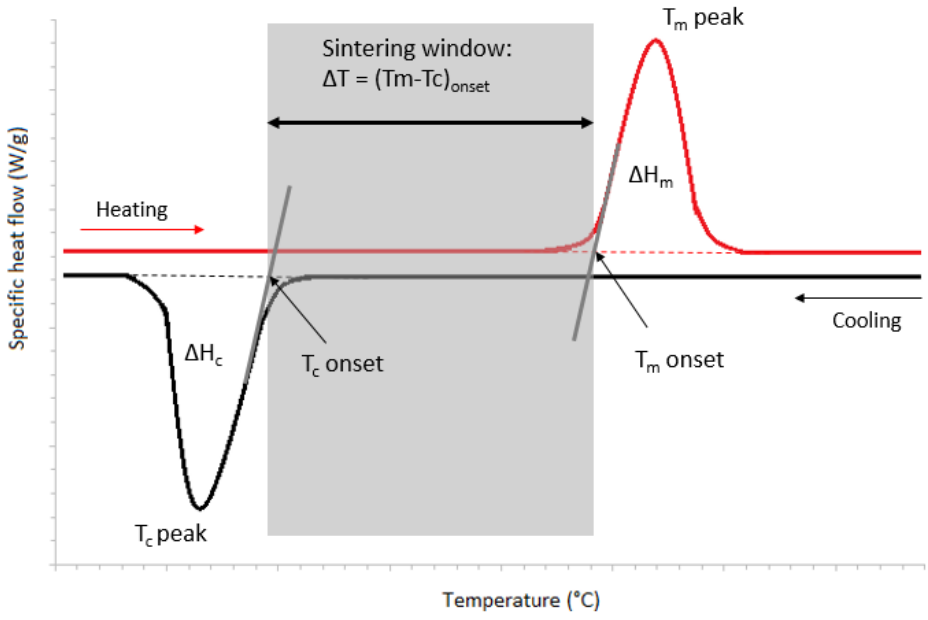

Figure 2.2. *An optimal DSC curve for SLS material with a wide sintering window and distinct melting and crystallisation peaks based on (Schmid & Wegener 2016).*

A large distance between the melting and crystallisation peaks in the DSC curve indicate slow re-crystallisation. Thus, the polymer remains longer in its liquid state during cooling. Delayed crystallisation minimises the risk of part distortion by preventing the accumulation of the residual stresses. Fast crystallisation during cooling, as well as the premature crystallisation in processing, can result in shrinkage and distortions to the part. However, a slow cooling rate results in a greater crystalline content, which in turn corresponds to lower ductility and higher shrinkage. This is due to the reduction of the amorphous regions that give the polymers the ability to yield without breaking. (Goodridge et al. 2012)

In addition to the wide sintering window, a narrow melt temperature range with a low zero viscosity and the low surface tension of the polymer melt are desired to enable successful SLS processing. A low viscosity combined with a narrow melt temperature range makes it possible to achieve fluidity rapidly without the need for excess energy. Furthermore, this enables raising the powder bed temperature closer to the melting temperature, which in turn minimises the required laser power to achieve consolidation. In addition, unlike some other processing methods, such as injection moulding, there is no additional compacting during processing, which makes low melt viscosity without shear stress especially important. (Goodridge et al. 2012; Schmid & Wegener 2016)

The flow behaviour during the laser sintering can be described with the zero shear viscosity, which can be determined by extrapolating the plateau region of the flow curve to zero shear stress or strain as presented in Figure 2.3. Basically, it tells the materials viscous behaviour at a specific temperature with no additional stress or strain. (Fiedler et al. 2007) Processing with SLS is found to be easier with the low melt viscosity. However, higher melt viscosity and molecular weight have been found to improve the mechanical properties, especially elongation at break. Furthermore, a low viscosity can result in a greater shrinkage and reduced accuracy. (Goodridge et al. 2012)

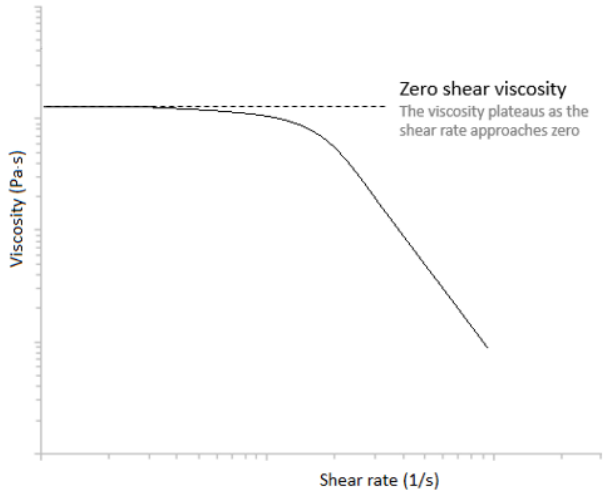

Figure 2.3. *Determination of the zero shear viscosity from the plateau region of the flow curve based on (Fiedler et al. 2007).*

In addition to the thermal and rheological properties, the optical properties are important to consider as well, when the SLS is used as the production method. In principle, three different effects can occur as the laser beam hits the polymer powder. The material absorbs the energy of the laser, but the reflexion and transmission of energy are also possible. Material needs to absorb the sufficient amount of the radiation to ensure an adequate consolidation. However, this is not a problem for most polymers since they consist of aliphatic compounds. At least in the majority of cases, these polymers have some group vibrations in the infrared region, making the sufficient absorption of CO_2 radiation possible. In addition, to induce an adequate layer adhesion between the sintered layers, some transmission of the radiation energy into the deeper layers is desired as well. Poor absorption and transmission capacity can be improved to some extent by increasing the laser energy power. However, using too high energy could cause degradation to the polymer. (Schmid & Wegener 2016)

2.2.2 Extrinsic properties

Different powder particle properties can have a great effect to the product when using selective laser sintering as a production method. The shape of a single powder particle is important factor when the flowing behaviour is considered. In addition, the powder bed density, the part surface roughness as well as the final part porosity are all dependent on the particle shape. Irregular particles can cause large irregular voids to the powder bed structure. Thus, spherical particles are preferred in the SLS process. (Bourell et al. 2014; Schmid et al. 2014; Schmid & Wegener 2016)

To determine the flowability of the powders the so-called Hausner ratio H_R can be calculated. The Hausner ratio can be calculated by dividing the tapped density with the bulk density as follows

$$H_R = \rho_{tap}/\rho_{bulk}, \quad (1)$$

Where ρ_{tap} is the tapped density and ρ_{bulk} is the bulk density. Regarding the literature when $H_R < 1.25$ powder has a free flowing behaviour and when $H_R > 1.4$ powder has fluidization problems. (Schmid et al. 2014; Schmid & Wegener 2016)

A certain particle size and particle size distribution are also important factors in the SLS. It is found that decreasing the particle size increases the part density, the surface quality and the accuracy of the parts. For commercial system, the particle size distribution is recommended to lie between 20 μm and 80 μm. (Goodridge et al. 2012; Schmid & Wegener 2016) Particle size and particle size distribution can be determined, for example, with a laser diffraction or sieve analysis (Żegleń et al. 2016). In addition, particle size distribution can be determined from scanning electron microscope (SEM), or other microscopic images.

2.2.3 Classic polymeric SLS materials

In principle, all materials that can be melted and re-solidified are suitable for the selective laser sintering. Originally, the SLS was developed for the production of plastic prototypes, but this technique has been extended to metals and ceramics as well. Nowadays, a quite broad range of different material groups, such as polymers, metals, ceramics and composites are employed in the SLS and are increasingly used in the direct manufacturing. (Gibson et al. 2015) However, since the aim of this study is to investigate the selective laser sintering of polyolefins the focus of the material overview will be on polymers.

Thermoplastic polymers are generally well suited for SLS since they have relatively low melting temperatures and low thermal conductivities. However, the availability of the polymeric laser sintering materials is highly limited. Thermoplastics can be further classified into the amorphous and semi-crystalline polymers, based on their crystallinity. The sintering behaviour of amorphous and semi-crystalline polymers is relatively different. (Gibson et al. 2015)

Due to its superior rheology, a semi-crystalline powder melt achieves a better coalescence and a higher density compared to the amorphous polymers. A problem with the semi-crystalline polymers is however, that they tend to shrink when they crystallise during cooling, which leads to distortions to the part. A wide processing window helps to postpone the crystallisation until the building process is completed. Powder should be preheated to the temperature just below the polymers melting temperature and kept there for a sufficient time after sintering. Controlling the cooling and re-crystallisation improves the dimensional accuracy and reduces the risk of distortions. (Goodridge et al. 2012; Gibson et al. 2015; Mys et al. 2016)

Amorphous polymers do not have a specific melting temperature, but they melt over a wide range of temperatures. Therefore, in SLS, they are heated equal or just below their glass transition temperature. However, amorphous polymers usually have a quite high zero shear viscosity even above their glass transition temperature, which can cause insufficient coalescence during the SLS. This leads to porous parts with a low density and a low strength. However, parts produced with the amorphous polymers have a high dimensional accuracy due to their low shrinkage during cooling. (Goodridge et al. 2012; Gibson et al. 2015; Mys et al. 2016; Schmid & Wegener 2016; Zhu et al. 2016)

When polymer materials are concerned, the material availability for the SLS is constricted mainly on PA12, PA11 and their different grades. In 2009, about 95% of the market consisted of PA12. (Goodridge et al. 2012) The popularity of using polyamide in the SLS can be explained with its properties and its good availability in a powder form. Polyamides have a good flowability, a low initial zero-shear viscosity as well as a small crystallisation shrinkage and a large degree of super-cooling. In addition, especially

PA12, has a very wide processing window. The combination of these properties lead to a low tendency to warp. The post-condensation behaviour, which is typical for the polyamides, is a major factor in establishing these properties. However, a major drawback with this behaviour is its highly negative effect to the recyclability of the powder and the consistency of the part properties. (Verbelen et al. 2016)

There are some other, less used, polymeric materials available in addition to the polyamide based powders. For example, there is a high-performance polymer, polyether ether ketone (PEEK), with an excellent temperature performance, strength, stiffness, wear and chemical resistance available to be used in the SLS. In addition, some polystyrene (PS) based powders, usually with a high dimensional accuracy and surface quality, are available as well. However, expanding the material availability further is important since the materials available nowadays, still do not have the properties required for the functional parts, or are too expensive to be used economically. There has been some extensive studies to find alternative materials suitable for the SLS process. However, the main developments are still constricted to the different variations of PA12 and PA11. (3D Systems 2017; Advanc3d Materials 2017; EOS e-Manufacturing Solutions 2017)

There are manufacturers that have some polypropylene-like SLS materials in their raw material selection. These materials are usually PA11 based powders with polypropylene simulating properties. For example, 3D Systems offers multiple polyamide based PP-like materials for SLS, such as DuraForm ProX PA, DuraForm PA, DuraForm EX Natural and DuraForm EX Black. In addition, Forecast 3D offers Nylon D80, Nylon EX and Nylon FR-106, which are all PA11 based materials that are said to have the toughness of injection-moulded polypropylene. (3D Systems 2017; Forecast 3D 2017)

In 2008, 3D Systems announced the first polypropylene based material DuraForm® PP 100 developed jointly with the TRIAL Corporation of Kanagawa (Wohlers & Gornet 2014, p. 13). However, that particular material is not currently available, at least not for consumer use. (3D Systems 2017)

There are some relatively new powder producers that offer actual polypropylene based as well as high-density polyethylene (HDPE) based materials for the SLS. Diamond Plastics GmbH offers different grades of PP powders for selective laser sintering with and without fillers. In addition, they have HDPE powder available as well. (Diamond Plastics 2017) Furthermore, a company Advanc3D Materials GmbH offers polypropylene material (PP flex) which is said to have 35% elongation at break. In addition, Advanc3d Materials provides Coathylene® Sint PP polypropylene powder manufactured by Axalta to be used in the SLS. (Advanc3D Materials 2017)

2.3 Processing considerations

In addition to the material properties affecting the SLS processing, some other processing parameters should be considered. These process parameters can be divided into four main categories: laser related parameters, scan related parameters, powder related parameters and temperature related parameters. In addition to these, the build size is dependent on the size of the equipment. Most of these parameters are highly dependent on each other and they affect both the production efficiency and the properties of the build parts. Especially, the mechanical behaviour and the density of the SLS parts are highly dependent on the accumulated laser energy density, the part bed temperature and the part orientation. Balancing the processing parameters is important to be able to meet the part requirements. (Gibson & Shi 1997; Bourell et al. 2014; Gibson et al. 2015) Laser, scan, powder and temperature related parameters are discussed in the following subchapters.

2.3.1 Laser related parameters

Laser related parameters include parameters, such as laser power, spot size, pulse duration and pulse frequency. Laser power is the power provided by the laser to the part bed surface. It is used to rapidly heat the powder above the part bed temperature. Laser power should be high enough to ensure that the temperature of the part bed surface rises above the melting temperature of the material during scanning. The material should reach its melt temperature to be able to fuse together with the surrounding particles. (Gibson & Shi 1997; Gibson et al. 2015)

A lower bed temperature requires a higher laser power and generally by increasing the bed temperature, the laser power can be decreased. The absorptivity characteristics that are dependent upon the powder shape, size and packing density, also affect the required laser power. The combination of the high laser power with the high part bed temperature generally provides dense parts. However, this combination can also reduce the recyclability of the powder and induce the part growth. On the other hand, a low laser power and part bed temperature provide a better dimensional accuracy, but the parts have lower density and higher risk of the layer delamination. (Gibson & Shi 1997; Gibson et al. 2015)

The total energy input that is needed to fuse the powder into a useable part is dependent on the several different parameters. In addition to the laser power, the spot size, pulse duration and the powder bed temperature have their input. If the laser power is low, the scanning speed should be slow enough to ensure a sufficient particle fusion. On the other hand, with higher laser power, scanning can be performed faster. A spot size is the diameter of the laser beam determining the area that the laser affects when remaining still. (Gibson & Shi 1997; Gibson et al. 2015)

2.3.2 Scan related parameters

Scan size is the distance that the scanners move in one time step with the laser on and it determines the laser beam speed. Laser beam speed on the other hand affects the laser power on specific point on the surface of the part bed, the building time as well as the energy density. Scan spacing is the distance between two neighbouring parallel scan vectors. Scan spacing should not be too wide and exceed the diameter of the laser beam in order to be able to sinter the whole cross-section completely. It is possible to increase the energy density by decreasing the scan size, laser beam speed and scan spacing as well as by increasing the laser power. Energy density can be calculated as follows

$$ED = \frac{P}{SS \cdot LS}, \tag{2}$$

Where P is the laser power in W, SS is the scan spacing in mm and LS is the laser beam speed in mm/s. Experimental results show that increasing the energy density results in increased tensile strength and part density. However, with a high energy density other problems, such as curling and distortions, can occur. (Gibson & Shi 1997; Caulfield et al. 2007)

Delay time affects the laser sintering process and it can be defined as a time difference for laser exposure between any two adjacent points on the successive scanning lines on a layer and it is dependent on the length of scan line and the speed of the laser beam. Delay time correlates closely with the scan speed thus long delay time means slow scan speed and small delay time means fast scan speed. Too short as well as too long delay time can lead to improper sintering characteristics. A long delay time thus slow scan speed, can result in thermal degradation, and thus lower strength. On the other hand, a small delay time thus fast scan speed, can result in insufficient bonding. The orientation of the part affects the length of the scan line and it can be varied to achieve the optimal length, and thus the optimal delay time. Experimental studies show that the delay time has a significant influence to the strength of the parts. Findings show that increasing the delay time increases the part strength until it reaches a maximum point from which the further increase of the delay time decreases the strength of the part. According to Jain et al. (2009) this can be attributed to the thermal degradation. (Jain et al. 2009)

To improve the accuracy and the surface finish properties, laser scanning can be performed in a contour mode and in a fill mode. This way, only the outline of the cross-section, of a specific layer, is first scanned in the contour mode and after that, the rest of the cross-section is scanned according to the fill pattern. Typically, the laser energy is lower for the contour mode to decrease the risk of overflown material, and thus ensure the dimensional accuracy. (Gibson et al. 2015)

2.3.3 Powder related parameters

As discussed earlier, the particle shape is preferred to be spherical and the particle size as small as possible. However, too fine particles can cause problems for the SLS process since static forces can make the spreading of the powder with fine particles difficult, causing problems to the flowability. Moreover, it is possible to the fine particles to "evaporate off" which could cause problems to the efficiency of the process by fogging the optics and heat elements. As a conclusion, the suitable particle size is highly dependent on the properties required for the laser sintered part, but if the negative influence to the process caused by very fine particles is not too significant, decreasing the particle size is usually recommended. (Goodridge et al. 2012; Schmid & Wegener 2016)

Particle size, shape and size distribution, have a great influence to the flowability and the packing density of the powder, but they also affect the powder bed thermal conductivity as well as the laser absorption characteristics. Since the finer particles have greater surface area, they can absorb the laser energy more efficiently compared to the coarser particles. Thus, the small particles coalesce at a faster rate than the large particles when kept in identical conditions. This can cause unwanted sintering next to the sintering area causing problems to the part accuracy. Large variations in the particle size can also cause the incomplete melting of the large particles, which can in some cases result in the porosity of the parts. (Goodridge et al. 2012; Bourell et al. 2014; Gibson et al. 2015)

Slice or layer thickness is the depth that the part piston lowers for each layer and it can affect the properties of the parts. The surface roughness of the parts can be decreased by using a small layer thickness, but the use of the small layer thicknesses also increases the build time. However, it should be noted that the layer thickness is dependent on the powder particle size, and thus it cannot be smaller, but it can exceed the largest particle size. A suitable powder spreading speed is also dependent on the flowability of the powder. These and all the processing parameters should be set to match the overall requirements of the application. (Gibson & Shi 1997)

2.3.4 Temperature related parameters

Temperature related parameters include properties, such as the powder bed temperature, feed powder temperature and the temperature uniformity. As was mentioned before, the appropriate laser energy is dependent on the powder bed temperature. The laser power should be adjusted to a level where the powder, at the powder bed surface, is heated near to the melting temperature of the material, by the effect of the laser. Usually, decreasing the laser power is possible when the bed temperature is increased. However, the part bed temperature should be kept in a sufficient level since too high part bed temperature can cause undesired bonding, a hard part cake and a poor dimensional accuracy. Due to the hard part cake, the removing of the part can became more difficult and the degree of recyclable powder reduced. On the other hand, a too low part bed temperature can cause

insufficient melting causing porosity and the curling of the corners and the edges of the part caused by the early crystallisation. Curling can result in distortions and warping to the product and furthermore ruin the whole process, if the curling causes the part to dislodge from its original position. This can happen, if the powder-spreading roller grabs the curled edge of the part, and moves the part from its original position and as a result, the following layers do not build up correctly on top of the previous layers. (Gibson & Shi 1997; Goodridge et al. 2012; Bourell et al. 2014)

For the semi-crystalline polymers, the sufficient part bed temperature is usually 3-4 ºC below the melt peak temperature of the polymer. In addition to reducing the required laser power, increased part bed temperature also prevents the molten polymer from crystallising. Too early crystallisation can cause localised solidification shrinkage and part distortion. In addition to the precise control of the powder bed temperature, the temperature of the feed powder, spread over the build area after each layer, should be considered. If the temperature of the new powder layer is too low, the previously sintered layer can start to cool too soon. On the other hand, too high feed powder temperature can cause problems with the flow and deposition of the powder. In addition, the time between layers thus the time that the new layer of the powder has to reach the correct part bed temperature, affects the temperature control but also the build time. (Goodridge et al. 2012; Bourell et al. 2014)

Temperature uniformity can be compromised by small variations to the powder bed temperature due to the conduction from previously heated powder layers and/or conduction through the part cake walls as well as thermal convection channels formed in the N_2 atmosphere above the part bed. In addition, irregular heating elements can cause inconsistent powder bed heating. Furthermore, a poor sealing, due to the gradual thermal degradation of the sealing elements between the chamber door and the machine frame, can cause temperature fluctuations as well as the risk of a potential oxygen exposure, risking the oxidation of the exposed part and the feedstock powder. These variations to the part bed temperature can lead to insufficient melting and coalescence if the temperature drops too much and on the other hand, temperature rise can cause melt overflows, and thus decrease the dimensional accuracy. Furthermore, too early cooling can be especially problematic for the materials with a narrow processing range thus sintering window. Thermoplastics start to crystallise already before reaching the crystallisation temperature peak and if the sintering window for processing is narrow, only a little drop to the temperature can start the crystallisation. (Goodridge et al. 2012; Bourell et al. 2014)

Conduction through the part chamber walls can cause temperature control related problems, especially for the large builds. In commercial laser sintering machines, the heat sources are the laser itself in addition to the infrared heaters above the part bed surface and below the part bed piston. Selectively heating the particular region of the part bed surface is not possible with these heating elements, and in addition, they can induce local

hot and cold spots. Thus, for large builds it is difficult to achieve a controlled and even temperature with just two heaters while the wall cooling and the thermal convection channels further complicate the situation. Improvement to these problems could be achieved with a multi-zone heater layouts. Integra has produced a 9-zone heater that can be used with 3D Systems laser sintering machines. This system enables the optimised thermal profile for the different part bed layouts and makes the mechanical properties, with more consistence, achievable. In addition, it is possible to decrease the overall part bed temperature and laser power. (Bourell et al. 2014)

2.4 Processing problems and limitations

Humidity and electrostatic charge can compromise the flowability of the powder, especially with the fine particles. Depending on the polymer used, drying is usually advised to prevent the problems caused by the absorbed humidity. (Goodridge et al. 2012.) However, drying can aggravate the effect of the electrostatic charge. Another problematic feature in laser sintering process, is the "fogging" of the laser window. This problem is also related to the fine powder particles since, as discussed earlier, they can evaporate off at high temperatures, causing fogging to the lens. The laser window protects the laser directional control mirrors from the airborne contaminants, but the fogging of the lens causes alterations to the energy and the shape of the laser beam. (Bourell et al. 2014)

The cooling of the SLS parts is quite different compared to, for example injection moulding, since in the SLS cooling can take several hours, while cooling in the injection moulding usually happens in the matter of seconds. The poor thermal conductivity of the polymer powder, in addition to the thermal contact resistance between the powder particles, limits the cooling rate, and thus cooling happens very slowly. As discussed earlier, a slow cooling rate leads to a greater crystalline content which affects the mechanical properties of the produced parts. The reduction of the amorphous regions corresponding to the higher crystalline content, which limits the polymers ability to yield without breaking, and thus decreases the ductility of the polymer. In addition, the higher crystalline content corresponds to a higher shrinkage. Especially, an uneven cooling, and thus shrinking throughout the part, can cause serious distortions to the part. (Goodridge et al. 2012; Bourell et al. 2014) However, a lower molecular chain activity that generally results from the higher degree of crystallinity, leads to lower porosity and better tensile properties. (Bai et al. 2016)

The major limitations in the SLS, from the production point of view, are available part size, production speed, material choices and in-situ process control. Moreover, to be able to produce functional parts, with properties comparable to the injection moulded parts, with the selective laser sintering, the parts need to be free of porosity and particle coring. To achieve this, incomplete particle melting and coalescence need to be overcome. Advanced part monitoring and laser control schemes may help to accomplish this.

However, even with a perfectly uniform temperature control, there is always some non-uniform melting and coalescence due to the variations in polymers properties, such as molecular weight, crystallinity and particle size and shape, requiring advanced powder bed monitoring and closed-loop feedback control techniques to be able to control them. (Bourell et al. 2014)

3. POWDER PRODUCTION FOR SELECTIVE LASER SINTERING

It is possible to produce fine polymer powders with several methods. These methods include some physiochemical methods, such as solution precipitation and spray drying, as well as some mechanical size reduction methods. Mechanical methods are the most commonly employed. However, as discussed earlier, the fulfilment of some rather specific requirements is necessary for the powder to be suitable for the SLS process. In addition to suitable particle size, it is preferred that the particles are spherically shaped and that the particle size distribution is at required range. Different pulverization techniques have their advantages and limitations when considering the SLS powder requirements, which should be considered when choosing the method. (Khait et al. 2001; Schmid et al. 2014) Different mechanical and physiochemical powder production methods are presented and discussed in the following subchapters.

3.1 Mechanical techniques

There are different mechanical actions for accomplishing the size reduction including crushing, impacting, cutting and exploding. The size reduction process usually employs one or more of these actions depending on the equipment used. Commercial equipment can be categorized in different kinds of crushers and mills based on the technique they are using. In addition, solid-state shear pulverization, also called powder extrusion, has been developed as an alternative method for the powder production, to overcome the limitations of the conventional grinding. Depending on the equipment, mechanical size reduction methods usually produce powder particles with irregular shape. Particle size and particle size distribution are dependent on the equipment used as well. (Khait et al. 2001)

Suitable equipment should be chosen based on the material properties as well as the desired powder properties, including particle size, shape and size distribution. In general, the production of the coarse powder happens with the shattering and crushing motions and fine and ultrafine powders form with the effect of tear, shear, abrasion or attrition. The commercial grinding machines, such as jet mills, usually employ impact motion for the size reduction of more brittle materials and cutting for the softer and more elastic materials. However, the mechanical size reduction equipment is not very efficient and is usually quite expensive to operate since only about 30% of the processed material achieves the desired particle size in one processing round. In addition, the batch nature of this kind of powder production can cause variations to the particle shape and size between the different batches. According to Khait et al. (2001), the energy consumption can be

reduced with the powder extrusion compared to the traditional grinding methods. (Khait et al. 2001; Bourell et al. 2014)

Different grinding methods have different properties and they can be compared for their suitability. Mys et al. (2016) have compared using ball milling and rotor milling for the production of a syndiotactic polystyrene powder at the ambient temperature. They found that the ball milling usually takes a lot of time and the powder produced often has too wide particle size distribution as well as undesired particle morphology. The spheronizers can be used to enhance the morphology of the pellets, but the desired range for the particle size distribution is still not achieved. Finer powder can be produced with longer milling times, but the obtained particles are non-spherical in nature. Milling times longer than 45 minutes can cause the flattening of the particles. (Mys et al. 2016)

On the other hand, the rotor milling is a short-contact milling method where the residence time of the material in the miller is minimized, and thereby the possibility of material degradation reduced. Material is fractioned by impacting on the rotor blades and further sheared between the rotor and sieve. The particle morphology obtained with this method is relatively spherical and the particle size is at the desired range. The rounding of the particles is believed to be caused by the extra shearing effect in the grinding. (Mys et al. 2016)

Suitable processing temperature can make the size reduction process more efficient. Materials that are not so easily affected by the temperature rise, and are inherently brittle, can usually be processed at ambient temperature. However, at the ambient temperature the wear of knives or blades as well as the generated frictional heat are quite significant, and thus for temperature sensitive materials, the temperature-controlled grinding is required. The ultimate increase in temperature during the grinding process should not exceed the glass-transition temperature of the material. For example, materials that are resilient at room temperature, like polyethylene and polypropylene, can be made more brittle and glass-like by reducing their temperature, and thus making the grinding more efficient. (Khait et al. 2001; Liang et al. 2002)

Temperature-controlled grinding needs a cooling agent to achieve the sufficient temperature for grinding. The most widely used cryogen is liquid nitrogen due to its large cooling capacity, rapid heat transfer, low-pressure storage, easily controlled flow and chemical inertness. However, to keep the temperature at sufficient level to prevent any damage to the material, a quite large amount of liquid nitrogen is required, leading to high operation costs. Moreover, in cryogenic grinding, both the material and the mill should be cooled. In addition, the production of especially very fine powders is highly energy consuming. (Liang et al. 2002; Wilczek et al. 2004)

Grinding can be conducted in a dry or wet conditions. In the wet grinding, some solvent is used to improve the grinding process. There are different solvents with different

properties that can be used. The selection of the suitable solvent is important since the solvent used can have a great effect to the powder properties. Decreasing the temperature usually increases the solvents viscosity, which by dampening the grinding bead motion decreases the grinding efficiency. This makes low viscosity solvents preferable for the wet grinding process, when the grinding is performed at reduced temperatures. (Schmidt et al. 2015)

Some post treatments can be employed to the irregular powder particles obtained with the mechanical grinding methods to improve their suitability for the SLS process. Schmidt et al. (2015) have tried to find a novel process route for the production of spherical polystyrene (PS) powder. They have found post treatment steps that can be conducted to improve the flowability and the packing density of the mechanically grinded powders. First, irregular particles obtained with wet grinding can be rounded by heating in a downer reactor. It is important that the rounding of the particles is done in a proper conditions and for a sufficient time. If the residence time is too short, the particles remain unchanged. The flowability of the rounded particles can then be further increased by dry coating powder particles with nanoparticles, which in turn increase the surface roughness. These steps increase the flowability of the powder remarkably as compared to the ground product. However, it was not reported if the dry coated nanoparticles had any other effect to the laser sintered parts. (Schmidt et al. 2015)

3.2 Physicochemical techniques

It is possible to obtain spherical powder particles with several physicochemical methods, such as precipitation, emulsion-based methods and spray drying. With these methods, it is usually possible to modify the particle size to a suitable range, by varying the process parameters. However, some difficulties exists, such as insufficient process control, high costs and the complexity of the processing. (Nandiyanto & Okuyama 2011) These methods will be discussed shortly in following paragraphs.

A possibility for the production of polyamide powders, which are widely used in the SLS, is precipitation by dissolving the polymer in a suitable solvent, typically under pressure, and at an elevated temperature. After dissolving, the temperature is decreased until the nucleation takes place without the precipitation. The temperature is held constant for a determined time. After reaching a suitable time, the temperature is decreased further to achieve the supersaturation. Then the polymer powder is precipitated and the resulting suspension is dried. (Baumann & Wilczok 1999) A similar procedure can be employed with polyethylene. However, with polypropylene the situation is more complex. When polypropylene is dissolved in a solvent and a non-solvent or even if it is first dissolved in a solvent and then a non-solvent, the powder form of polypropylene is difficult to obtain. Instead, this procedure usually results in a non-pulverous lumpy mass. According to the literature, even a slightest mechanical movement during precipitation can cause the precipitation products to form in filaments or tough skins. (Körsgen & Weller 1985)

An alternative approach for producing a polypropylene powder includes novel manner elements in both the mechanical comminution and the physiochemical methods. The grinding of the coarse polypropylene particles into fine powder is not very efficient as its own, but according to Körsgen & Weller (1985) pretreating polypropylene with solvents can ease the grinding in great deal. According to the invention, pretreated and dried polypropylene can be ground into fine and free flowing powder quite efficiently. Controlling the particle size is possible by adjusting the pretreatment conditions and the conditions during the mechanical comminution. Processing steps include dissolving polypropylene at elevated temperature and cooling the solution in very steady conditions, where no mechanical agitation occurs. In these conditions, polypropylene re-precipitates and the precipitated polypropylene can be separated from the liquid and dried. Dried polypropylene can then be subjected to mechanical comminution. Screening can be performed to obtain the required particle size. (Körsgen & Weller 1985)

In melt emulsification, the formation of the pre-emulsion happens by heating the dispersed phase above its solidification temperature in a stirred tank. This typically happens in the presence of a continuous phase and emulsifier. Pre-emulsion is then transferred to a rotor-stator device. The formation of the melt emulsion happens due to the shear and elongation stress in the rotor-stator device. The suspension of spherical particles is obtained when the formed droplets are cooled and they solidify. It is important to maintain the colloidal stability during the droplet breakup, phase change from liquid to solid and after cooling. To ensure this, the emulsifier needs to be effective during the whole process. In addition, emulsifier needs to assure a long-term stability during storage to avoid agglomeration and it cannot decompose at the process temperature. The obtained product needs to be dried before the SLS, typically with a spray drying process. (Fanselow et al. 2016)

The spray drying can be used to obtain dry products with varying particle size from fine powders to granulates. The size of the droplets and their distribution has a high influence to the final powder particle size and particle size distribution. Thus, if the droplet size can be reliably predicted, the final powder properties can be controlled. The feed material can be in the form of solution, suspension, slurry or paste. There are three main process stages in the spray drying including the atomization, spray-air mixing and moisture evaporation and the separation of the dry product from the exit air. Atomization is the most important operation since the type of atomizer determines the energy required to form the spray. In addition, the drop size and size distribution, as well as their trajectory and speed, are determined based on the atomizer, and thus the final particle size is dependent on the atomizer as well. (Mujumdar 2014, p. 193-194)

The rotary wheel atomizers and the pressure nozzle single-fluid atomizers are the most commonly used atomizers. The pneumatic two-fluid nozzles are used only in very rare occasions. (Mujumdar 2014, p. 193) A wheel atomizer can produce a wide range of mean droplet sizes with a high homogeneity spray. They can handle high feed rates in a single

wheel and are suitable to be used even with abrasive materials. The wheel speed has a high effect to the droplet size. Thus, the size distribution can be controlled by varying the wheel speed. However, changing the feed rate does not give a similar effect. In addition, this equipment is very flexible and can be easily tuned to meet the necessary requirements. (Mujumdar 2014, p. 196) However, the wheel atomizers have higher energy consumption and capital costs compared to the pressure nozzles. Furthermore, a large chamber is required due to the broad spray. The pressure nozzles have a simple and compact construction with no moving parts. On the other hand, the pressure nozzles have tendency to clog and the swirl nozzles cannot be used for the suspensions due to the phase separation. (Mujumdar 2014, p. 199)

3.3 Powder recycling

Reusing the non-consolidated excess powder of the powder bed chamber is desired for the economical purposes, as well as for minimising the produced waste. It is possible for the unfused powder to be sieved and reused, but it should be considered that even though the surrounding powder is not melted, it goes through a significant thermal cycle during the SLS process. An elevated temperature can cause the powder bed to fuse and can induce changes to the molecular weight of the polymer. In addition, in the presence of the reactive atmospheric gases the chemical nature of the polymers can change as well. The magnitude of these effects vary for different materials. (Goodridge et al. 2012; Gibson et al. 2015)

To maintain the uniform quality for the produced parts, different recycling methodologies have been developed. The easiest recycle method is the fractional mixing of the unused powder and the used powder. The amount of the fresh powder required is polymer dependent. In addition, the used powder should be separated to the overflow/feed powder and the loose powder from the part-bed since their thermal exposure differs from each other. Furthermore, the mixing of the unused and used powders should be thorough to ensure the uniform base material and comparable parts. However, the batch nature of this kind of recycling method always results in differences between the batches due to the inconsistencies of the different build layouts. Moreover, there can be severe variations to the parts quality when comparing parts manufactured from the used and unused powder. (Goodridge et al. 2012; Gibson et al. 2015)

To be able to overcome the problems existing in the fractional mixing, and to improve the uniformity of the recycled material, a method employing the powders melt flow index (MFI) has been developed. The MFI is the measure of molten thermoplastic material flow through an extrusion apparatus, carried out under prescribed conditions. To ensure the repeatability, ASTM and ISO standards can be followed. With a MFI based recycling method, the target MFI is determined based on experience. The goal is to achieve this value by mixing the used and unused powder in suitable proportions. The MFI can be

measured for the powder mixture and the proportions of the different powders can be modified if necessary, to achieve the target value. (Gibson et al. 2015)

Wegner & Ünlü (2016) have carried out some studies considering the re-usage of the pre-commercial version of ROWAK Rolaserit PP powder. The effects for the processing and the part quality have been investigated using the fresh powder, the excess powders from the SLS process as well as the refreshed powder with the refresh rate of 50%. To understand the flow characteristics of the different powders, the measurements for the melt volume rate (MVR), Hausner ratio, relative bulk density and relative packing density were conducted. In addition, tensile specimens and density cubes were produced for testing. For the tensile tests, the specimens were produced in different build directions. (Wegner & Ünlü 2016)

Based on the findings of Wegner & Ünlü (2016), the aging effects seem to have only little effect on the materials viscosity and Hausner ratio. However, the bulk and packing densities of the powders were reduced when the material was reused. However, according to their results, aging has only little effect to the density, Young´s modulus and tensile strength of the SLS produced parts when the used energy density was high enough. On the other hand, elongation at break (EAB) is a sensitive value regarding aging effects and shows the significant reduction of values for all studied energy density levels, possibly due to the reduction in the packing density. These results are comparable to the values of the commercially used PA12 powders. (Wegner & Ünlü 2016)

4. SELECTIVE LASER SINTERING OF POLYOLEFINS

There have been studies that investigate the suitability of different polymeric materials to be used in the SLS process in addition to the polyamide based powders. These studies include using polyolefins, such as polypropylene and polyethylene. This chapter will give an outer view of the basic properties of the polyolefins, focusing on polypropylene and polyethylene. In addition, Subchapter 4.2 sums up shortly some of the previous studies considering the selective laser sintering of these polymers.

4.1 Polyolefins

Polyolefins are the group of thermoplastic polymers containing only carbon and hydrogen atoms. They are formed by the polymerisation of olefins, such as propylene, ethylene, isoprene, and butanes, which in turn are commonly obtained from the natural carbon sources, such as crude oil and gas. After the development of the Ziegler-Natta catalysts in 1950, polyolefins have been widely used in different applications. The Ziegler-Natta catalysts improved the molar mass control of polyolefins and made it possible to produce them with lower costs as well as in higher quantities. (Al-Ali AlMa'adeed & Krupa 2016, p.1) Nowadays, polyolefins are widely produced and the production of polyethylene and polypropylene alone occupies 50% of the plastic production worldwide. (Al-Ali AlMa'adeed & Krupa 2016, p. 51)

To make a polyolefin, at least three components are required: a monomer/co-monomer, a catalyst/initiator and a polymerisation reactor. The route of polymerisation has a great influence to the molar mass and the degree of crystallinity of the polymer. Furthermore, the catalyst used in the polymerisation determines how the monomers will be linked in the polymer chain, influencing the polymer microstructure and properties. There are four main types of olefin polymerisation catalysts including the Ziegler-Natta catalysts, the Phillips catalysts, the metallocene catalysts, and the late transition metal catalysts. In addition, a system that promotes the polymer chain growth is required for the manufacturing process. For the industrial applications, both the free radical initiators and the coordination catalysts are suitable to make a polyethylene but for the polypropylene production, only the coordination catalysts are used. Controlling the polymer microstructure is more efficient with the coordination catalysts than with the free radical initiators. (Soares & McKenna 2012, p. 1-2; Al-Ali AlMa'adeed & Krupa 2016, p. 2)

In general, polyolefins have a high electrical resistivity and a high dielectric strength. In addition, they are chemically very stable. They are also insoluble in water, in polar solvents and in unipolar organic solvents when the temperature is below 60 °C. (Al-Ali

AlMa'adeed & Krupa 2016, p. 2) Furthermore, polyolefins have a low surface energy and a poor adhesion. (Al-Ali AlMa'adeed & Krupa 2016. p. 7)

The most common types of polypropylenes can be classified into isotactic, syndiotactic and atactic polypropylenes, based on the location of the methyl groups in their molecular structure. In the isotactic form, the methyl groups are placed on the same side of the backbone, in the syndiotactic from they are on the alternating sides and in the atactic form they are arranged in a random order. Figure 4.1 shows the isotactic, syndiotactic and atactic forms of polypropylene. Atactic polypropylene is seldom used due to its amorphous nature. Isotactic and syndiotactic polypropylenes are both semi-crystalline polymers, however isotactic polypropylene dominates the market likely due to its relatively easy produceability with the Ziegler-Natta and metallocene catalysts. Syndiotactic polypropylene can only be produced with some metallocene catalysts, which can explain its lesser commercial use. (Soares & McKenna 2012, p. 10-11)

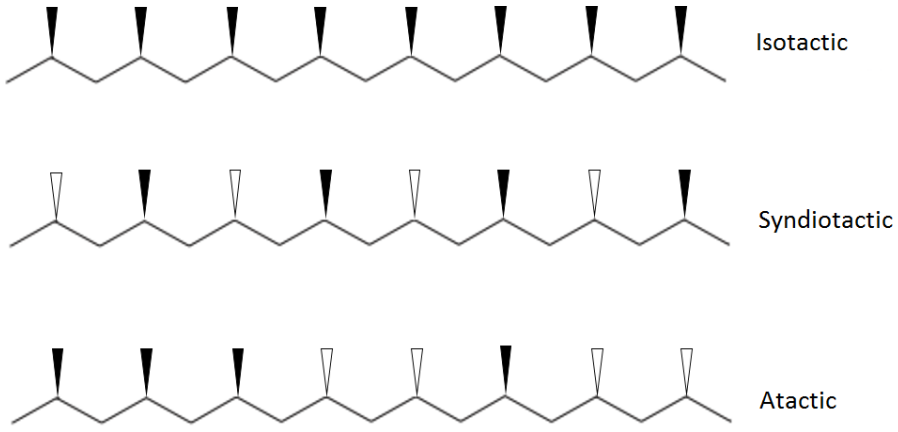

Figure 4.1. *The common types of polypropylene based on (Soares & McKenna 2012, p. 11).*

The polyethylene resins can be classified into three main types, including a low-density polyethylene (LDPE), a linear low-density polyethylene (LLDPE) and a high-density polyethylene (HDPE), based on their density range and branching structure. Figure 4.2 shows the branching structure of the main types of polyethylene. It is possible to divide LLDPE to smaller segments, MDPE (medium-density polyethylene), LLDPE and VLDPE (very low-density polyethylene), based on the density range, but from the structural point of view they are very similar, and thus can be categorized to LLDPE. In addition, polyethylene with the molecular weight of several millions is called ultrahigh molecular weight polyethylene (UHMWPE), but it is structurally very similar to HDPE. LDPE is made by the free radical initiators and it has both short and long chain branches in its structure. HDPE and LLDPE are made with coordination catalysts, which generally forms only short chain branches. The Ziegler-Natta or the Philips catalyst is generally used for the production of the most commercial HDPE and LLDPE grades. (Soares & McKenna 2012, p. 4-5)

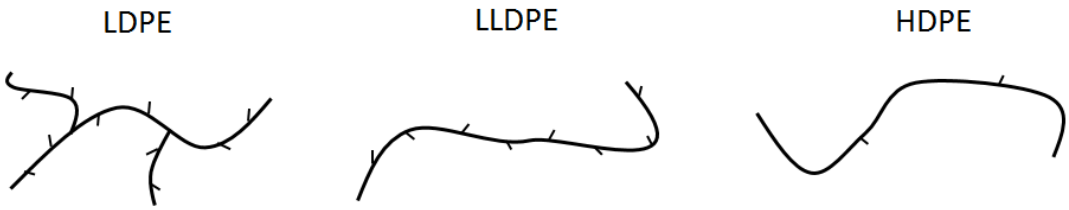

Figure 4.2. *The branching structure of the common types of polyethylene based on (Soares & McKenna 2012, p. 5).*

The comparison of the properties of polypropylene and polyethylene shows that there are many similarities but also some specific differences. Polypropylene is a semi-rigid and tough polymer with a good chemical, fatigue and heat resistance. Polyethylene is more flexible but has a good chemical resistance as well. Polypropylenes have lower density, better temperature resistance as well as higher rigidity and hardness than polyethylene. In addition, polypropylene is the number one choice for living hinges. However, polypropylene and polyethylene are both vulnerable to the UV degradation and oxidation and they have poor resistance to chlorinated solvents and aromatics. Moreover, coating them is difficult due to their poor adhesion properties. However, both of these polymers are very popular materials for many applications despite of these shortcomings. (Hindle 2017)

4.2 Studies on polyolefins in SLS applications

Theoretically, any thermoplastic polymer that is available in powder form can be laser sintered with optimised processing parameters. Especially, due to their relatively low melting temperature, thermoplastic polymers are well suited. However, there is a very limited number of different polymers commercially available for the SLS process. On the other hand, the materials used nowadays, cannot completely meet the requirements of all the applications. (Bai et al. 2016) Since the main interest for this study, is to investigate the suitability of polypropylene and polyethylene in SLS, the following subchapters focus mainly on the previous studies performed with these polymers.

4.2.1 Polypropylene in SLS

Fiedler et al. (2007) and Zhu et al. (2016) have investigated the suitability of polypropylene powders in the selective laser sintering. Approaches with these studies are somewhat different. Studies performed by Fiedler et al. (2007) focus on the available commercial PP materials, and their properties and suitability for the SLS, while Zhu et al. (2016) investigates how commercial PP materials should be modified, to be better suited for the SLS. Following paragraphs give the outer view of these studies and their findings.

Studies by Fiedler et al. (2007) consider the commercial PP powders available for the rotational moulding, high-speed injection moulding as well as some ultrafine powders recommended to be used as additives. In addition, commercial PA12 powder, already used for the SLS, and some of its substitutes, were applied as well, as reference materials. Several tests were carried out by Fiedler et al. (2007) to determine the intrinsic and the extrinsic properties of the investigated PP powders. Studies showed that there were significant differences when comparing the different PP powders and PP and PA powders with each other. Some properties, such as the sintering window and the stability regarding thermal degradation, were found to be superior for some of the PP powders compared to the PA powders. The viscosity measurements were not comparable between the PP and PA powders, yet there were some differences when different PP powders were compared. It was found that one powder, used in rotational moulding, had too high viscosity, while other PP powders showed sufficient values with some variations with each other. (Fiedler et al. 2007)

The crystallinity of the PP powders, investigated by Fiedler et al. (2007), was found to exceed the values for PA powders about 100%. In addition, the ability to absorb the CO_2 laser power was higher for PA powders. Moreover, the particle size of the PP powders used in the rotational moulding was found to be too coarse and the PP powder produced with the precipitation too fine. Powders meant for the masterbatch application were found to be the most similar to those of PA powders but still with a too narrow particle size range. Fiedler et al. (2007) conclude, that the particle size and size distribution need to be modified to meet the requirements needed for SLS. In addition, the crystallinity of PP powders should be reduced to decrease the amount of shrinkage and the absorbance of the CO_2 laser should be improved. (Fiedler et al. 2007)

To ensure the sufficient mechanical properties, the commercial PP usually has relatively high isotacticity, and thus a high degree of crystallinity. As mentioned before, the high degree of crystallinity is found to cause the high level of shrinkage, which can cause the deformation of the SLS parts. Studies conducted by Zhu et al. (2016) investigate the possibility of modifying the chemical structure of PP to decrease the crystallinity and improve its SLS processability. Comparing the low-isotacticity and high-isotacticity PP shows that low-isotacticity leads to the lower melting temperatures as well as to a lower degree of crystallinity. Furthermore, these properties can improve the processability of the low-isotacticity PP. In theory, the reduction of the part bed temperature, shrinkage and part deformation is possible by lowering the melting temperatures and the degree of crystallinity. Moreover, the warping and curling behaviour can be avoided by minimizing the thermal gradient between the molten and supporting powder by preheating the material to a certain temperature before laser sintering. For the semi-crystalline polymers, this temperature should be close to the melting temperature. (Zhu et al. 2016)

The SLS processing causes relatively high thermal load to the polymer during the processing cycle, which can cause degradation to the polymer. However, the degradation

temperature for PP, investigated by Zhu et al. (2016), is significantly higher than the powder bed temperature in the SLS processing, which indicates that this PP has sufficient thermal stability to be used in the SLS. However, there can be seen a distinctive decline at the degradation temperature when PP parts produced with SLS are compared to the raw powder. According to Zhu et al. (2016), this could be explained with the thermal oxidation degradation since polyolefins are known to be quite sensitive to the thermal oxidation. As discussed in Subchapter 3.3, the excess non-sintered powder can be recycled, but it should be considered that the properties of the parts produced with the recycled powder and the new powder can differ in great deal. (Zhu et al. 2016)

Zhu et al. (2016) also studied the effect of the energy density in the SLS. At relatively low energy densities, powder particles are slightly bonded together and the sintering necks can be observed giving only low-density parts. By increasing the energy density, a connected structure with improved specimen densities could be achieved, but there were still some un-melted particles found on the surface. Less apparent and more compact morphology was achieved by further increasing the energy density, but there was some spherical voids formed on the fracture surface when the certain level of the energy density was achieved. According to Zhu et al. (2016), this could be explained with gas generated from the degradation of the polymer. In addition, the tensile strength increased when the energy density was increased but only to this certain energy density level. Increasing the energy density further from that point decreases the tensile strength, due to the degradation of the polymer. (Zhu et al. 2016)

4.2.2 Polyethylene in SLS

Bai et al. (2016) have studied the usability of polyethylene in the SLS. Their studies show that even though the spreading of the PE powder was relatively easy, compared to commercial PA12, PE powder exhibited inferior flowability. Further studies show that the PE powder contained irregular and non-spherical particles, which is known to have a negative effect to the flowability of the powder, as well as to the density and mechanical properties of the laser sintered parts. In addition, the particle size distribution was found to be larger than the suggested particle size range for the SLS. This can affect to the surface finish and the density of the produced parts. (Bai et al. 2016)

The melting and crystallisation behaviour of the PE powder can be determined using the differential scanning calorimetry. Since the powder bed is generally heated close to the melting temperature of the material during SLS, processing material with more than one melting range is difficult, and thus fixed and controlled melting and crystallisation temperature peaks are preferred. However, if there are several peaks they should be in very close range. According to the DSC measurements conducted by Bai et al (2016), PE powder had single distinct melting and crystallisation peaks. (Bai et al. 2016)

When semi-crystalline polymer, such as PE, is heated above its melting temperature, the change from the solid state to a viscous liquid can happen quite fast. However, the higher level of volume change on cooling through the melting temperature causes semi-crystalline polymers to shrink. This shrinkage can cause distortion to the part and variation to the part dimensional accuracy. As discussed earlier, these kind of issues are usually greater for the semi-crystalline than amorphous polymers. By preheating and post-heating the polymer powder at the range of the sintering window, these issues can be minimized. When the cooling of the part happens slowly, the shrinkage will happen more evenly inside the part, and major part distortions can usually be avoided. A clear sintering window, and thus the temperature range between the melting and crystallisation peaks, helps to determine the right temperature for different steps during the processing of the parts. (Bai et al. 2016)

According to the literature, PE parts could be successfully laser sintered with a laser power from 3 W to 11 W with a 2 W interval. It was noticed that the increase to the laser power had effect to the geometry of the laser sintered parts. When higher laser powers from 7 W up to 11 W were used, the parts showed obvious swell at the bottom of the part and further increasing the power caused the geometry to change from near square, to trapezoid, to semi-circular. The higher laser power allows the larger powder particles to melt more completely leading to the lower viscosity melt. This causes the flowability to increase and the melt to flow outwards causing the swollen bottom of the part. The heat of the next sintered layer could transmit to the first layer and accumulate there, causing further outwards flow and the expansion of the first layer. According to Bai et al. (2016), this could be a factor causing the irregularities to the geometry of the laser sintered parts. (Bai et al. 2016)

Further studies, by Bai et al. (2016), showed that with the lower laser powers of 3 W – 5 W, the dimensional accuracy of the parts was significantly better with much less swell. However, using the lower powers was also found to lead to porous and weak parts. The use of the double laser scan was introduced to solve this problem. With this method, each powder layer is scanned both in the vertical and horizontal directions. It is found that with the double laser scan the laser energy can be delivered more gradually to each layer, which enables greater definition and significantly reduced shrinkage. (Bai et al. 2016)

Mechanical tests, employed for the produced PE parts by Bai et al. (2016), showed variations with the different test specimens, even though they were built with the same laser. It was found, that the scanning order had significance. Parts that had a longer cooling time and a slower cooling rate, had better tensile properties and lower porosity. According to Bai et al. (2016), this can be explained with the molecular structure of the polymer. The long molecule chains have more time to rearrange at the high temperature when the cooling rate is slow, which usually increases the degree of crystallinity. The higher degree of crystallinity generally results in the lower molecular chain activity and porosity, enabling better tensile properties. (Bai et al. 2016)

Based on the finding of Bai et al. (2016), it is possible to produce well-defined polyethylene parts with precise laser sintering parameters. In addition, the laser energy input could be increased with the double laser scanning which also could increase the strength of the laser sintered parts and help to achieve a well-defined geometry. It also seems that with a slower cooling rate, stronger sintered parts can be produced. (Bai et al. 2016)

5. MATERIALS AND METHODS

This chapter presents the materials and the different analysis and test methods that have been used in this study. Three different polypropylenes and one polyethylene were employed to this investigation, to determine and compare their suitability to be used in the SLS. The characterisation of the different materials was performed to evaluate their suitability for the SLS and the parts produced with the SLS were tested for their mechanical properties.

5.1 Materials

This investigation includes four different polyolefin materials, three different polypropylenes and one polyethylene. One of the investigated polypropylenes PP-1 as well as the investigated polyethylene PE-1 are commercial materials for the injection moulding. Thus, they are provided in a granulate form. Two of the polypropylenes are commercial SLS powders provided by two different suppliers. PP-2 polypropylene powder, manufactured by Axalta, was acquired from Advanc3d Materials Gmbh and PP-3 polypropylene powder was acquired from Diamond Plastics Gmbh.

In addition to the four polyolefin materials, four different polyamides were investigated as well. Investigation regarding PA powders were conducted only with SEM, to compare the extrinsic properties of the investigated polyolefins to the commercially used PA powders. The investigated PA powders included fresh PA powder (PA-1), mixed PA powder with 50% refresh rate (PA-2), completely recycled PA powder (PA-3) and bad quality PA powder (PA-4) that does not work in the SLS anymore. The unsuitability of the PA-4 powder was determined based on its insufficient flowability in the SLS machine.

5.2 Powder production and characterisation methods

Different measurements and analyses were made to investigate the different properties of the different materials, and thus their suitability to be used in the SLS. In the thermal analysis, differential scanning calorimetry as well as thermogravimetric analyses were carried out to understand the melting and crystallisation behaviour as well as the thermal degradation behaviour of the investigated materials. In addition, rotational rheometry measurements were made at different temperatures to understand the melt flow behaviour of the materials. Furthermore, an analysis regarding the powder particles, their size and shape, were conducted using a scanning electron microscope.

5.2.1 Cutting mill

Two of the investigated materials were provided in a granulate form, and thus needed to be converted into fine powders. A cutting mill, with different sieve sizes, was used to pulverize these materials. Liquid nitrogen was used to cool the material before grinding to ensure the brittle behaviour of the material, as well as to delay the heating of the equipment during grinding. Figure 5.1 presents the cutting mill equipment that was used in this study.

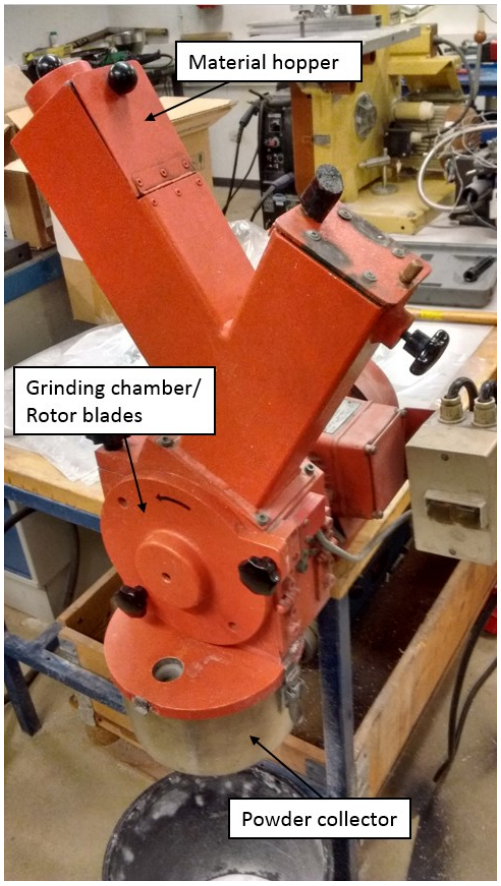

Figure 5.1. *The cutting mill equipment used to pulverize materials from granulate form into fine powders.*

Cutting mill uses cutting and shearing forces to achieve the size reduction. The material is fed through a hopper from where it passes to a grinding chamber. Material is comminuted into a smaller size between the stationary cutting bars and the rotor blades. After the material has comminuted into a suitable size, it passes through the sieve at the bottom of the equipment and into a powder collector. The sieves sizes of 1.5 mm and 1 mm were used in grinding to achieve coarse powders and the sieve sizes of 500 µm and 250 µm were used to achieve fine powders.

5.2.2 Differential scanning calorimetry

A differential scanning calorimetry (DSC) is a thermal analysis method which measures the difference between the rate of the heat flow into a specimen and a reference specimen as the function of temperature and/or time. During this measurement, both the specimen and the reference are in a specific atmosphere and subjected to the same controlled temperature program. DSC can be used to examine for example materials physical transitions, such as melting and crystallisation as well as chemical reactions, the stability to oxidation and the heat capacity. (Finnish Standards Association 2016)

As have been discussed earlier, knowing the materials sintering window is important in SLS and the sintering window can be determined based on the melting and crystallisation peaks presented in the DSC curve. The DSC measurements for the investigated materials were carried out to determine the melting and crystallisation behaviour of the materials. Measurements were performed with Netzsch DSC 204 F1. The temperature range for heating was set from -20 °C to 220 °C and for cooling from 220 °C to room temperature. The heating and cooling rates were set to 10 °C/min.

5.2.3 Thermogavimetric analysis

A thermogravimetric analysis (TGA) can be used to determine the temperature and the rate of the decomposition of polymers. Generally, the mass of the test specimen changes due to decomposition, oxidation reactions or the volatilisation of a component and this change in mass is recorded as a thermogravimetric curve. This thermogravimetric data can be used to estimate the thermal stability of the material as the change in mass as the function of temperature and the extent of the change serve as indicators to the thermal stability. (Finnish Standards Association 2014)

The thermogravimetric analysis was performed based on the standard ISO 11358-1, which is applicable to liquids and solids, and thus suitable for powders. Measurements were carried out in dynamic mode and in nitrogen atmosphere. In dynamic mode, the mass change versus temperature or time is investigated under a programmed conditions. Thermogravimetric analyser Netzsch STA 409 was used to determine the onset degradation temperatures for the investigated materials. The temperature range for measurements was set from 55 °C to 900 °C with the 10 °C/min heating rate.

5.2.4 Rotational rheometry

Different kind of rheometers are used to measure different rheological properties. A Rotational rheometer can be used to measure the viscosity as well as stress coefficient functions as the functions of shear rate and temperature. There are different geometries that can be used in the measurements, such as the cone-plate and parallel-plate. However,

since the cone-plate system provides a constant shear rate in the conical gap, it is preferred in the most cases. (Osswald & Rudolph 2015 p. 187,191, 195)

As discussed earlier, the flow behaviour during the laser sintering can be described with the zero shear viscosity, which can be determined by extrapolating the plateau region of the flow curve to zero shear stress or strain. (Fiedler et al. 2007) The flow behaviour of the different investigated materials was determined using rotational rheometer Anton Paar MCR301 with a cone-plate system. The measurements were carried out at three different temperatures: 170 °C, 190 °C and 210 °C with the shear rates from 0.1 to 100 1/s.

5.2.5 Scanning electron microscope

A scanning electron microscope (SEM) uses the focused beam of electrons to produce the images of the sample. The images are formed when the high energy electrons generate the variety of signals when interacting with the atoms of the specimen. SEM can be used to examine the samples external morphology, chemical composition and crystalline structure. In addition, it is possible to analyse selected point locations on the sample, for example, when determining the chemical compositions with the energy-dispersive x-ray spectroscopy (EDS). Samples that are insulating materials need to be coated with some conductive materials before the SEM analysis, most commonly with carbon or gold. (Swapp 2017)

SEM was used to determine the extrinsic properties, such as particle size, particle morphology and particle size distribution, for the investigated SLS powders. In addition, EDS was used to determine the elemental composition for some powders. Samples were prepared by attaching the powders to the specific sample holders equipped with a carbon tape. Since the investigated powders are electrically insulating materials, they were coated with gold before the SEM analysis. To ensure the dryness of the samples, they were held in a desiccator over night before coating them with gold. After coating, the samples were held in the desiccator again over night before the SEM analysis. Scanning electron microscope Zeiss ULTRAplus and Scanning electron microscope Philips XL-30 were used for the SEM analyses.

5.3 SLS equipment

Evaluations for the powder flowability and the production of the test specimens with a SLS equipment were conducted with a collaboration with Aalto University and with Materflow Corporation. Both of these facilities provided their own equipment and staff for managing the use of their equipment.

The SLS equipment at Aalto University has been built by the students, and thus the machine has adjustable parameters. Powder chamber size for the equipment is 300×300×200 mm and the temperature inside the chamber can be adjusted between 100-

150 °C. The equipment uses CO_2 laser with the maximum capacity of 100 W, but usually the laser is used with about 20% capacity. The layer thickness can be varied from less than 200 µm to several millimetres. The flowability of powders PP-1 and PP-2 was evaluated at Aalto University by using different layer thicknesses, powder spreading speeds and powder bed temperatures. Furthermore, a silica based additive was used to improve the flowability of the PP-2 powder.

Materflow uses EOSINT P 395 SLS equipment manufactured by EOS. Maximum part size with this equipment is 330×330×620 mm. It is possible to use the layer thicknesses of 0.1 mm, 0.12 mm and 0.15 mm. The equipment uses CO_2 laser with 20 W power. Three batches of tensile specimens were produced at Materflow by using different energy densities to evaluate the optimal energy density for the experimented material PP-3. The same silica based additive that was used at Aalto University, was used also at Materflow to improve the powder flowability.

5.4 Test methods for the test specimens

The properties of the parts produced with the SLS technique were analysed using different test methods. The tensile properties were determined with tensile testing and the porosity and sintering quality were analysed with SEM. Analysation includes the three batches of tensile specimens produced with three energy density levels. Furthermore, some tensile specimens were also built in different build directions.

5.4.1 Tensile test

The tensile properties of the test specimens can be determined with the tensile test. With this method, the tensile strength, tensile modulus as well as other stress/strain relationship aspects can be determined under defined conditions. The test is performed by extending the test specimen along its major longitudal axis at a constant speed until the specimen fractures or until some pretermined value of stress or strain is reached. The load and the elongation are measured during this procedure. (Finnish Standards Association 2012)

A mechanical tensile testing machine Instron 5967 was used to determine the tensile properties of the SLS specimens. The modulus, tensile stress at break as well as extension at break were determined based on the tensile measurements. Test speed was set to 20 mm/min and the power sensor of 30 kN was used for the measurements. The dimensions of each specimen were measured before the testing.

5.4.2 Sintering quality and porosity evaluation

Some estimation about the sintering quality and the porosity of the parts produced with SLS could be determined based on the SEM images. For this evaluation, the fracture surfaces of the tensile specimens were analysed with SEM and the acquired SEM images

were analysed using the programme ImageJ. Suitable samples were cut from the tensile specimens and similar sample preparations were conducted as with the powder samples for SEM. Thus, samples were coated with cold and held in a desiccator overnight, before and after the coating, to ensure the dryness of the samples. Scanning electron microscope Philips XL-30 was used to obtain the SEM images for this evaluation.

6. RESULTS AND DISCUSSION

This chapter presents the results and observations made during the experiments presented in Chapter 5. Test results for the powder characterisation, the flowability evaluation and the test specimens are presented separately.

6.1 Production and characterisation of the SLS powders

This subchapter includes the powder production from granulates to powders as well as powder characterisation measurement results. Commercial polypropylene powders PP-2 and PP-3 were provided in a powder form with a suitable particle size, and thus they were not processed with the cutting mill. In addition, Subchapter 6.1.5 offers some comparison between the investigated PP powders and the commercially used PA powders.

6.1.1 Powder production

Some very fine powders could be achieved with the setup described in Subchapter 5.2.1. However, grinding process itself was very ineffective and slow. The heating of the equipment during the grinding caused severe problems. Even though the material was cooled before grinding, it heated up relative quickly during grinding to a point where it started to melt. At that point, grinding chamber had to be unloaded from the hot material and replaced with a cooled material. The constant need to unload the hot material from the mill slowed down the process significantly.

If it would be possible to cool down the whole process, or more precisely the cutting blades and the chamber, it could be possible to obtain powder particles with the right size straight from the granulates. However, since the cooling restricted only to the material before pulverizing, grinding was done in segments moving from coarser powder to finer powder by decreasing the sieve size. Every time the sieve was changed to a smaller size the material was cooled again in liquid nitrogen. Even though a relatively fine powder was obtained with this approach, the production of the powder was not very efficient since even with this setup, the overheating of the material could not be avoided.

It was realised that this method was not sufficient enough to produce very large amounts of the powder, and thus the grinding was focused to only one of the materials available in granulate form: PP-1. Decision was made based an assumption that polypropylene has better chance to succeed in the SLS than polyethylene. Literature evaluation supports this assumption. Enough polypropylene PP-1 powder was produced to be able to categorise it and compare it with other the powders as well as experiment its flowability in a SLS machine.

6.1.2 Thermal properties

Differential scanning calorimetry was used to find the sintering windows for the different powders. The DSC measurements were performed to all the investigated materials, including injection moulding grade polypropylene and polyethylene as well as commercial polypropylene SLS powders from Advanc3d Materials Gmbh and Diamond Plastics Gmbh. The DSC curve of polyethylene PE-1 is presented in Figure 6.1 and it shows that the melting and crystallisation peaks are very close together, which indicates a narrow sintering window.

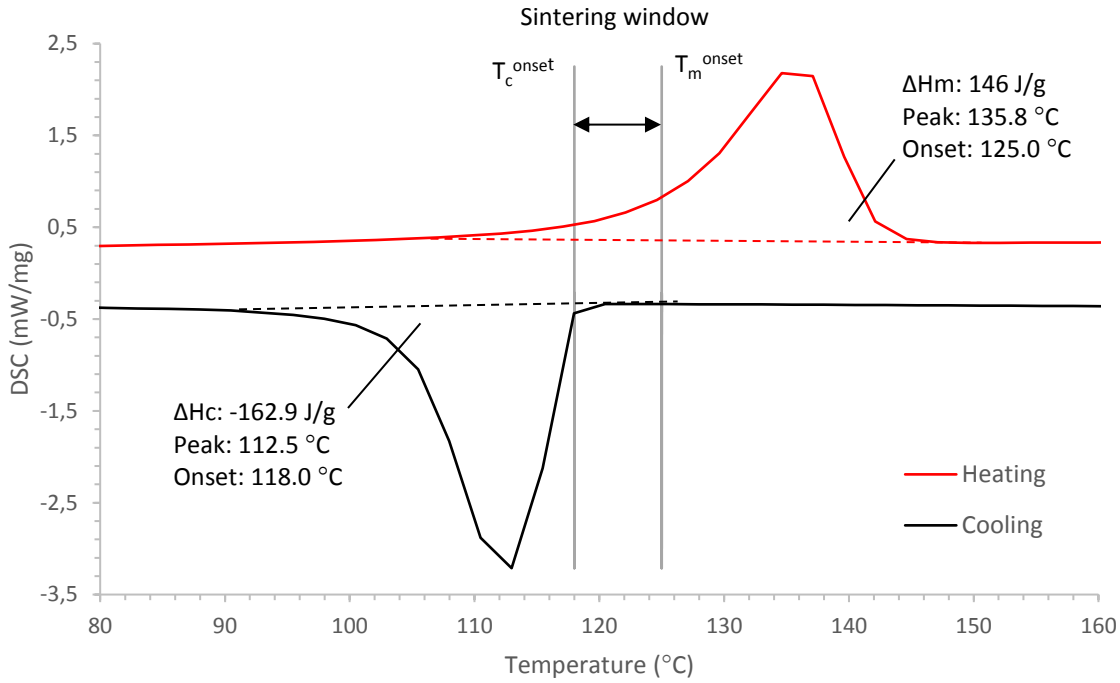

Figure 6.1. *DSC curve for the Polyethylene PE-1.*

Based on the onset melting and crystallisation temperatures shown in Figure 6.1, the sintering window for polyethylene PE-1 is only 7 °C. Wegner (2016) has investigated PE grade with the sintering window of 11.2 °C. According to his study, it was possible to process that grade of PE with SLS with only little warping. However, as discussed in the second chapter, a narrow sintering window can make laser sintering very difficult due to the increased risk of part distortions caused by the early crystallisation thus shrinkage. As the sintering window for polyethylene PE-1 is even lower than the PP grade investigated by Wegner (2016), it was decided to be discarded from further inspection based on its too narrow sintering window.

Figure 6.2 shows the melting and crystallisation behaviour of PP-1 powder. The sintering window for this grade of polypropylene is 22.1 °C, which is superior compared to the sintering window of PE-1. Sintering window of PP-1 should be wide enough to be experimented in the SLS.

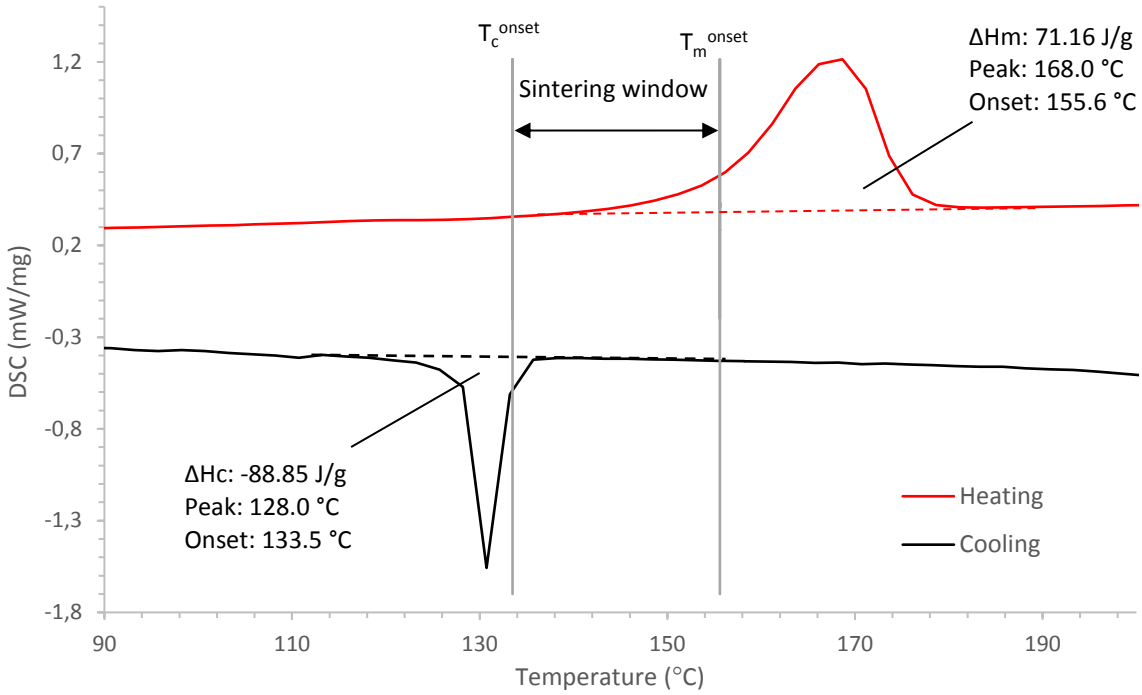

Figure 6.2. *DSC curve for the polypropylene PP-1.*

DSC curve for the commercially available polypropylene powder PP-2 is presented in Figure 6.3. According to the DSC curve, PP-2 has the sintering window of 35.1 °C. Thus, the sintering window of PP-2 is significantly wider than the sintering window of PE-1 and exceeds the sintering window of PP-1 as well.

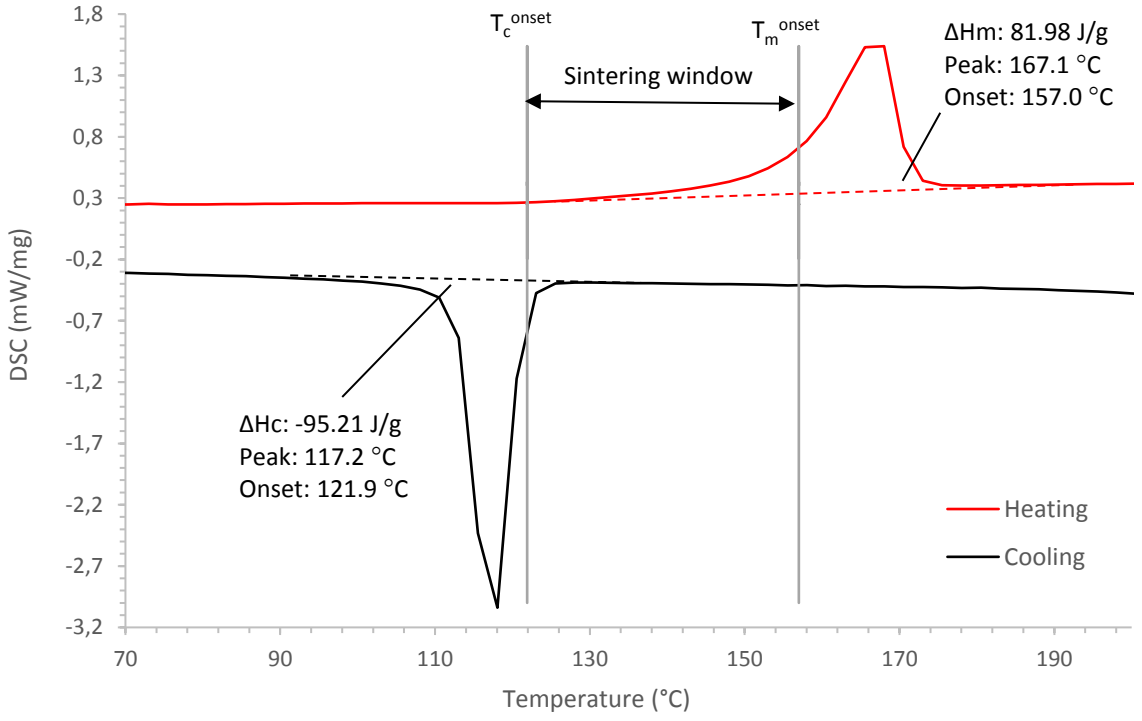

Figure 6.3. *DSC curve for the commercial SLS powder PP-2.*

DSC curve for the commercial polypropylene powder PP-3 is presented in Figure 6.4. According to the DSC curve, PP-3 polypropylene powder has the sintering window of 28.8 °C which is wider than for PP-1 but smaller than the other commercial SLS powder PP-2.

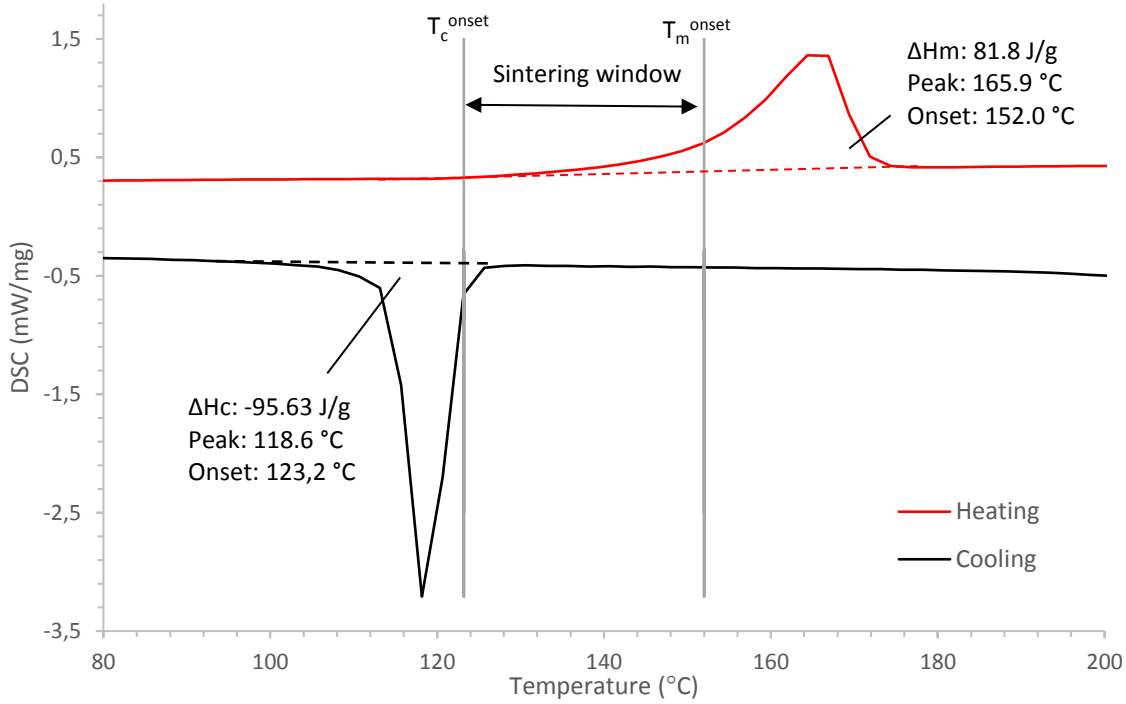

Figure 6.4. *DSC curve for the commercial SLS powder PP-3.*

Table 6.1 summarizes the peak and onset melting temperatures as well as the peak and onset crystallisation temperatures for all the investigated materials determined from the DSC measurements. The sintering windows for each material, calculated based on the onset melting and crystallisation temperatures, are also presented in Table 6.1.

Table 6.1. *Temperature related data collected from the DSC curves and calculated sintering windows for the investigated materials.*

Material	T_m onset (°C)	T_m peak (°C)	T_c onset (°C)	T_c peak (°C)	Sintering window (°C)
PP-1	155.6	168.0	133.5	128.0	22.1
PP-2	157.0	167.1	121.9	117.2	35.1
PP-3	152.0	165.9	123.2	118.6	28.8
PE-1	125.0	135.8	118.0	112.5	7.0

Study conducted by Fiedler et al. (2007) showed that sintering window for different PP grades can vary from 17.5 °C to about 34 °C. In addition, Wegner (2016) has studied a PP grade with the sintering window of 27.3 °C. PP grades investigated in current study

fall in the same range as with the other studies and the PP grade PP-2 even exceeds the highest value found in the other studies. Sintering windows of the investigated materials can also be compared to the sintering windows of the commercially used PA powders which are found to be around 32 – 34 °C (Fiedler et al. 2007; Bourell et al. 2014; Wegner 2016). Sintering windows of the investigated commercial PP powders are comparable to PA powders. Thus, the sintering window of PP-2 is even higher and the sintering window of PP-3 is only a little bit lower compared to commercial PA powders. However, the sintering window of PP-1 is somewhat lower compared to the PA powders.

Based on the DSC measurements, the processing of the commercial PP SLS powders is probably easier in the SLS process compared to the PP-1 polypropylene grade, at least in the thermal point of view, due to the wider sintering windows. Thus, with wider sintering window small fluctuations to the temperature can usually be accommodated without significant distortions.

The degree of crystallinity is also an important property which can be determined from the DSC curve. The melting enthalpy of the investigated polymer material can be compared to the enthalpy of 100% crystalline polymer material, and thus the degree of crystallinity can be calculated using following equation

$$C\% = \frac{\Delta H_m}{\Delta H_m^0} \cdot 100\%, \tag{3}$$

Where ΔH_m is the melting enthalpy determined from the DSC curve and $\Delta H_m{}^0$ is the literature value for the melting enthalpy of the 100% crystalline material. The values of the melting and crystallisation enthalpies for the different powders and degrees of crystallinity for these powders, calculated with equation (3), are presented in Table 6.2. For 100% crystalline polypropylene theoretical melt enthalpy is 209 J/g (Wypych 2012, p. 481) and for 100% crystalline polyethylene it is 295 J/g (Wypych 2012, p. 150-151). However, the estimation of the melt entaphy of 100% crystalline polymers is difficult and there are some differences in the values depending on the reference.

Table 6.2. *The melting and crystallisation enthalpy values and the degrees of crystallinity of the different investigated materials.*

Material	ΔH_m (J/g)	ΔH_c (J/g)	Degree of crystallinity (%)
PP-1	71.16	-88.85	34.05
PP-2	81.98	-95.21	39.22
PP-3	81.8	-95.63	39.14
PE-1	146.0	-162.9	49.49

The PP grades investigated by Fiedler et al. (2007) had the degree of crystallinity from 45% to 55%. However, all the PP grades investigated in current study had the degree of crystallinity below 40% and only the investigated PE grade had the degree of crystallinity close to 50%. This indicates that processing of the PP grades investigated in this study could be easier than the PP grades investigated by Fiedler et al. (2007). However, as discussed earlier, the degree of crystallinity affects both the SLS processability and the final part properties. The high degree of crystallinity usually results in higher shrinkage and lower ductility but also lower porosity and better tensile properties (Goodridge et al. 2012; Bourell et al. 2014; Bai et al. 2016).

The onset temperature for the thermal degradation was determined with the TG analysis. Figure 6.5 presents the mass loss as the function of temperature for all the investigated polypropylene materials where the temperature, where thermal degradation occurs, can be seen.

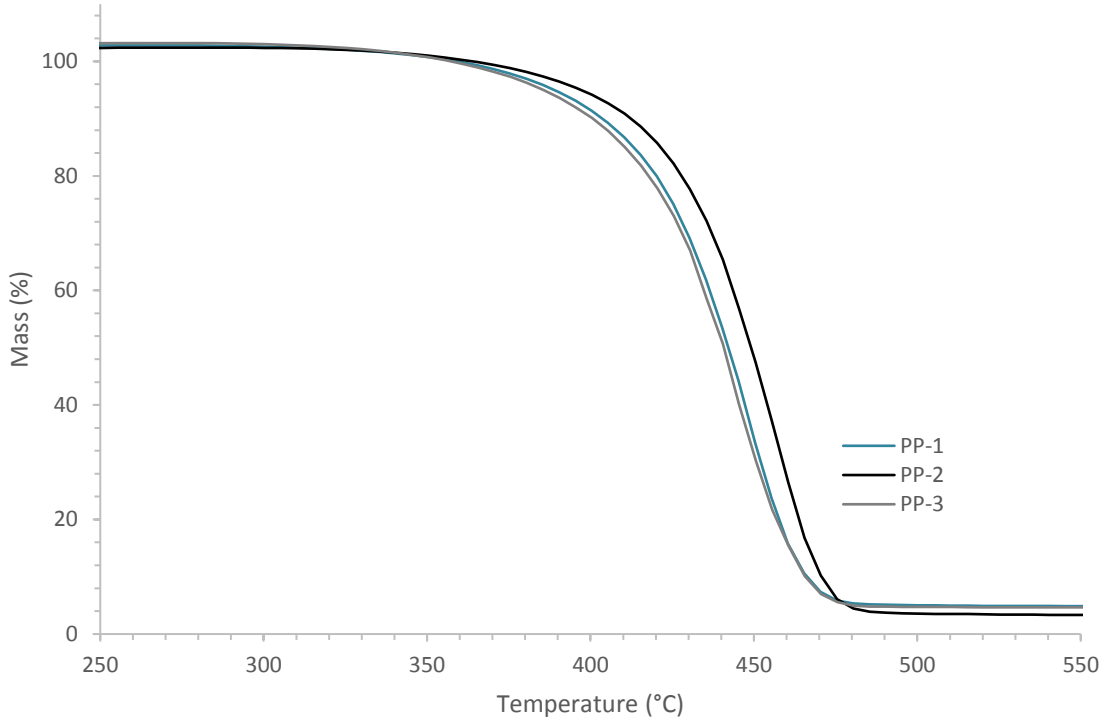

Figure 6.5. *Thermogravimetric analysis for the PP-1, PP-2 and PP-3 powders.*

Onset degradation temperatures for the investigated materials are presented in Table 6.3. The degradation temperatures for all of these materials are above 400 °C and in very close range with each other, especially PP-1 and PP-3. PP-2 has slightly higher degradation temperature compared to the other two powders. Fiedler at al. (2007) investigated PP grades with thermal degradation temperatures from 450 °C to 455 °C, which are higher than the values found in current study. However, all the investigated PP powders should have sufficient thermal balance to be used in SLS, since the temperatures should never rise as high as above 400 °C in the SLS process, at least not in the case of polymers.

Table 6.3. *Onset degradation temperatures for the investigated materials.*

	PP-1	PP-2	PP-3
T_{onset} (°C)	411	421	409

The characterisation of the thermal properties show that the investigated polyethylene material was not suitable to be used in the SLS. However, all the investigated polypropylene materials have sufficient thermal properties and shall be investigated further.

6.1.3 Rheological properties

Figure 6.6 shows the estimated zero shear viscosities for different polypropylene materials at different temperatures. Zero shear viscosities are determined based on the plateau regions of the flow curves presented in Appendix A. Based on the rheological measurements, PP-1 has the highest viscosity at every measured temperature. Especially significant difference can be seen at the temperature of 170 °C, which is also closest to the actual sintering temperature. In higher temperatures, the difference is not that severe but still quite significant. Commercial powders have similar viscosities with each other but, it can be seen that PP-3 has slightly lower zero shear viscosity values at every measured temperature compared to PP-2.

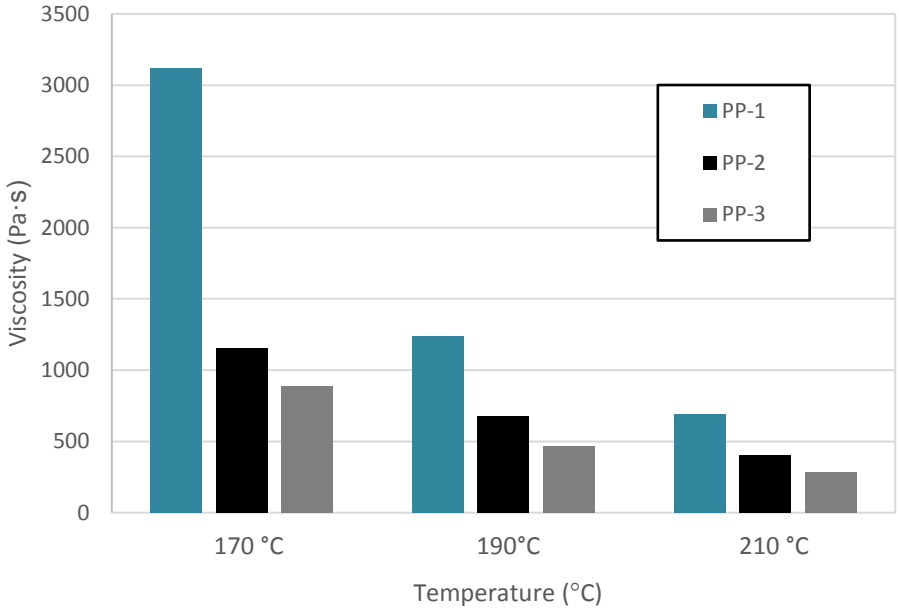

Figure 6.6. *The zero shear viscosities of PP-1, PP-2 and PP-3 at different temperatures.*

Numerical values for the zero shear viscosities of the investigated materials PP-1, PP-2 and PP-3 are presented in Table 6.4. Values are presented separately for all the measured

temperatures. Fiedler et al. (2007) measured the zero shear viscosities for different PP grades from 750 Pa·s to over 3500 Pa·s when measurement were made at the temperature of 180 °C. The PP grade with the zero shear viscosity over 3500 Pa·s at 180 °C was declared inadequate compared to other PP grades by Fiedler et al. (2007).

Table 6.4. *Numerical values for the zero shear viscosities of PP-1, PP-2 and PP-3 at different temperatures.*

Temperature (°C)	Zero shear viscosity (Pa·s)		
	PP-1	**PP-2**	**PP-3**
170	3121	1153	890
190	1241	674	465
210	692	401	284

Current study found that PP-1 has significantly higher zero shear viscosity compared to other investigated powders PP-2 and PP-3. However, the zero shear viscosity value of PP-1 is still lower than the highest measured value by Fiedler et al. (2007), even though the PP-1 powder was measured in lower temperature thus in 170 °C. However, the zero shear viscosity of PP-1 is still quite high and can cause problems to the coalescence of the powder melt. The commercial PP powders have significantly lower zero shear viscosities at every temperature compared to PP-1 and should not have major coalescence problems based on these measurements.

6.1.4 Extrinsic properties

An estimation about the particle size, particle size distribution and particle morphology were determined from the SEM images. Images were taken from every investigated PP powder using SEM Zeiss ULTRAplus. The analysation of the images was conducted with the programme ImageJ. However, due to the elongated structure of the grinded PP-1 powder, the determination of the particle size distribution for that powder was relative difficult and could not be done using automated analysis methods. On the other hand, some estimation could be performed by manually collecting particles from the image and calculating some estimation from that data. Due to the elongated structure some average diameters could only be determined. PP-2 as well as PP-3 had relative spherical morphology, and thus the particle size distribution should be determined from SEM images quite easily.

Figure 6.7 presents the SEM images of PP-2 powder with different magnifications. SEM images show that powder particles are relatively spherical in shape and roughly estimated in proper particle size range. For more precise size estimation programme ImageJ was used.

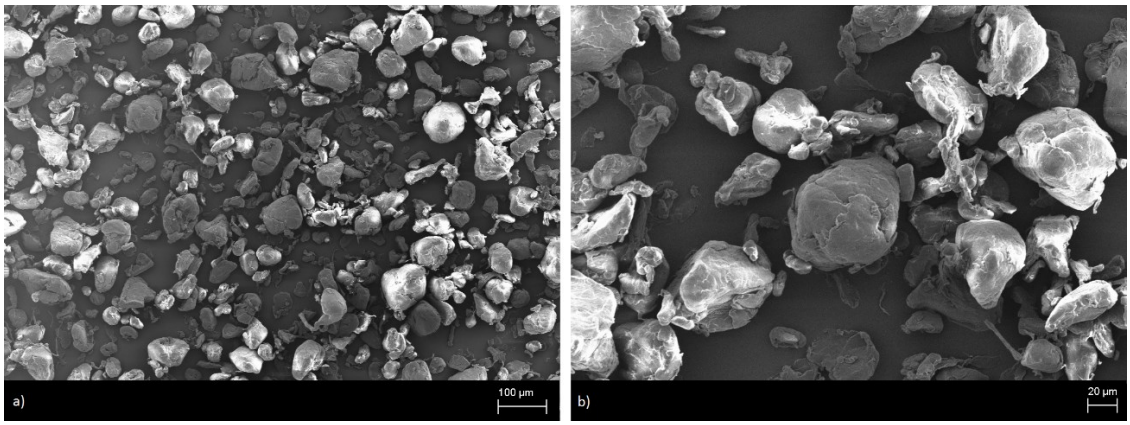

Figure 6.7. *The SEM images of the PP-2 powder with the magnifications of a) 100 µm and b) 20µm.*

Figure 6.8 presents the graphical estimation about the cumulative volume and number distribution for PP-2. Data for this graph was determined from the SEM images using ImageJ. The programme ImageJ can identify the areas of the powder particles. However, automated particle analysis neglected some of the particles giving inaccurate particle size distribution. More accurate determination could be made by manually selecting the areas of the particles. The diameters of the particles could then be determined with the assumption that the particles are spherically shaped. At least two images were analysed for each material to achieve reliable results.

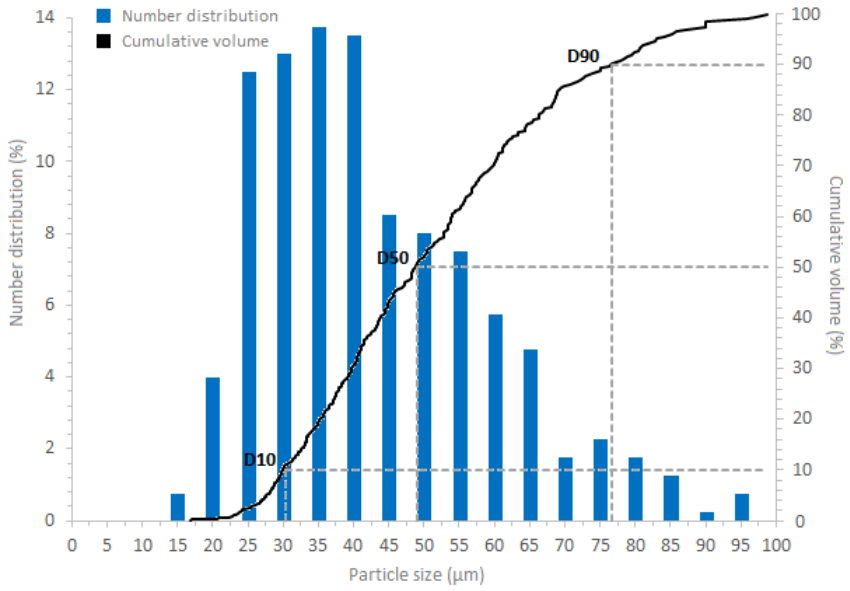

Figure 6.8. *Particle size analysis for the PP-2 powder.*

Figure 6.9 presents the SEM images of the PP-3 powder with different magnifications. The PP-3 powder particles are relatively spherical in shape and roughly estimated in proper particle size range. Compared to PP-2, PP-3 seems to have more small particles

especially on the surfaces of the larger particles. EDS was used to determine if the surface particles could be some additive. EDS results for PP-3 are presented in Appendix B.

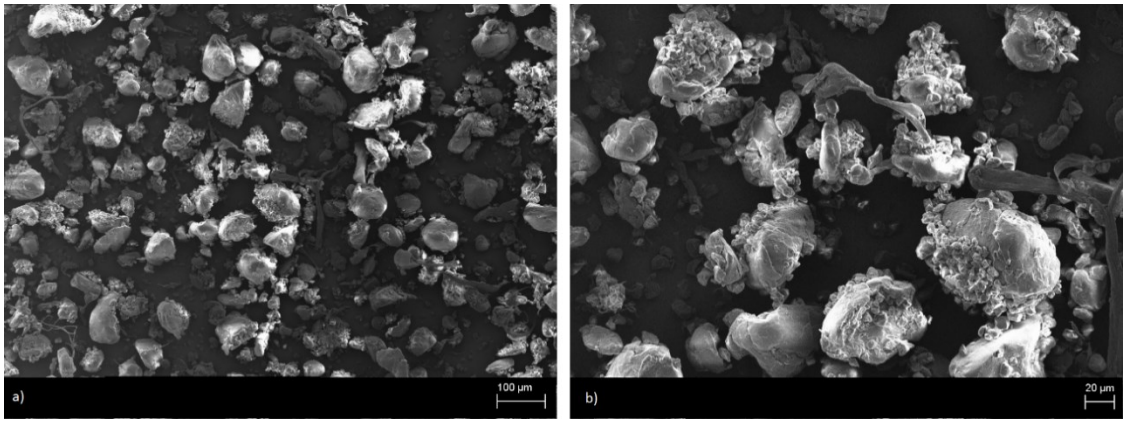

Figure 6.9. *The SEM images of the PP-3 powder with the magnifications of a) 100 µm and b) 20 µm.*

Based on the EDS, the inspected small particles on the surface of the larger powder particles could be some silica additive. This could also be probable because using additives, such as hydrophobic silica, is found to improve the flowability of some SLS powders (Lexow & Drummer 2016). According to the EDS, PP-3 contains 0.55 wt% of silica.

Figure 6.10 presents the graphical estimation about the cumulative volume and number distribution for the PP-3 powder. Like with the PP-2 powder, the data for this graph was determined from the SEM images using ImageJ.

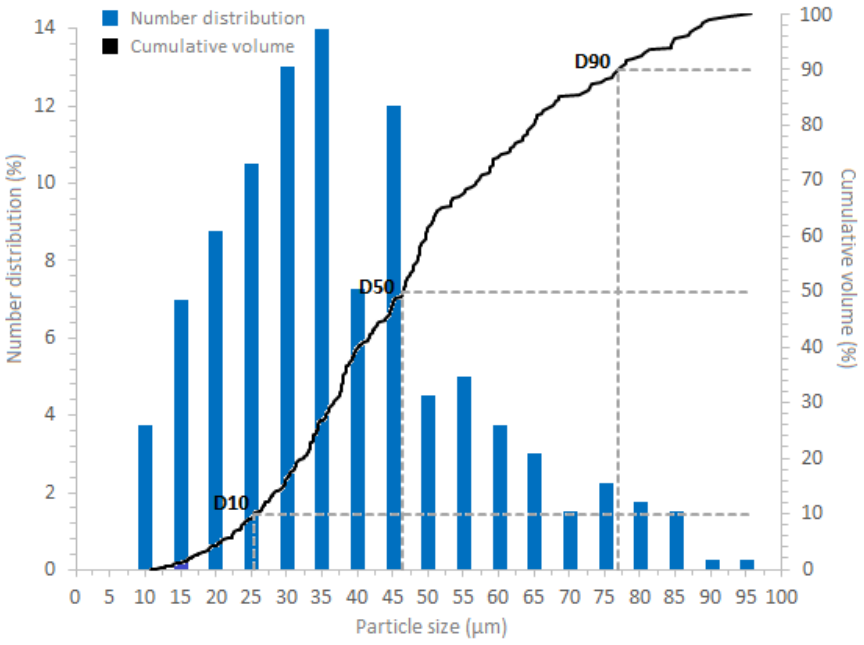

Figure 6.10. *Particle size analysis for the PP-3 powder.*

Table 6.5 summarises the particle properties for commercial PP SLS powders PP-2 and PP-3. If these commercial powders are compared with each other, it can be seen that the PP-3 powder includes more small particles than the PP-2 powder. However, the small silica additive particles can affect this analysis. Otherwise, these commercial PP powders are relatively similar in their particle size, size distribution and morphology.

Table 6.5. *The summary of particle size properties for PP-2 and PP-3 powders.*

	Particle size (µm)	
	PP-2	**PP-3**
Min	16.77	10.87
Max	98.77	95.64
Average	45.57	40.59
D10	30.29	25.39
D50	49.01	46.50
D90	76.64	76.95

Figures 6.11 and 6.12 present the SEM images of the PP-1 powder, grinded with the cutting mill, with different sieve sizes. Images show that the particle structure is very irregular. Due to the irregular structure of the particles, comparable particle size distribution with the commercial powders cannot be determined. However, some kind of estimation about the maximum and minimum particle sizes can be made. When making an estimation, it should be noted that due to the elongated structure, very long particles can go through the sieve during grinding. From the SEM image it can be inspected that particles, with diameters as high as 1.5 mm, can go through the sieve, if the diameter in the other direction is small enough.

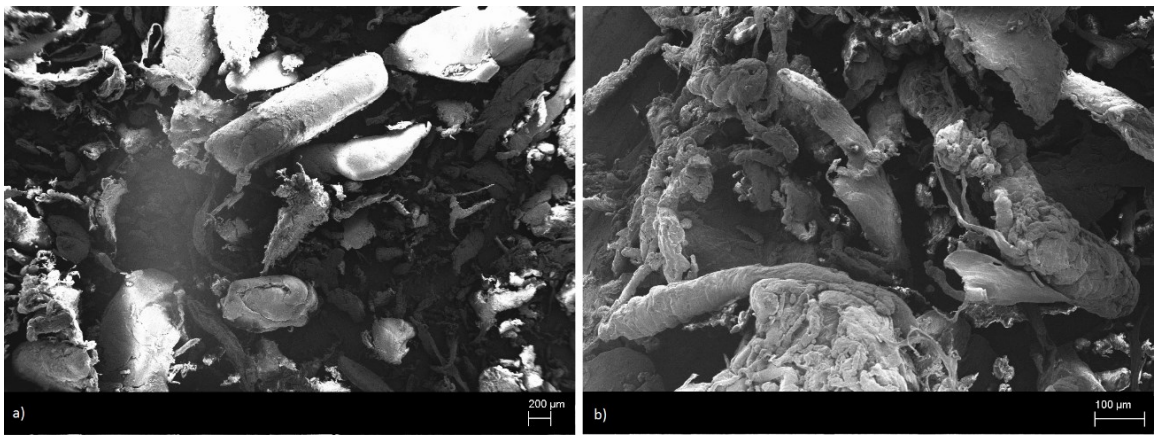

Figure 6.11. *The SEM images of the PP-1 powder grinded with 500 µm sieve with the magnifications of a) 200 µm and b) 100µm.*

Further sieving was used to see, if it could erase some of the undesired particles. Some improvement was achieved with sieving regarding the large particles, but the powder still contained a large amount of elongated particles. In addition, the amount of the powder collected with sieving was very small.

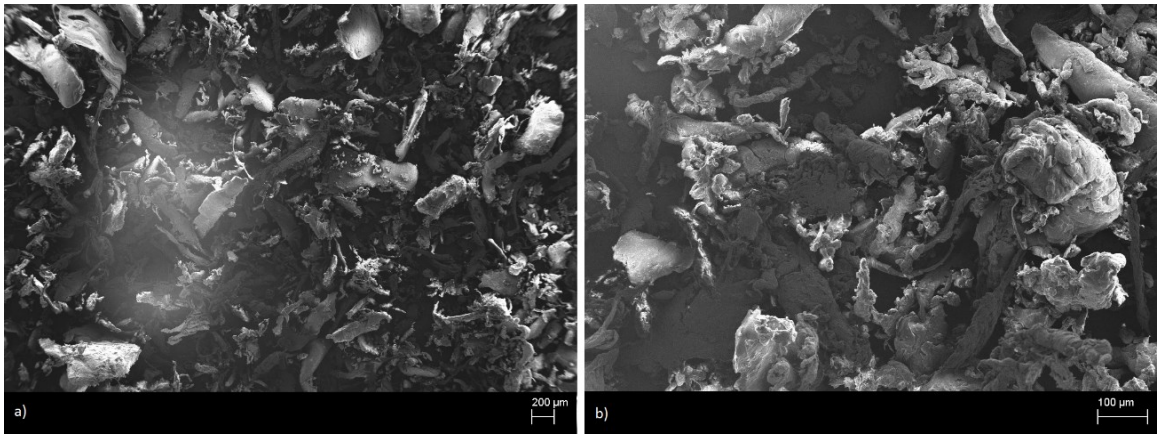

Figure 6.12. *The SEM image of the PP-1 powder grinded with 250 µm sieve, and then sieved with 112 µm sieve, with the magnifications of a) 200 µm and b) 100µm.*

Based on the SEM image evaluation, it would seem that the commercial PP powders have relatively good chances to work in the SLS. However, the grinded PP-1 is likely to have some severe flowability problems.

6.1.5 Comparison between PA and PP SLS powders

As discussed in Chapter 2.2.2, the extrinsic properties have a great effect to the processability of the powders in the SLS. The particle size and morphology determine the flowability and the packing of the powder particles thus they are very important properties to consider when SLS is used as a production method. Since PA powders are so widely used in the SLS it makes sense to compare them to the PP powders investigated in this current to offer some reference to the properties of the PP powders.

The SEM images of the polyamide powders were taken with SEM Philips XL-30 to offer some reference to the polypropylene powders. Four different polyamides were analysed with SEM: PA-1 that was a fresh powder, PA-2 that was a mixed powder with 50% refresh rate, PA-3 that was a completely recycled powder and PA-4 that was a bad quality powder that does not work anymore in the SLS. The SEM images of the PA powders are presented in Figure 6.13.

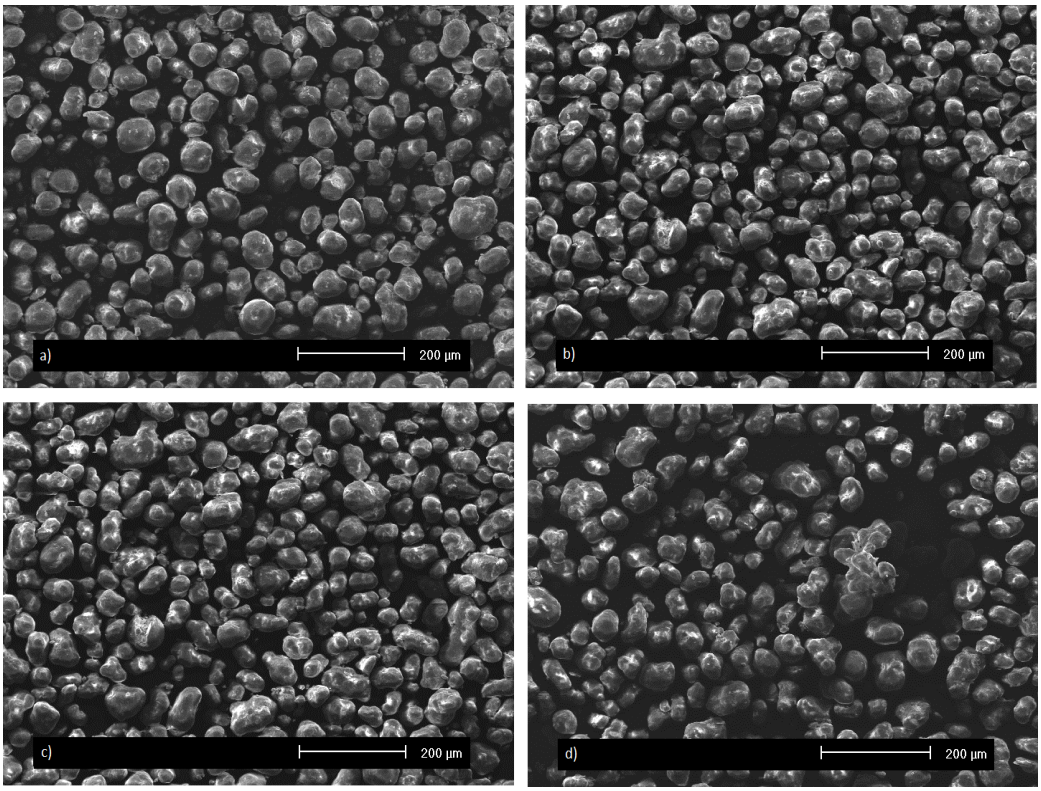

Figure 6.13. The *SEM images of the PA SLS powders a) PA-1 b) PA-2 c) PA-3 and d) PA-4.*

Table 6.6 summarizes the particle size properties for the different PA powders. Graphical presentations for determining these values are presented in Appendix C. Overall, it would seem that the particle size increases when moving from PA-1 to PA-4. In addition, the visual inspection of the SEM images show that the shape of the particles changes from spherical to somewhat irregular when fresh and used powders are compared. Furthermore, as seen in Figure 6.13 d), some clusters of the partly coalesced particles can be seen in PA-4 powder, which can be one reason why it does not work properly in the SLS anymore.

Table 6.6. *The Summary of the different PA powder properties.*

	Particle size (µm)			
	PA-1	**PA-2**	**PA-3**	**PA-4**
Min	14.05	26.18	27.91	34.22
Max	89.30	86.80	93.63	96.17
Average	49.02	51.25	54.13	58.14
D10	38.58	39.59	42.80	46.70
D50	51.11	52.71	55.21	59.45
D90	63.60	68.55	71.59	74.79

Figure 6.14 presents the SEM images of the commercial PP SLS powders PP-2 and PP-3 as well as PP-1 powder grinded with the cutting mill and PA-1 powder. Based on the SEM images it seems that PA-1 powder has only little variation in the particle size when commercial PP powders have quite much variation. In addition, PA seems to have smoother particle surfaces. Grinded PP-1 is not comparable to the other powders.

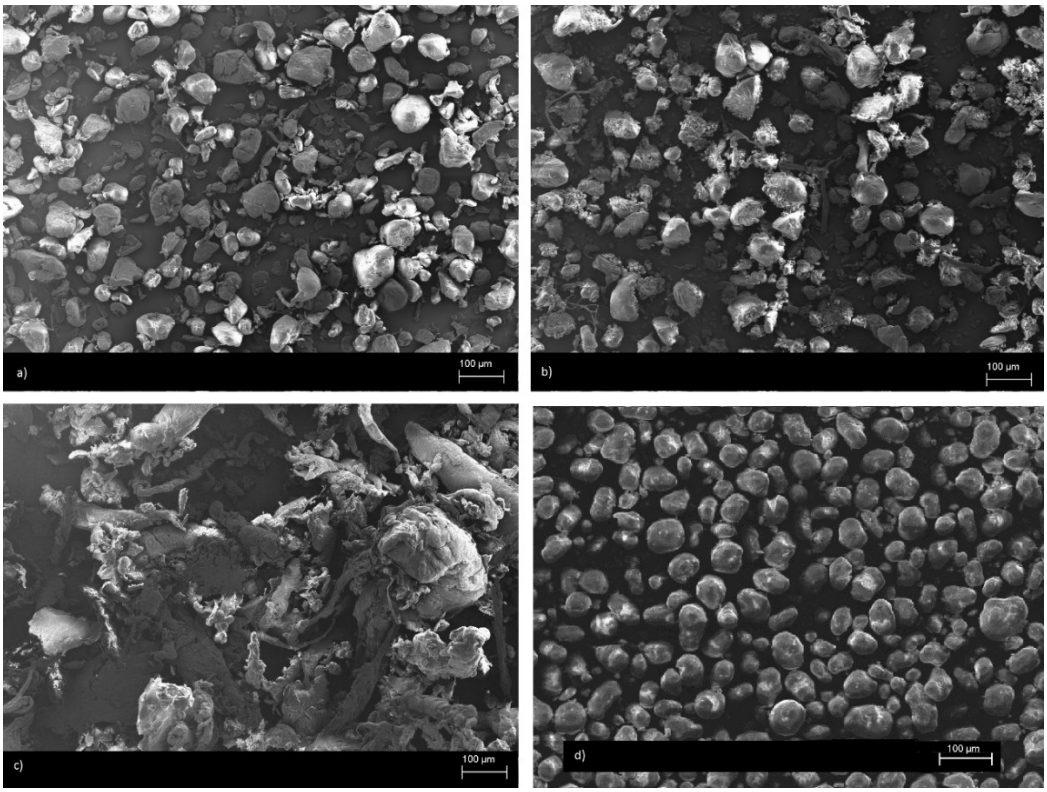

Figure 6.14. *The SEM images of the a) PP-2, b) PP-3, c) PP-1 and d) PA-1 powders.*

Figure 6.15 shows a graph where the particle size distribution of PP-2, PP-3 and PA-1 powders are compared. Table 6.7 combines the results regarding PA-1 powder particle properties and the properties of commercial PP SLS powders PP-2 and PP-3 that have been established earlier.

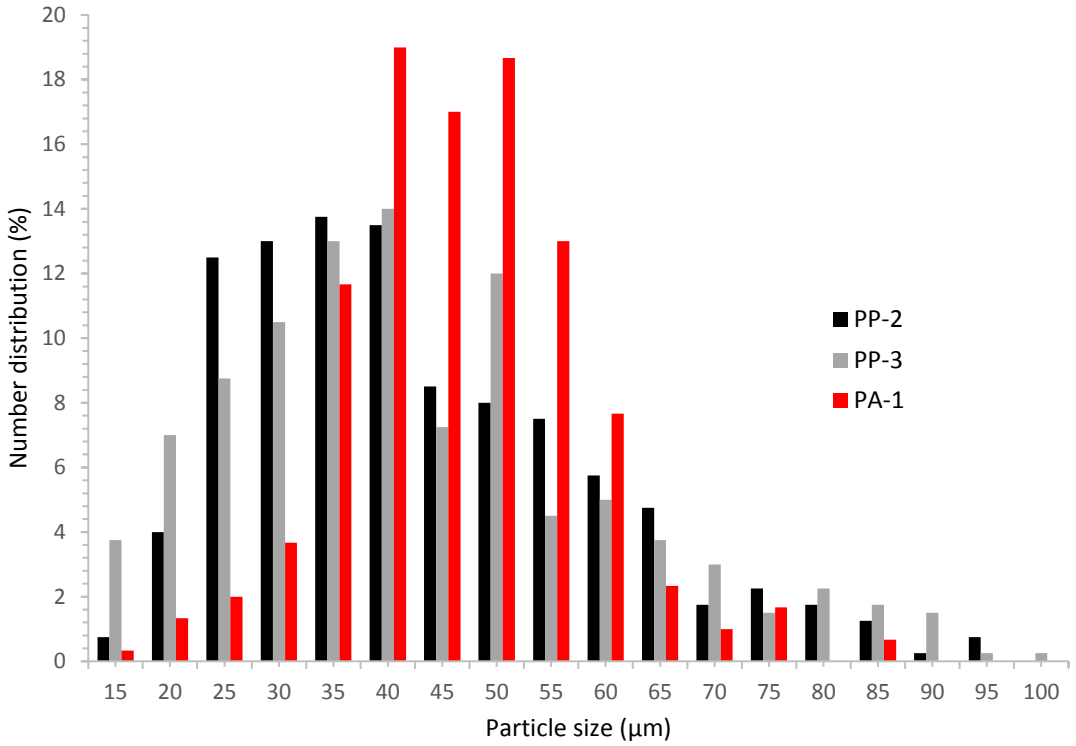

Figure 6.15. *The comparison of PP-2, PP-3 and PA-1 particle size distribution.*

If the PA-1 powder and commercial PP SLS powders, that are also fresh powders, are compared, it can be seen that PP powders have wider particle size distribution range thus they have more small particles but also more large particles. On the other hand, PP powders have smaller average particle size compared to the PA powders.

Table 6.7. *The comparison of the PA-1, PP-2 and PP-3 powder particle properties.*

	Particle size (µm)		
	PA-1	**PP-2**	**PP-3**
Min	14.05	16.77	10.87
Max	89.30	98.77	95.64
Average	49.02	45.57	40.59
D10	38.58	30.29	25.39
D50	51.11	49.01	46.50
D90	63.60	76.64	76.95

The fact that PP powders have more small particles can have a positive effect to the packing density, and thus the density of the laser sintered parts. However, as discussed earlier, small particles can also cause problems to the flowability of the powder due to the static forces as well as the fogging of the laser window and heat elements. In addition, the

faster coalescence of the smaller particles compared to larger particles can cause unwanted sintering next to the sintering area decreasing the part accuracy. Large variations in the particle size can also result in the porosity of the parts due to the incomplete melting of the large particles.

6.2 Evaluation of the powder flowability with SLS equipment

Since there was no suitable SLS equipment available at TUT for the laser sintering of polymers, some cooperation needed to be done with other facilities. Experiments with the SLS machine were performed at Aalto University and at Materflow. Both facilities made their own flowability evaluation, but this subchapter focuses on the experiments carried out at Aalto University. The experiments were conducted with the commercial PP powder PP-2 and with the grinded PP powder PP-1.

The effect of a silica (SiO_2) additive, which is known to improve the flowability of some powder materials, was evaluated to see, if it has any effect on the flowability of PP-2 powder. To find the optimal values for the processing parameters, different parameter combinations were evaluated as well. All the results and analysations that are presented in subchapters 6.2.1 and 6.2.2 are based on the experiments conducted by Aalto University.

6.2.1 Flowability evaluation for PP-1

Different layer thicknesses and recoating speeds were tested for the grinded PP-1 powder in attempts to achieve suitable flowability. The PP-1 powder could be spread on to the powder bed, however, not very smoothly. Significant amount of defects existed on the powder bed surface with every experimented layer thickness and recoating speed. Due to the defects and unevenness of the powder bed surface, it was not possible to use PP-1 powder in SLS, at least not in its current shape. This was expected due to the very irregular morphology of the powder. Figure 6.16. presents the powder bed of the PP-1 powder with the layer thickness of 1 mm, where holes and defects of several millimetres can be detected on the bed surface.

Figure 6.16.*The powder bed of the PP-1 powder with 1 mm layer thickness (provided by Aalto University).*

Some post treatments could be employed to improve the flowability of the grinded powder, as was discussed in Subchapter 3.1. However, as the grinding itself was so insufficient and the particle size of the produced powder was still too large, achieving the necessary requirements does not seem very likely. For future work, some other type of mill could be employed to see, if the required particle size could be achieved and if the morphology of the particles could be improved. As discussed in 3.1, rotor mill has been found to achieve relatively spherical particles with a suitable particle size.

6.2.2 Flowability evaluation for PP-2

The effect of the silica additive, to the flowability of the PP-2 powder, was evaluated by using constant parameters for the spreading of the powder and evaluating the defects formed on the surface of the powder bed. The defects were recognised by using a custom made mathlab script and image recognition algorithms, which detect the level of lighting, pixel by pixel, per each image. Threshold values were set to provide a sum of pixels, which were considered as “surface damage”. Lastly, the pixel values were converted to centimetres. Multiple pictures were used for the analysation to ensure reliable results. Figure 6.17 presents the differences with the flowability of the PP-2 powder with and without the silica additive, where the purple areas show the defected areas.

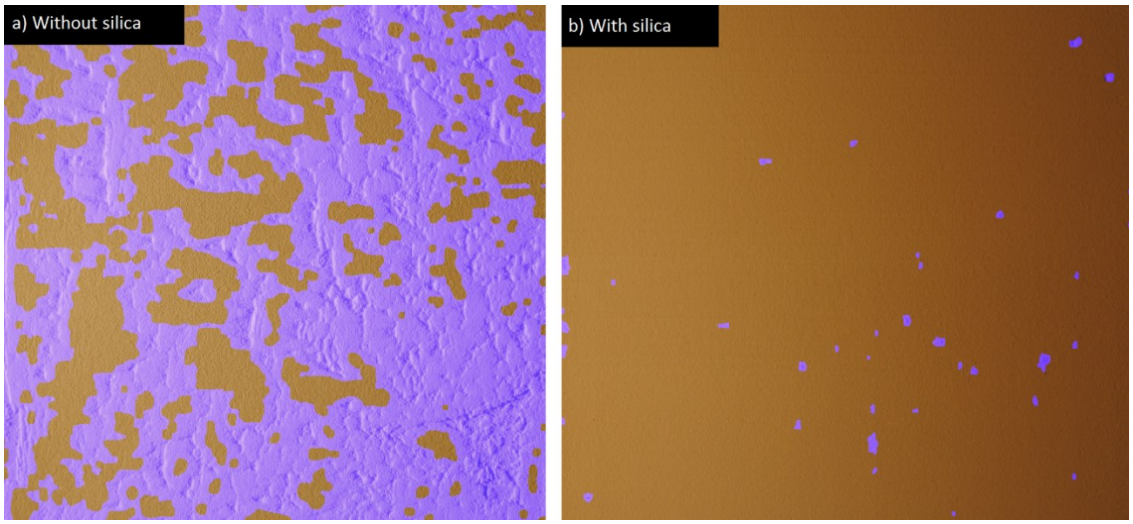

Figure 6.17. *Flowability evaluation for the PP-2 powder where the purple areas indicate defect on the surface of the powder bed a) without silica additive and b) with silica additive (provided by Aalto University).*

The flowability of the PP-2 powder improves remarkably when a specific amount of the silica additive is added to the powder. Figure 6.17 a) shows a significant amount of defects on the powder bed surface while Figure 6.17 b) shows only a little amount of small defects.

The flowability of the PP-2 powder was also experimented by employing different layer thicknesses, powder bed temperatures and recoating speeds and evaluating and comparing the defects formed to the powder bed surface. The defect areas were identified from multiple pictures to ensure reliable evaluation with the setup described earlier. These experiments were conducted both with and without the silica additive to be able to compare the effects of different parameters to the powder flowability and to see the effects of the silica additive to the different parameters.

Figure 6.18 presents average values for the effects of the different parameters to the flowability of the PP-2 powder. Average values are calculated based on several different measurements conducted with different parameter combinations, with and without the silica additive. The evaluation is made based on the defects formed on the surface of the powder bed thus smaller defects on the bed area value correlates with better flowability and larger defects on the bed area value correlates with inferior flowability.

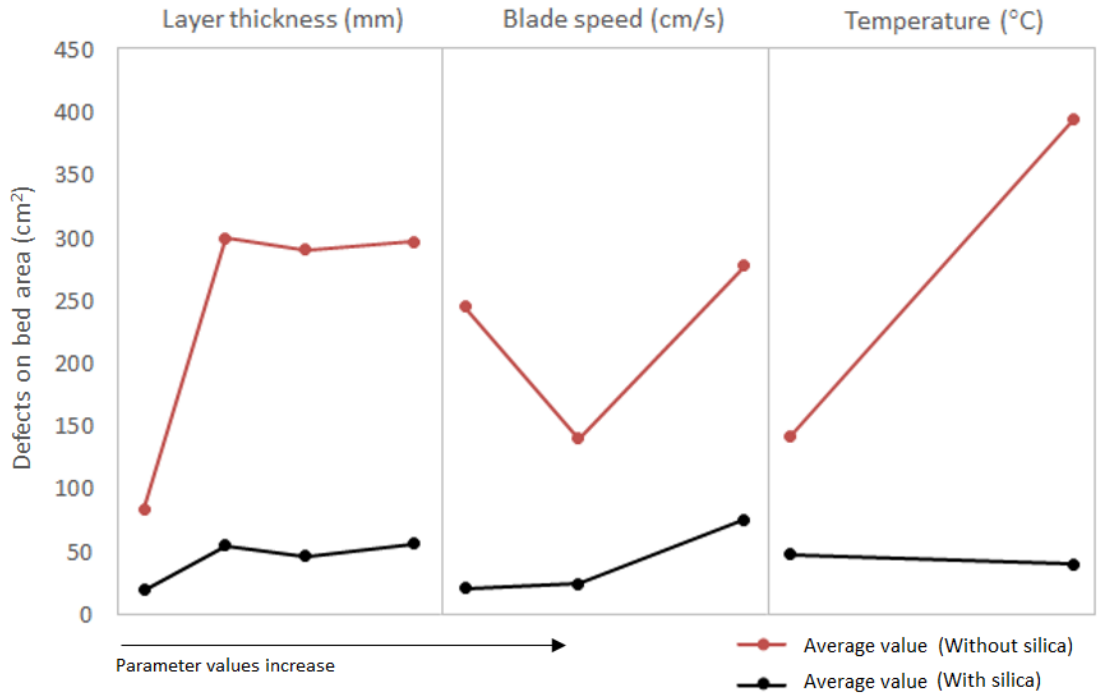

Figure 6.18. *The average values for the effects of the parameters to the flowability of the PP-2 powder with and without the silica additive presented as the area of defects on the bed area based on the data provided by Aalto University.*

Based on Figure 6.18, when there is no silica additive at use, a clear trend can be seen, where increasing the layer thickness and the temperature, increases the amount of defects on the bed surface, and thus diminishes the flowability. However, the further increase of the layer thickness do not seem to make much further difference. The diminishing effect to the flowability of the powder, caused by the temperature increase, can be due to the humidity decrease resulted from the temperature rise, and thus the forming of electrostatic charges. On the other hand, the decrease in the flowability can also result from the softening of the PP powder particles above their glass transition temperature since soft particles are more difficult to spread evenly than tough and solid particles. When the blade speed is evaluated, the increase of the blade speed first improves the flowability but further increase causes inferior flowability.

However, Figure 6.18 also shows that adding the silica additive improves the flowability of the PP-2 powder quite significantly. It can also be seen that the effects of the different parameters to the flowability of the powder are less significant when the silica additive is used. Increasing the layer thickness diminishes the flowability as does the increasing of the blade speed. On the other hand, increasing the temperature improves the flowability when the silica additive is used, which is the opposite reaction to the effect of temperature increase when the silica additive was not used. This can be due to the possible antistatic behaviour of the silica additive, which could decrease the negative effect to the flowability caused by the electrostatic charge, and thus improve the flowability. In

addition, the tough silica particles could help the PP powder particles to remain more rigid also in the higher temperatures. However, the effects of the process parameters with the silica additive are very subtle compared to the effects of the parameter modifications without the silica additive.

The effect of the silica additive, to the part properties, has not been reported in the previous studies. This can be due to the fact that it is impossible to produce parts with some powders without the silica additive, and thus it has not been possible to do the comparison between the parts with and without silica, as was also the case in the current study. However, it could be assumed that since the silica improves the flowability of the powder, and thus the packing density, also the mechanical properties would improve. In addition, the amount of the silica additive required to improve the flowability is very small. Based on flowability evaluation results and the assumption that the silica additive does not decrease the mechanical properties, the use of this additive is highly recommended at least for this specific material.

6.3 Test specimens

Both commercial PP powders PP-2 and PP-3 were evaluated for their flowability in a SLS machine at Materflow. However, similar data, as presented in the previous chapter for PP-2 powder, was not available for the experiments conducted at Materflow. According to their experiments, it was not possible to spread the PP-2 powder evenly enough to be able to use it for the part production. However, the PP-3 powder showed suitable flowability. Since there is not similar data available about the effects of different process parameters to the flowability of the PP-3 powder, it is assumed that the effects are similar as for the PP-2 powder studied in the previous chapter. PP-3 powder was used to produce tensile specimens at Materflow to evaluate the tensile properties of the products manufactured with the SLS.

Three batches of the specimens with different energy densities were produced to determine the optimal energy density level for the investigated material. Specimens were produced according to the standard ISO 20753. Energy density level can be calculated based on equation (2), and thus the energy density level was altered by changing the laser beam speed. Decreasing the laser beam speed increases the energy density. The first batch V1, with the lowest energy density, included eight specimens and the second batch V2, with the highest energy density, included ten specimens. The third batch V3, with middle energy density value, included 15 specimens, where seven specimens were produced in y-direction, four specimens in x-direction and four specimens in z-direction. Figure 6.19 shows the different build directions that were used for the production of batch V3.

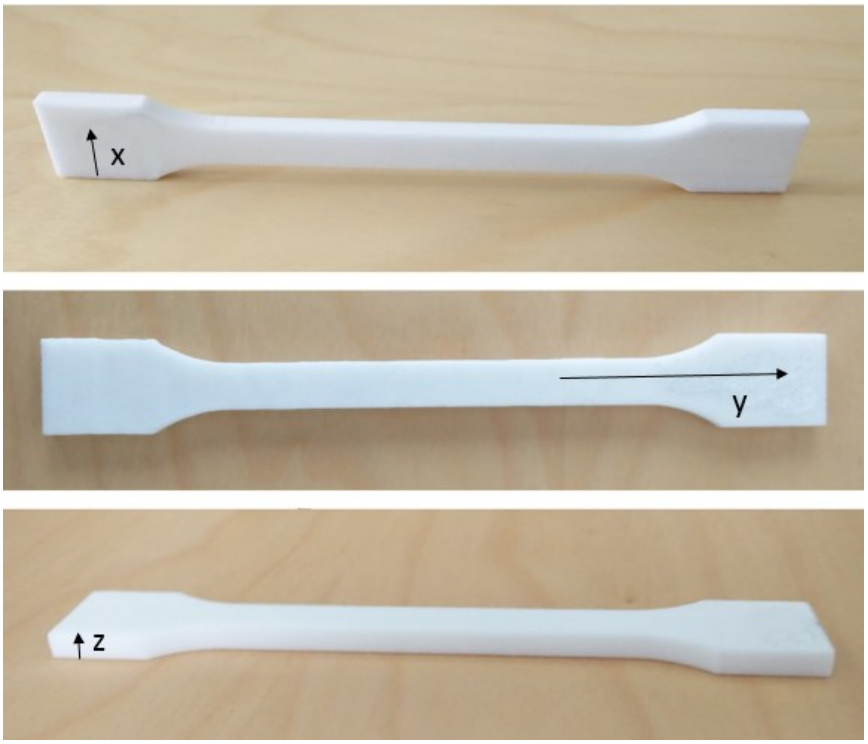

Figure 6.19. *The tensile specimens of batch V3 with different build directions.*

It was found during the experiments at Materflow, that changing the energy density and the powder bed temperature also affected the powder flowability in the SLS machine. With the highest experimented energy density level (batch V2), a smooth powder bed surface was achieved due to the easy spreading of the powder. With the second highest energy density level (batch V3) it was not possible to achieve as smooth powder bed surface than with the highest level, but the spreading was still sufficient. With the lowest energy density level (batch V1), the spreading was sufficient enough to produce some tensile specimens, but a clear difference could be seen to the other two energy density levels. Thus, batch V1 had inferior flowability compared to other two batches.

On the other hand, with the lowest energy density level, a little bit lower powder bed temperature was also employed, which could also be one reason for the varying flowability behaviour. It was noticed during the flowability experiments for PP-2 powder that by increasing the powder bed temperature, with the silica additive, the flowability subtly improves. These observations would indicate that the powders PP-2 and PP-3 respond similarly to the change in the powder bed temperature with the silica additive. The powder bed temperature for the batches V2 and V3 was the same.

Subchapter 6.3.1 presents the tensile test results that were conducted to the different batches of tensile specimens. In addition, subchapter 6.3.2 presents the evaluation of the sintering quality and porosity of some of the tensile specimens.

6.3.1 Tensile properties

The tensile properties of the test specimens were evaluated to understand their mechanical behaviour. Three different batches produced with different parameters were evaluated. In addition, in batch V3, the specimens were built in three different directions, which are evaluated separately. Figure 6.20 presents the average tensile test curves for all the batches and investigated build directions. Curves are presented as the stress as a function of the strain. Individual tensile test curves, for each measured tensile specimen, are presented in Appendix D.

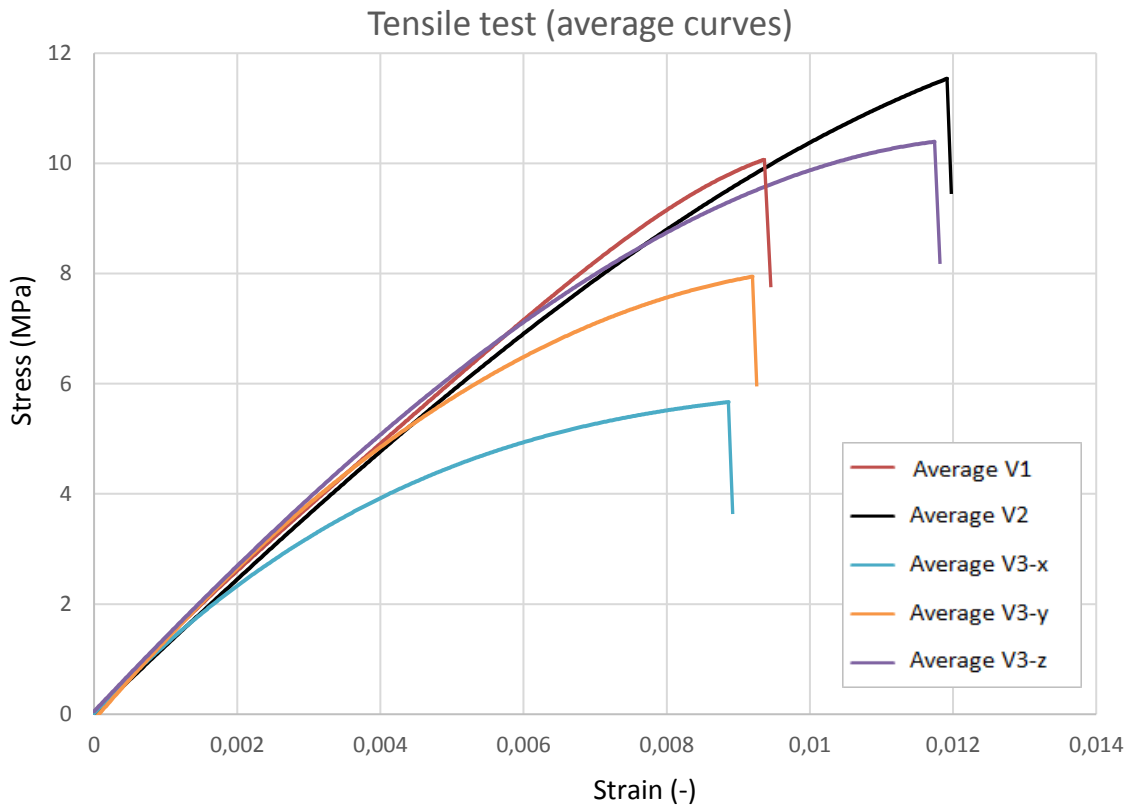

Figure 6.20. *The average tensile test curves for the different batches V1, V2, V3-x, V3-y and V3-z.*

Overall, the curves show that the specimens produced with SLS are very brittle since they break at quite low strains without yielding. Due to the brittleness of the specimens, it could be assumed that the specimens produced with SLS have quite high porosity. Porosity of the specimens will be evaluated further with SEM in the next subchapter.

Comparing the average curves of the batches V1, V2 and V3-z, which are the batches built in the same build direction, the effect of the energy density can be seen. To be able to see the effect of the energy density even more clearly, Figure 6.21 presents the tensile strength as the function of the energy density. The tensile strengths are presented as average values with their standard deviations.

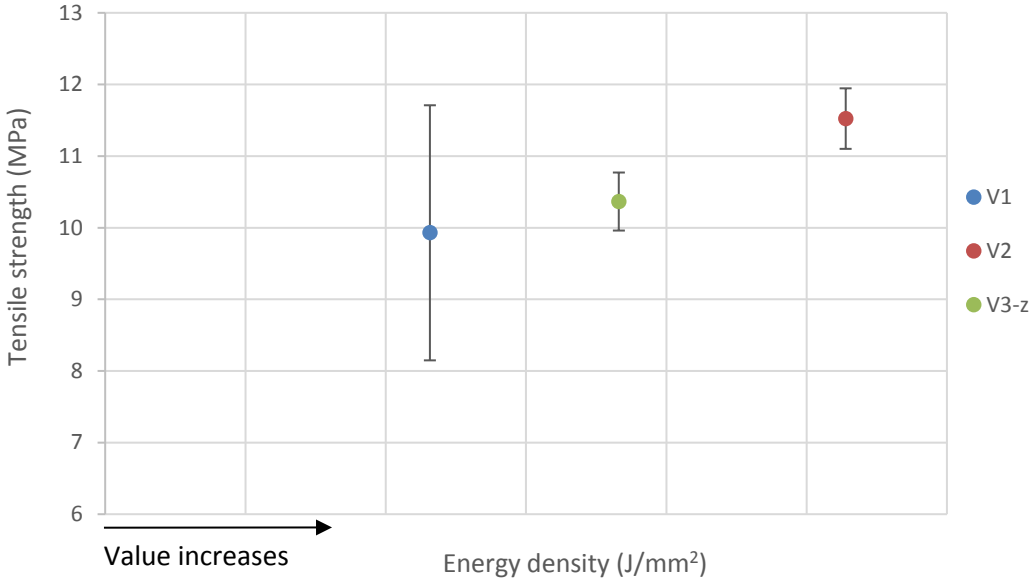

Figure 6.21. *The effect of the energy density to the tensile strength presented by the average tensile strengths with their standard deviations.*

From the Figure 6.21, it can be seen clearly that the highest experimented energy density results in the highest tensile strength (V2) and the lowest experimented energy density results in the lowest tensile strength (V1). Batch V3 had the energy density level between the values of V1 and V2, and it also had the middle tensile strength value. This corresponds to the previous studies conducted by Zhu et al. (2016), who also found that increasing the energy density increases the tensile strength to a certain point, from which the further increase to the energy density level decreases the tensile strength due to the thermal degradation. The point where the thermal degradation would decrease the tensile strength was not found in the current study, but the highest experimented energy density level gave the best tensile properties.

On the other hand, the build direction also has a significant effect to the tensile properties of the SLS parts. When the different build directions used for the batch V3 are evaluated, it is quite clear that the specimens produced in the x -and y-directions have inferior tensile properties compared to the specimens produced in the z-direction. Similar observations about the effect of the build direction have also been made in the previous studies (Caulfield et al. 2007; Jain et al. 2009; Wegner & Ünlü 2016). Furthermore, the scan pattern can affect to the tensile properties.

The average values for the modulus, tensile stress at break and elongation at break for the different batches with their standard deviations are presented in Table 6.8. Based on the average values, batch V2 has the highest tensile stress at break and elongation values. Results also show that the specimens built in x- and y-directions have significantly lower tensile stress at break values compared to the batches V1, V2 and V3-z.

Table 6.8. *The average values for the modulus, tensile stress at break and elongation at break with the standard deviations determined based on the tensile tests for the different batches.*

Batch	Modulus (MPa)	Tensile stress at Break (MPa)	Elongation at Break (%)
V1	816.87 ± 11.13	9.93 ± 1.78	0.94 ± 0.20
V2	773.23 ± 18.54	11.52 ± 0.42	1.19 ± 0.061
V3-z	851.03 ± 11.86	10.37 ± 0.40	1.11 ± 0.10
V3-x	784.60 ± 62.75	5.74 ± 1.03	0.89 ± 0.16
V3-y	826.82 ± 14.21	7.04 ± 0.99	0.85 ± 0.39

Individual tensile test measurements showed that there was significantly greater amount of variation between different specimens in batches V1, V3-x and V3-y compared to batches V2 and V3-z. For example for batch V1 the measured tensile stress at break varied from 7.5 MPa to 12.3 MPa. Furthermore, batches V3-x and V3-y had more variations in their tensile test results compared to batches V2 and V3-z.

Variation between batch V1 and batches V2 and V3 can be explained by the inferior powder flowability of the V1 powder, at least to some level. When there is variation to the powder flowability, it is likely to have differences in the specimens produced as well. On the other hand, the specimen arrangement in the powder chamber can also inflict differences to the produced parts. For example, the studies by Bai et al. (2016) discovered that parts that had a longer cooling time and a slower cooling rate, thus the parts that were manufactured first, had better tensile properties and lower porosity. This could explain the differences between specimens in batches V3-x and V3-y.

6.3.2 Sintering quality and porosity

Fracture surfaces of the tested tensile specimens were investigated with SEM to evaluate the sintering quality and porosity of the parts. SEM images were taken from every batch and each build direction thus V1, V2, V3-x, V3-y and V3-z, to be able to compare the possible differences.

Figure 6.22 presents the SEM images of the batches V2, V3-z and V1, thus the batches produced in the same build direction, with the different energy density levels. There are two different magnifications used for the specimens for each batch to enable the evaluation from wider perspective but still to get a closer look to the structure as well. Sintering quality and part porosity analysations were made based on the visual inspection of the SEM images by evaluating the coalescence of the particles and the amount of voids visible on the fracture surfaces of the parts.

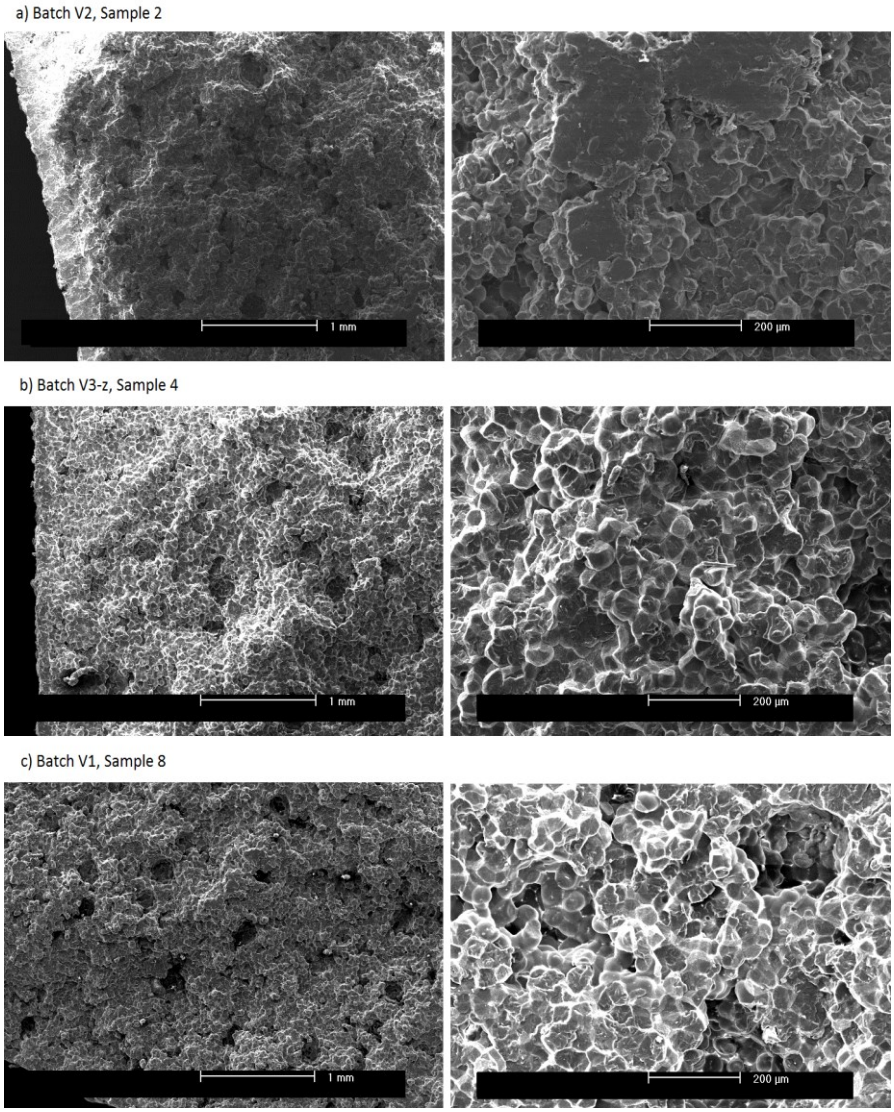

Figure 6.22. *SEM images of the fracture surface of the tensile specimens from batches produced in z-direction with different magnifications a) batch V2, b) batch V3-z and c) batch V1.*

It can be seen from Figure 6.22, that with all the experimented energy density levels the individual powder particles are still visual, even with the highest energy density level thus batch V2. In addition, clear voids can be seen in the structure of all the investigated specimens. The brittle behaviour that the tensile test results indicated, probably result from the very porous structure of the specimens visual in the SEM images.

The flowability of the powder also has influence to the porosity of the parts since sufficient flowability improves the packing density of the powder, and thus enables the lower porosity. It was found during the flowability experiment conducted for PP-2 powder that when the silica additive was used, increasing the temperature subtly improves the flowability of the powder. Observation made during the production of the tensile

specimens with the PP-3 powder indicated that the effect of the powder bed temperature is similar for the powders PP-2 and PP-3.

Comparison of the SEM images of the different batches, presented in Figure 6.22, shows that the particles of the batch V2 seem to have significantly better coalescence compared to batches V3-z and V1. Tensile test results also support this conclusion since batch V2 had the highest tensile strength results. In addition, the flowability of the powder of the batch V2, was reported to be superior compared to the batches V1 and V3-z. There is not so significant difference between the coalescence of batches V3-z and V1, but the differences in their tensile strengths was not so significant either.

Figure 6.23 presents the SEM images of batches V3-x, V3-y and V3-z thus the batches produced in the different build directions.

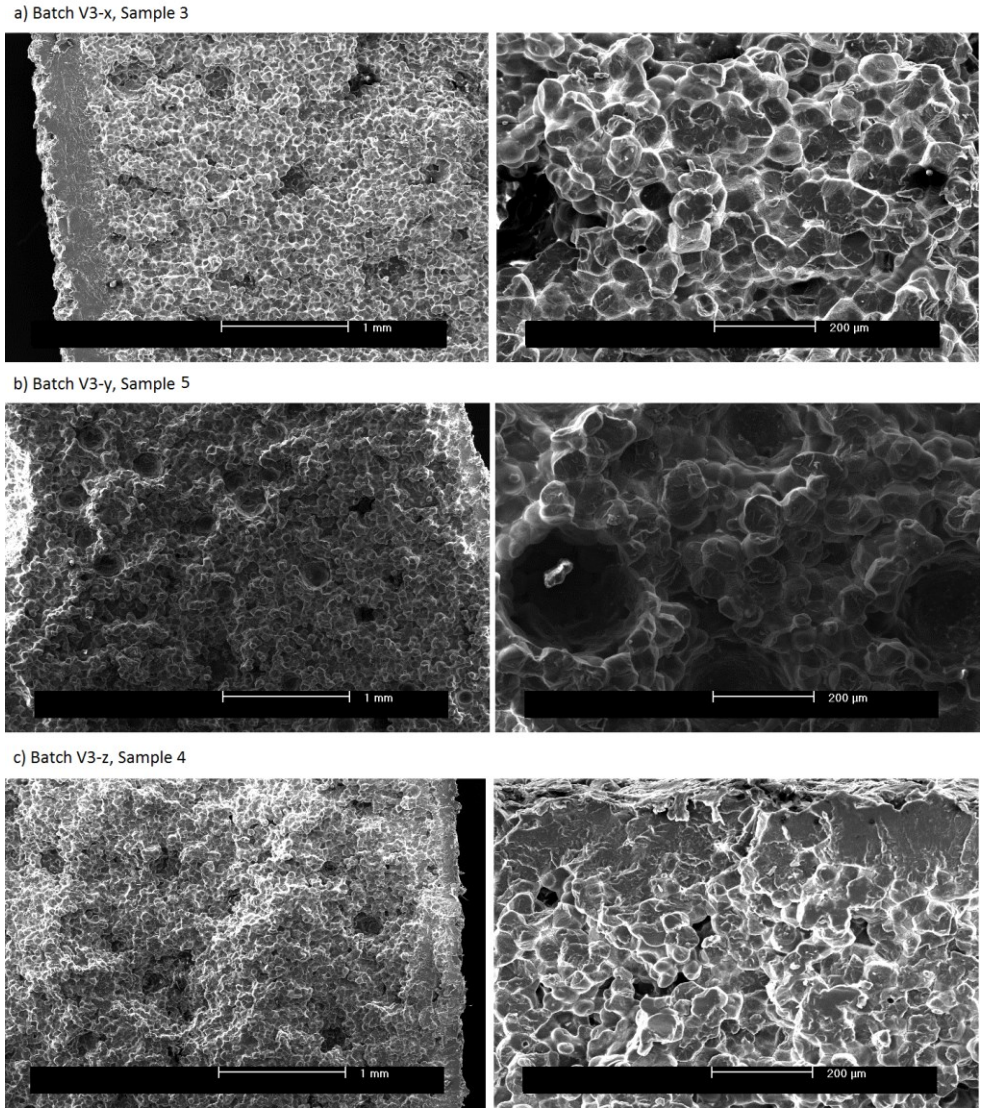

Figure 6.23. *SEM images of the fracture surface of the tensile specimens from batch V3, produced in different build directions, with different magnifications a) batch V3-x, b) batch V3-y and c) batch V3-z.*

Based on the SEM images presented in Figure 6.23, there do not seem to be so much variations in the sintering quality and the porosity of the parts built in different directions as there was when different energy density levels where compared. However, voids as large as over 200 µm are visible in the structure of the specimens in every build direction. It is not possible to explain the differences of the tensile test results between different build directions based on these SEM images, and thus the sintering quality and porosity of the parts are not the main reasons for these differences.

The experimented process parameters and their effect to the flowability of the powder and the tensile strength and sintering quality of the SLS parts are summarised in Table 6.9.

Table 6.9 *The summary of the effects of the process parameters to the flowability, tensile strength and sintering quality.*

	Flowability	**Tensile strength**	**Sintering quality**
Increasing energy density	Positive	Positive	Positive
Adding silica	Positive	Indirect[a] positive	Indirect[a] positive
Build orientation	No effect	x: worst, y: middle, z: best	No known effect
Increasing layer thickness (with and without SiO_2)	Negative	Indirect[a] negative	Indirect[a] negative
Increasing blade speed (without SiO_2)	Inconsistent: First positive then negative	Inconsistent: First indirect[a] positive then indirect[a] negative	Inconsistent: First indirect[a] positive then indirect[a] negative
Increasing blade speed (with SiO_2)	Negative	Indirect[a] negative	Indirect[a] negative
Increasing powder bed temperature (without SiO_2)	Negative	Indirect[a] negative	Indirect[a] negative
Increasing powder bed temperature (with SiO_2)	Positive	Indirect[a] positive	Indirect[a] positive

[a] Effect that results indirectly from the flowability behaviour

These investigations show how complicated process the SLS really is, as the effects of the different parameters are not always consistent, and thus finding the optimal values for processing is difficult. As Table 6.9 presents, changing just one factor in the SLS process, like adding the silica, can change the effect of the other parameters quite significantly. Furthermore, Table 6.9 shows that the flowability of the powder has a very significant role in the SLS process since the changes in the flowability have a strong indirect effect

to the tensile strength and sintering quality as well. It is important to determine the optimal values for all the materials processed with the SLS separately to ensure the optimal part properties. Furthermore, the determined values are usually machine dependent, and thus the values should also be determined separately for the different SLS machines.

Based on the tensile test results and the SEM evaluations, it could be concluded that experimenting even higher energy density levels with this material could be advisable. It is probable that with the higher energy density levels, better coalescence, and thus lower porosity could be achieved which could lead to higher tensile strengths. In addition, it would seem that the higher energy density also improves the flowability of the powder. However, it should be considered that increasing the energy density level too high can cause thermal degradation, and thus decrease the tensile properties.

7. CONCLUSIONS

Additive manufacturing is a rising manufacturing field as the use of AM in the producing of the functional parts is increasing. AM techniques are especially equipped to produce small batches and individual parts. These kind of parts usually require a lot of additional tooling when they are manufactured with some more traditional methods. It is not economical to produce these kind of products with, for example injection moulding, since manufacturing a mould for the injection moulding is quite expensive, and thus economical only with large volumes. Different AM techniques could be an economical solution for the production of these small batches. However, there are still limitations with many AM techniques that need to be overcome before they can be used in a large scale.

SLS has many advantages compared to some other AM methods. The freedom of design is one of the main advantages since almost any kind of 3D object can be built without any support structures. Only limitation is that hollow closed parts cannot be made since the surrounding powder, supporting the part during sintering, would stay inside the part. However, major limitation with SLS is the limited raw material availability. Even though polyamides work well in the SLS and accurate parts can be produced, polyamides do not have the required material properties to achieve suitable properties for many functional parts. Commodity plastics, such as PP and PE, are therefore interesting materials to be investigated as possible materials for SLS.

One major limiting factor, in the investigation of the selective laser sintering of polyolefins, is the limited availability of polyolefins in a suitable powder form. During experiments, it was found that grinding with a cutting mill is not very effective way to produce powder and that the powder produced with grinding has insufficient morphology and also still too large particle size. There are commercial suppliers for polypropylene SLS powders, such as Diamond Plastics Gmbh that provides PP powder with different additives and Advanc3d Materials Gmbh that provides PP powder manufactured by Axalta. Commercial manufacturers have some kind of special grinding method that they use for the grinding of these PP powders, giving the powder particles suitable morphology and particle size.

The availability of suitable powder is critical since the SLS process requires that the powder spreads very evenly on the powder bed for each layer. If the powder has insufficient particle morphology or particle size, the spreading of the powder is difficult or impossible. Larger particle size can be compensated by increasing the layer thickness but only to some level since increasing the layer thickness too much causes its own problems. Increasing the layer thickness decreases the accuracy and requires an increase to the energy density. However, if the spreading is insufficient, the actual sintering cannot

be performed at all. Thus, determining the required part properties and balancing the processing parameters accordingly is essential.

Another limiting factor in these investigations have been finding a suitable SLS machine to experiment with the polyolefin materials. SLS machines are quite complex and expensive to buy or build. In addition, commercial SLS machines for polymers are mainly focused for the PA powders and have usually fixed parameters to fit the requirements of the PA powders. Machines with the open parameters are usually even more expensive.

Since polyamides are found to work in the SLS, some estimation about the suitability of polypropylene powders can be made by comparing them to the polyamides. SEM images showed that the PA powder particles are more spherical and smooth on the surface compared to the commercial PP powders. The extrinsic properties of the PA powders give them the required flowability to be used in SLS. In addition, the particle size distribution range is smaller with PA powders than with the investigated PP powders. On the other hand, PP powders have smaller average particle size due to the greater amount of small particles. These small particles could have positive effect to the packing density, and thus decreased porosity, but the negative effect that the small particle could cause to the process cannot be neglected. Furthermore, wide particle size distribution range could cause the insufficient melting of the large particles, and thus increase the porosity.

Based on the powder characterisation, the thermal properties of all the investigated polypropylenes were sufficient for the SLS, even for the injection moulding grade PP-1. However, at least the investigated polyethylene PE-1 had too narrow sintering window to be used in SLS, and thus was discarded from further studies. Rheological inspection showed that PP-1 has significantly higher zero shear viscosity compared to commercial SLS powder grades. This could lead to the porosity of the parts due to the insufficient coalescence. Extrinsic property evaluation shows that grinded PP-1 had insufficient morphology and the poor flowability behaviour, caused by the inferior particle morphology and size, was also experimented in an actual SLS machine. Due to the poor flowability of PP-1 the actual sintering could not be experimented with this powder.

For future work, it could be useful to investigate the powder processing methods further, to be able extend the amount of different materials that can be experimented in the SLS. Since there are commercial manufacturers for PP powder, the manufacturing of the powder with the suitable extrinsic properties is possible. As was mentioned earlier, experimenting the usability of some other kind of mill, than what was used in current study, could be advisable. Furthermore, if a method with a sufficient efficiency can be found, some post processing methods could be experimented as well.

The flowability of the PP-2 powder was also tested in a SLS machine. The flowability was significantly better compared to the grinded PP-1 but not as good as with a PA12 powder. To improve the flowability some hydrophobic silica was added as an additive to

the PP-2 powder to improve the flowing behaviour. It was quite clear that the silica additive improved the flowability of this powder significantly and it decreased the effect of different process parameters to the flowability behaviour. However, even with the silica additive, it was not possible to spread the PP-2 powder evenly enough to be able to use it for the laser sintering, at least not at Materflow. However, the commercial powder PP-3 showed sufficient flowability and was used for the production of tensile specimens with the SLS.

Comparing the properties of the powders gives only an estimation of the properties of the final parts. The real part properties can only be analysed by producing and investigating the actual parts. Especially properties, such as shrinkage as well as sintering quality thus porosity, are very difficult to determine based on just powder properties. Tensile specimens produced with the commercial powder PP-3 were investigated for their tensile properties as well as sintering quality and porosity. The tensile specimens were produced with three different energy density levels to determine the optimal energy density value for the PP-3 powder. In addition, different part build directions were experimented to evaluate the effect of the build orientation to the properties of the SLS parts. The level of the shrinkage of the tensile specimens was not reported by the manufacturer so it could not be evaluated. However, there was no significant distortions visible in the tensile specimens, and thus at least for these parts, the shrinkage did not seem to cause any major problems. The relatively wide sintering window of the PP-3 powder could be one factor compensating the shrinking behaviour, by preventing the too early crystallisation.

Tensile tests showed that the specimens produced with the SLS are very brittle since they break at quite low strains without yielding. However, increasing the energy density level in the SLS increased the tensile strength of the SLS specimens. Furthermore, the SEM evaluations regarding the sintering quality and porosity of the specimens support this result. Thus, higher energy density levels seem to lead to higher sintering quality and lower porosity. However, even with the highest experimented energy density level the tensile strengths were quite low and the porosity of the specimens quite high. The coalescence of the melt powder particles can also effect the porosity. However, the experimented PP-3 powder did have the lowest zero shear viscosity value compared to the other investigated powders. This means that achieving appropriate coalescence should be easiest for the PP-3 powder, and thus the processing of the other powders could be even more difficult. Based on these results it could be advisable to investigate the effect of even higher energy density levels in SLS. So long as the increase does not cause any thermal degradation to the material, it has been found that increasing energy density increases the tensile strength and decreases the porosity.

REFERENCES

3D Systems. (2017). Plastic materials: Polypropylene-like Materials, website. Available (accessed on 6.4.2017): https://www.3dsystems.com/materials/plastic#polypropylene-like-materials

Advanc3D Materials. (2017). Powders for SLS applications, website. Available (accessed on 7.4.2017): http://www.advanc3dmaterials.com/sls-powders.html

Al-Ali AlMa'adeed, M. & Krupa, I. (2016). Polyolefin Compounds and Materials: Fundamentals and Industrial Applications, Springer International Publishing, Switzerland, 354 p.

Bai, J., Zhang, B., Song, J., Bi, G., Wang, P. & Wei, J. (2016). The effect of processing conditions on the mechanical properties of polyethylene produced by selective laser sintering, Polymer Testing, Vol. 52 pp. 89-93. Available: http://www.sciencedirect.com/science/article/pii/S0142941816301854.

Baumann F. E. & Wilczok N. (1999). Preparation of precipitated polyamide powders of narrow particle size distribution and low porosity, US5932687A.

Bourell, D.L., Watt, T.J., Leigh, D.K. & Fulcher, B. (2014). Performance Limitations in Polymer Laser Sintering, Physics Procedia, Vol. 56 pp. 147-156. Available: http://www.sciencedirect.com/science/article/pii/S1875389214003022.

Caulfield, B., McHugh, P.E. & Lohfeld, S. (2007). Dependence of mechanical properties of polyamide components on build parameters in the SLS process, Journal of Materials Processing Tech, Vol. 182(1), pp. 477-488. Available: http://www.sciencedirect.com/science/article/pii/S0924013606007886.

Diamond Plastics (2017). Products, website. Available (accessed on 6.4.2017): http://www.diamond-plastics.de/en/products.html.

EOS e-Manufacturing Solutions (2017). EOS Plastic Materials for Additive Manufacturing, website. Available (accessed on 30.6.2017): https://www.eos.info/material-p

Fanselow, S., Emamjomeh, S.E., Wirth, K., Schmidt, J. & Peukert, W. (2016). Production of spherical wax and polyolefin microparticles by melt emulsification for additive manufacturing, Chemical Engineering Science, Vol. 141 pp. 282-292. Available: http://www.sciencedirect.com/science/article/pii/S0009250915007368.

Fiedler, L., Garcia Correa, L.O., Radusch, H., Wutzler, A. & Gerken, J. (2007). Evaluation of Polypropylene Powder Grades in Consideration of the Laser Sintering Processability, Journal of Plastic Technology, Vol. 3(4), pp. 1-14. Available: https://www.researchgate.net/publication/289628738.

Finnish Standards Association. (2016). Plastics. Differential scanning calorimetry (DSC). Part 1: General principles, SFS- ISO 11357-1, Helsinki, 37 p.

Finnish Standards Association. (2014). Plastics - Thermogravimetry (TG) of polymers - Part 1: General principles, SFS-ISO 11358-1, Helsinki, 9 p.

Finnish Standards Association. (2012). Plastics. Determination of tensile properties. Part 1: General principles, SFS-ISO 527-1, Helsinki, 23 p.

Finnish Standards Association. (2008). Plastics. Test specimens. SFS-EN ISO 20753, Helsinki, 15 p.

Forecast 3D. (2017). SLS Materials, website. Available (accessed on 6.4.2017): http://www.forecast3d.com/sls_materials.html

Gibson, I., Rosen, D. & Stucker, B. (2015). Additive manufacturing technologies: 3D Printing, Rapid Prototyping, and Direct Digital Manufacturing, 2nd ed. Springer-Verlag, New York, 498 p.

Gibson, I. & Shi, D. (1997). Material properties and fabrication parameters in selective laser sintering process, Rapid Prototyping Journal, Vol. 3(4), pp. 129-136. Available: http://search.proquest.com/docview/214030510.

Goodridge, R.D., Tuck, C.J. & Hague, R.J.M. (2012). Laser sintering of polyamides and other polymers, Progress in Materials Science, Vol. 57(2), pp. 229-267. Available: http://www.sciencedirect.com/science/article/pii/S0079642511000648.

Hindle, C. (2017) Polypropylene (PP), British Plastics Federation, website. Available (accessed on 5.4.2017): http://www.bpf.co.uk/plastipedia/polymers/PP.aspx.

Hopkinson, N., Hague, R.J.M. & Dickens, P.M. (2006). Rapid manufacturing: an industrial revolution for the digital age, John Wiley & Sons, Ltd, Chichester, England, 285 p.

Jain, P.K., Pandey, P.M. & Rao, P.V.M. (2009). Effect of delay time on part strength in selective laser sintering, The International Journal of Advanced Manufacturing Technology, Vol. 43(1-2), pp. 117-126. Available: http://link.springer.com/article/10.1007/s00170-008-1682-3.

Khait, K., Carr, S.H. & Mack, M.H. (2001). Solid state shear pulverization, Technomic Publishing Company Inc., Lancaster, Pensylvania, 185 p.

Körsgen, H. & Weller, W. (1985). Process for the production of polypropylene powders, US4510305A.

Lexow, M. & Drummer, D. (2016). New Materials for SLS: The Use of Antistatic and Flow Agents, Research article, Journal of Powder Technology, 9 p. Available: https://www.hindawi.com/archive/2016/4101089/cta/

Liang, S.B., Hu, D.P., Zhu, C. & Yu, A.B. (2002). Production of Fine Polymer Powder under Cryogenic Conditions, Chemical Engineering & Technology, Vol. 25(4), pp. 401-405. Available: https://www.researchgate.net/publication/243803660.

Mujumdar, A.S. (2014). Handbook of industrial drying, CRC Press, 1348 p.

Mys, N., Verberckmoes, A. & Cardon, L. (2016). Processing of Syndiotactic Polystyrene to Microspheres for Part Manufacturing through Selective Laser Sintering, Polymers, Vol. 8(11), pp. 383. Available: http://search.proquest.com/docview/1849302257.

Nandiyanto, A.B.D. & Okuyama, K. (2011). Progress in developing spray-drying methods for the production of controlled morphology particles: From the nanometer to submicrometer size ranges, Advanced Powder Technology, Vol. 22(1), pp. 1-19. Available: http://www.sciencedirect.com/science/article/pii/S0921883110001883.

Osswald, T. & Rudolph, N. (2015). Polymer Rheology, Hanser, München, 225 p.

Schmid, M., Amado, A. & Wegener, K. (2014). Polymer Powders for Selective Laser Sintering (SLS). Zürich: ETH-Zürich. Available (accessed on 31.1.2017): http://dx.doi.org/10.3929/ethz-a-010336188.

Schmid, M. & Wegener, K. (2016). Additive Manufacturing: Polymers Applicable for Laser Sintering (LS), Procedia Engineering, Vol. 149 pp. 457-464. Available: http://www.sciencedirect.com/science/article/pii/S1877705816312073.

Schmidt, J., Sachs, M., Blümel, C., Winzer, B., Toni, F., Wirth, K. & Peukert, W. (2015). A Novel Process Chain for the Production of Spherical SLS Polymer Powders with Good Flowability, Procedia Engineering, Vol. 102 pp. 550-556. Available: http://www.sciencedirect.com/science/article/pii/S1877705815001241.

Soares, J.B.P. & McKenna. (2012). Polyolefin reaction engineering: Introduction to polyolefins, Wiley-VCH, pp.1-13.

Swapp, S. (2017). Scanning Electron microscope, Geochemical Instrumentation and Analysis, website. Available (accessed on 12.7.2017): https://serc.carleton.edu/research_education/geochemsheets/techniques/SEM.html.

Verbelen, L., Dadbakhsh, S., Van den Eynde, M., Kruth, J., Goderis, B. & Van Puyvelde, P. (2016). Characterization of polyamide powders for determination of laser sintering processability, European Polymer Journal, Vol. 75 pp. 163-174. Available: http://www.sciencedirect.com/science/article/pii/S0014305715300938.

Wegner, A. (2016). New polymer materials for the laser sintering process: polypropylene and others, Physics Procedia, Vol. 83, pp.1003-1012. Available: http://www.sciencedirect.com/science/article/pii/S1875389216302127

Wegner, A. & Ünlü, T. (2016). Powder Life Cycle Analyses for a New Polypropylene Laser Sintering Material, pp. 834-846. Available: https://sffsymposium.engr.utexas.edu/sites/default/files/2016/067-Wegner.pdf

Wilczek, M., Bertling, J. & Hintemann, D. (2004). Optimised technologies for cryogenic grinding, International Journal of Mineral Processing, Vol. 74 pp. S434. Available: http://www.sciencedirect.com/science/article/pii/S0301751604000432.

Wohlers, T. & Gornet, T. (2014). Wohlers report: History of additive manufacturing, Wohlers Associates, Inc., 34 p.

Wypych, G. (2012). Handbook of polymers, ChemTec Publishing, Toronto, 696 p.

Zhu, W., Yan, C., Shi, Y., Wen, S., Han, C., Cai, C., Liu, J. & Shi, Y. (2016). Study on the selective laser sintering of a low-isotacticity polypropylene powder, Rapid Prototyping Journal, Vol. 22(4), pp. 621-629. Available: http://search.proquest.com/docview/1826442548.

APPENDIX A: RHEOLOGICAL MEASUREMENTS

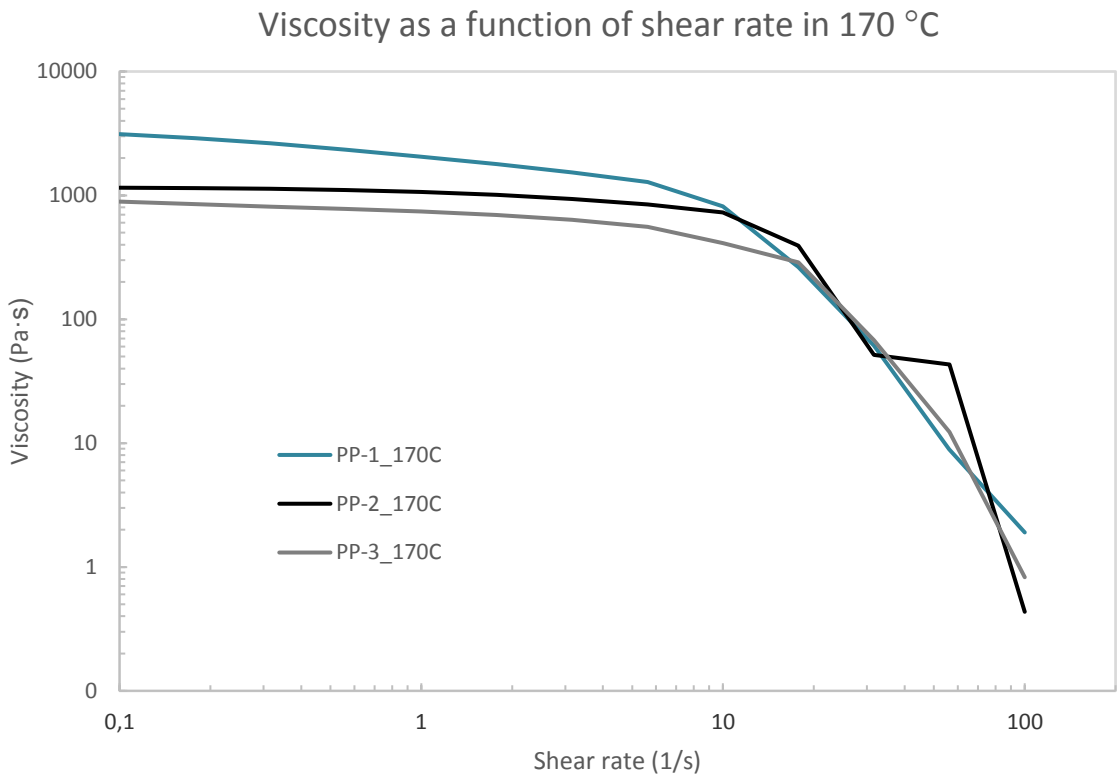

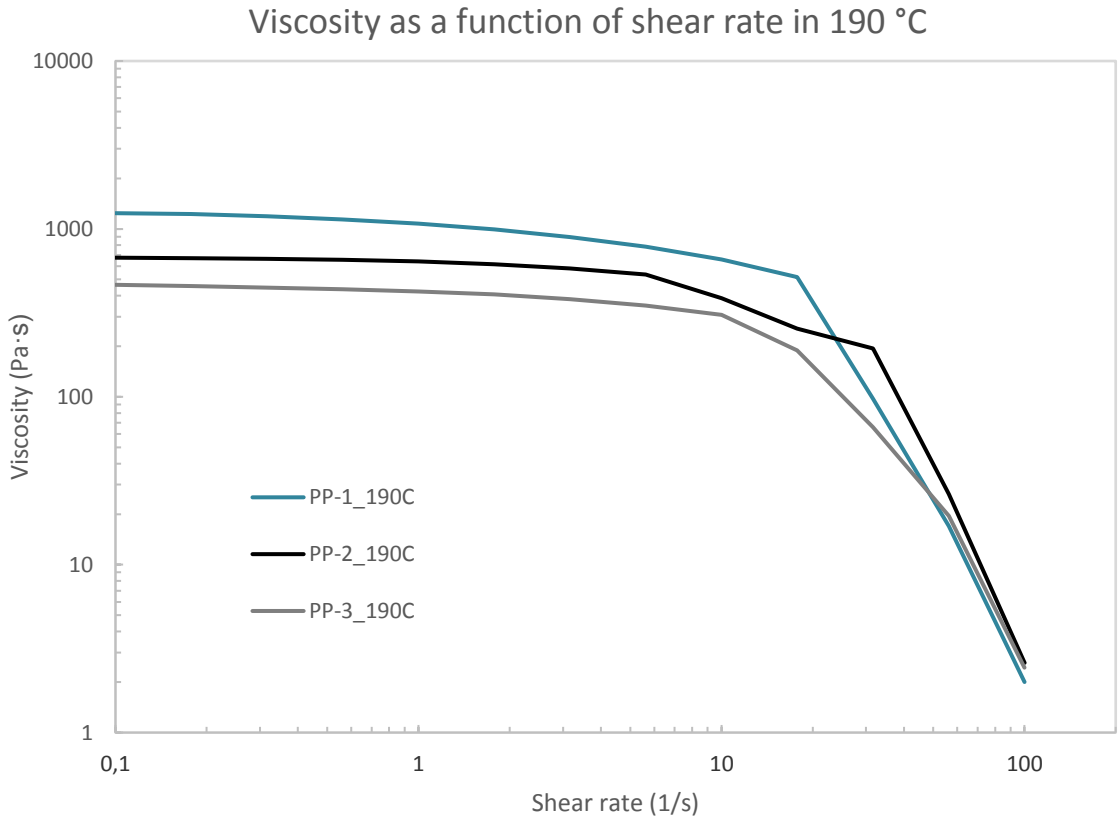

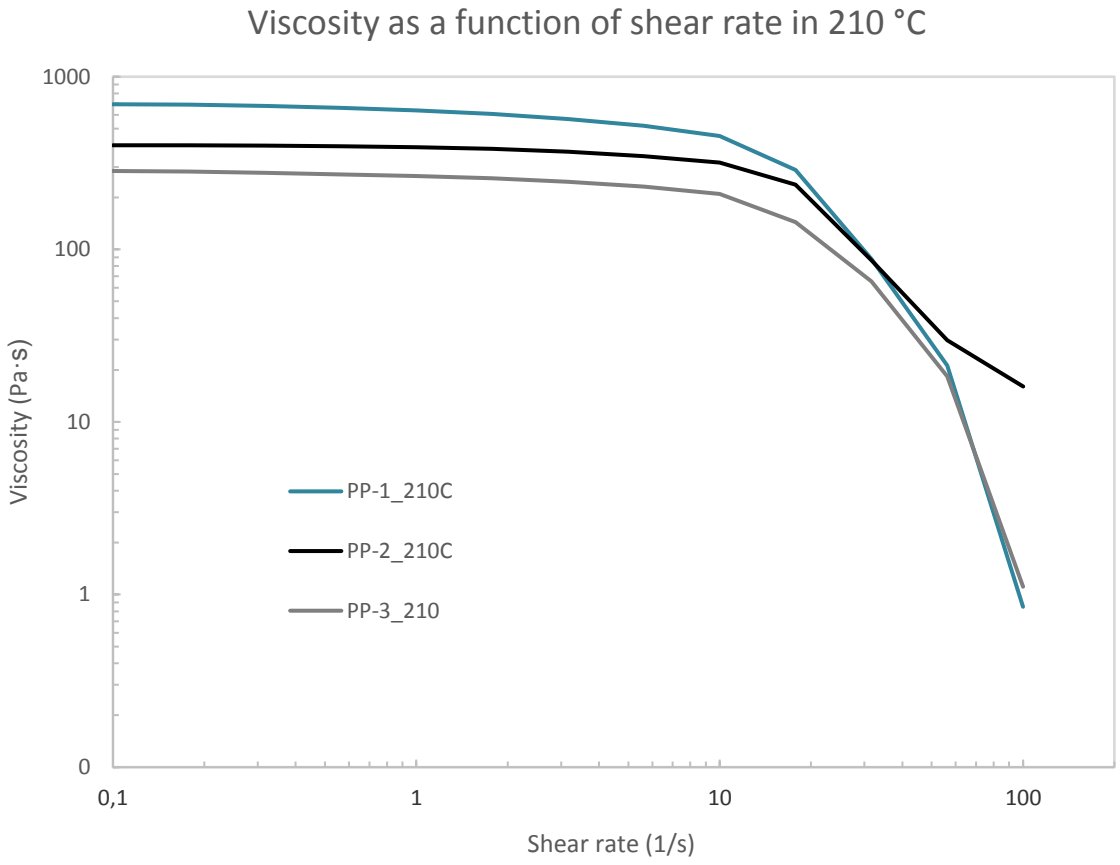
Viscosity as a function of shear rate in 210 °C
1000
100
10
1
0
Viscosity (Pa·s)
0,1
1
10
100
Shear rate (1/s)
PP-1_210C
PP-2_210C
PP-3_210

APPENDIX B: EDS FOR PP-3

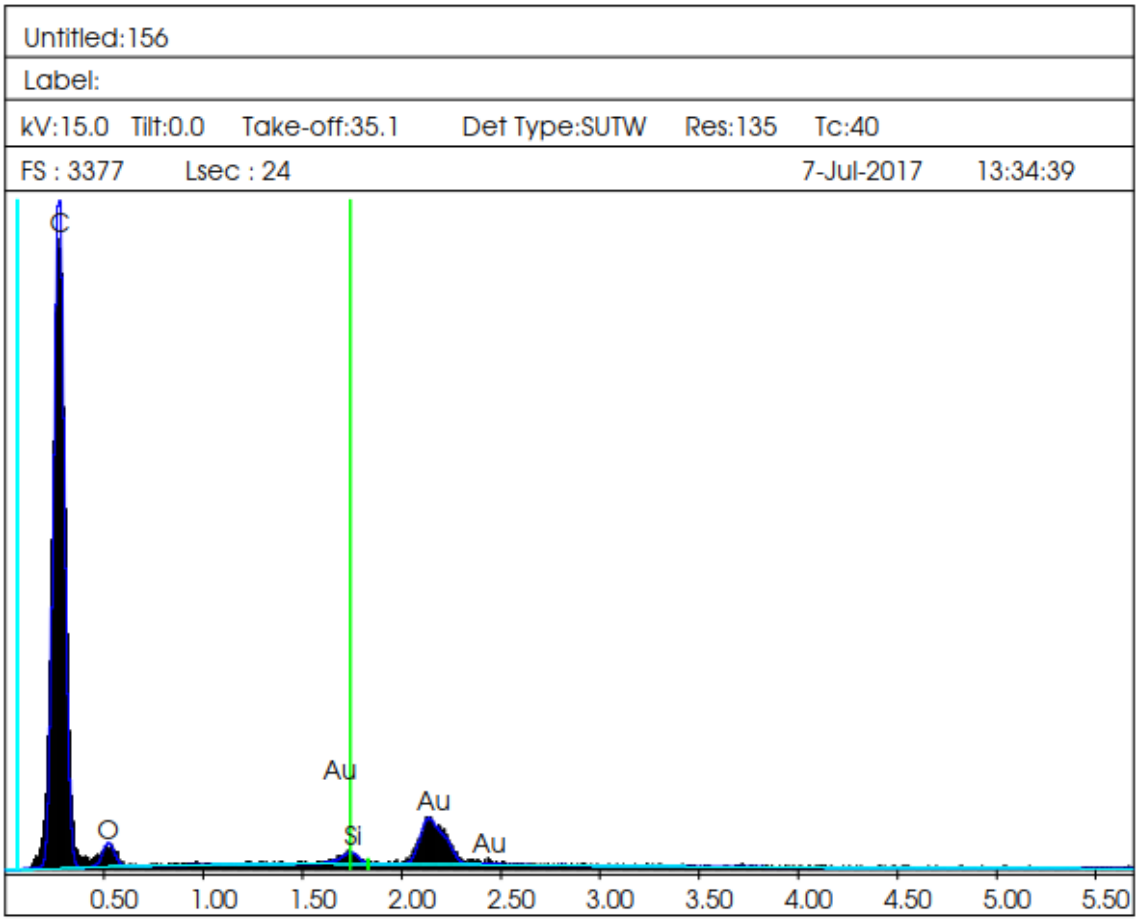

EDAX ZAF Quantification (Standardless)
Element Normalized
SEC Table : Default

Element	Wt %	At %	K-Ratio	Z	A	F
C K	83.92	94.05	0.5751	1.0228	0.6699	1.0000
O K	5.99	5.04	0.0117	1.0036	0.1947	1.0000
SiK	0.55	0.26	0.0048	0.9514	0.9294	1.0000
AuM	9.55	0.65	0.0770	0.6487	1.2429	1.0000
Total	100.00	100.00				

Element	Net Inte.	Bkgd Inte.	Inte. Error	P/B
C K	753.93	1.84	0.74	408.80
O K	29.51	5.41	4.05	5.45
SiK	16.67	11.07	6.40	1.51
AuM	79.63	11.19	2.42	7.12

APPENDIX C: PARTICLE SIZE DISTRIBUTION GRAPHS FOR PA POWDERS

PA-1 (fresh powder)

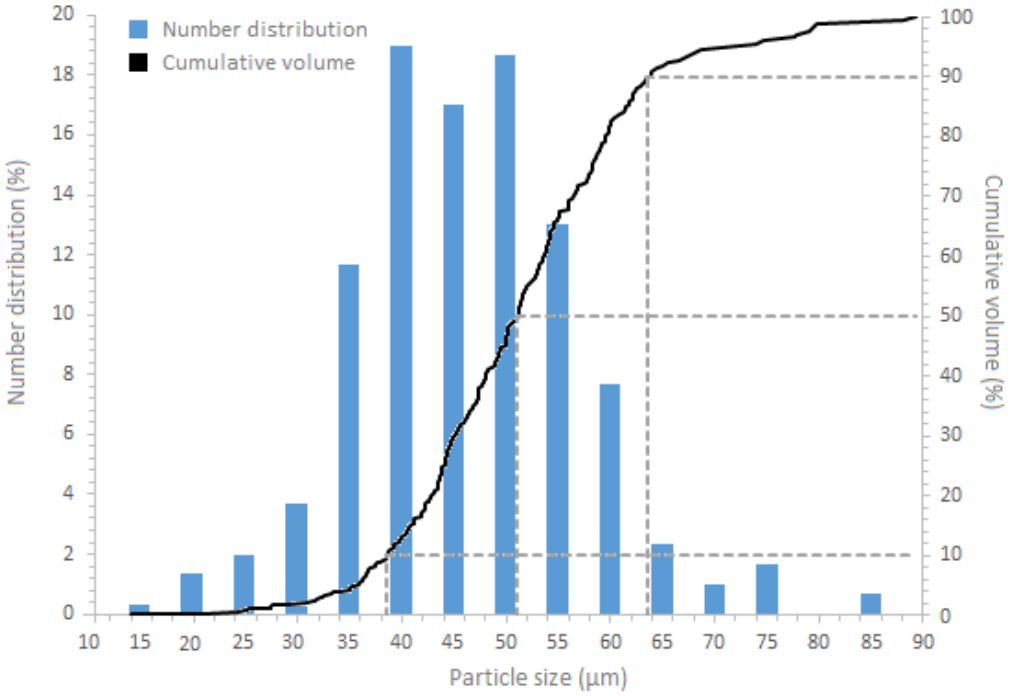

PA-2 (mixed powder with 50% refresh rate)

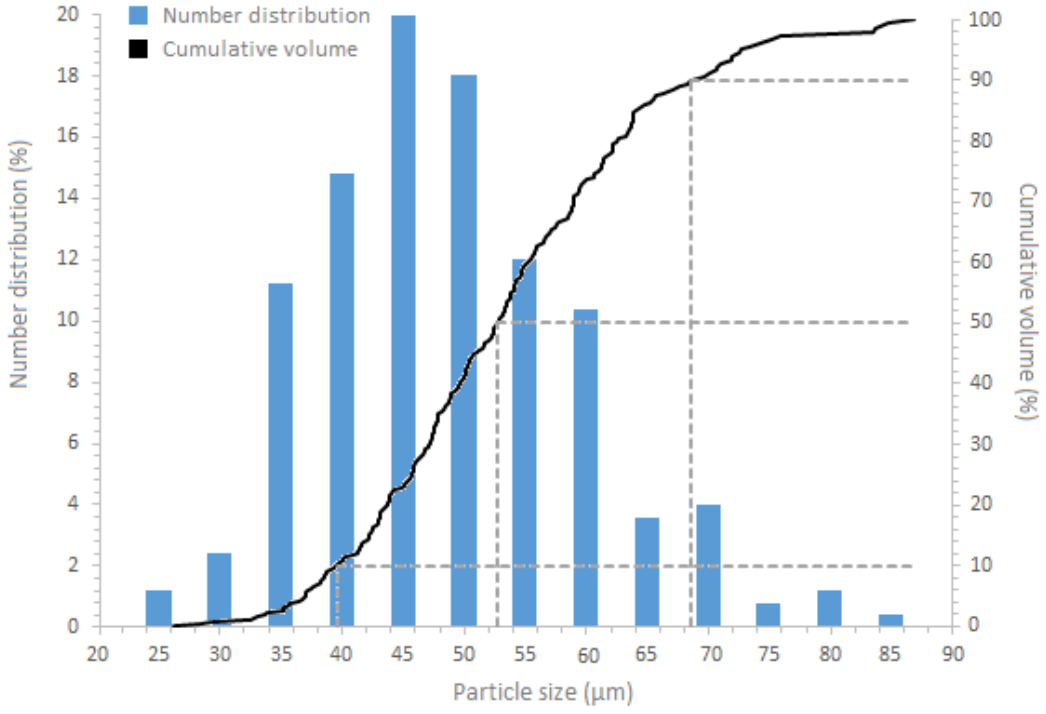

PA-3 (Recycled powder)

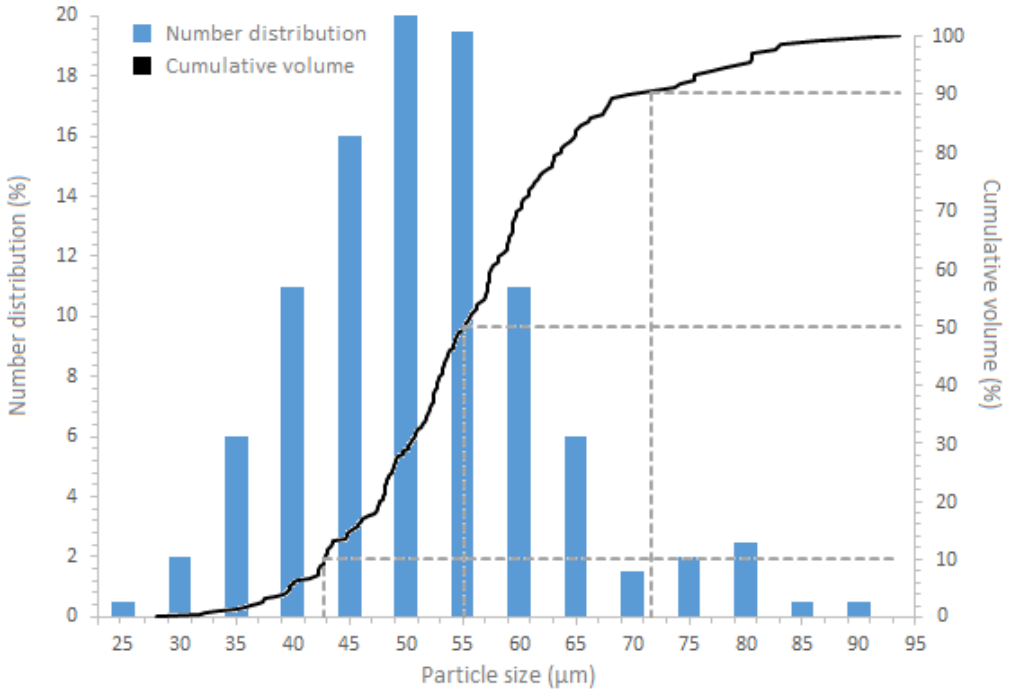

PA-4 (Bad quality powder)

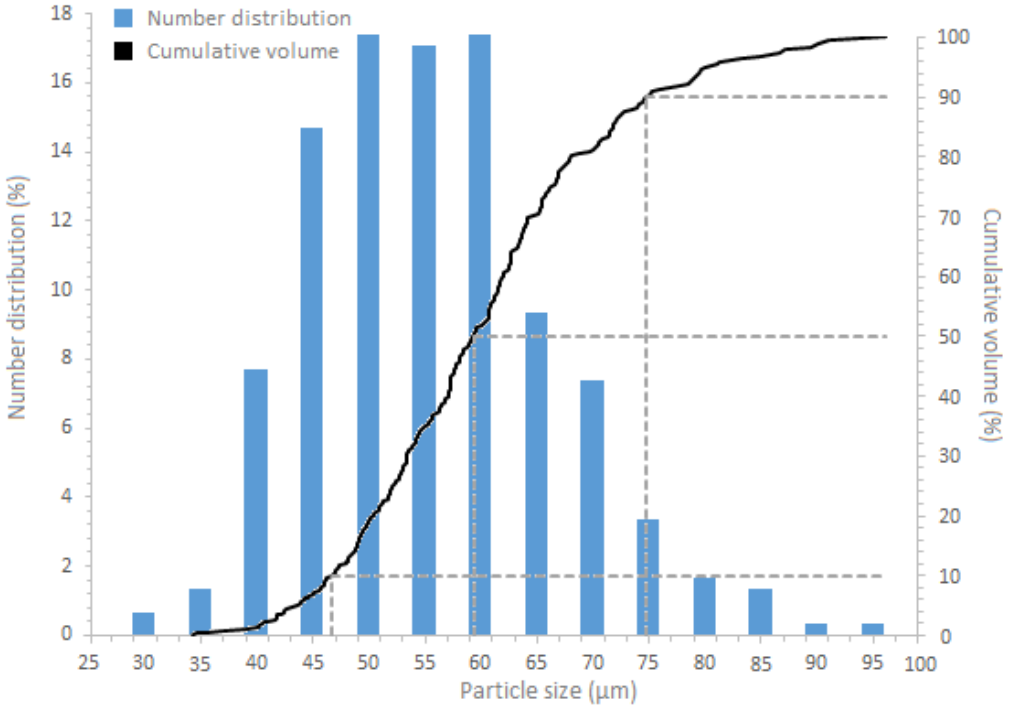

APPENDIX D: TENSILE TEST RESULTS

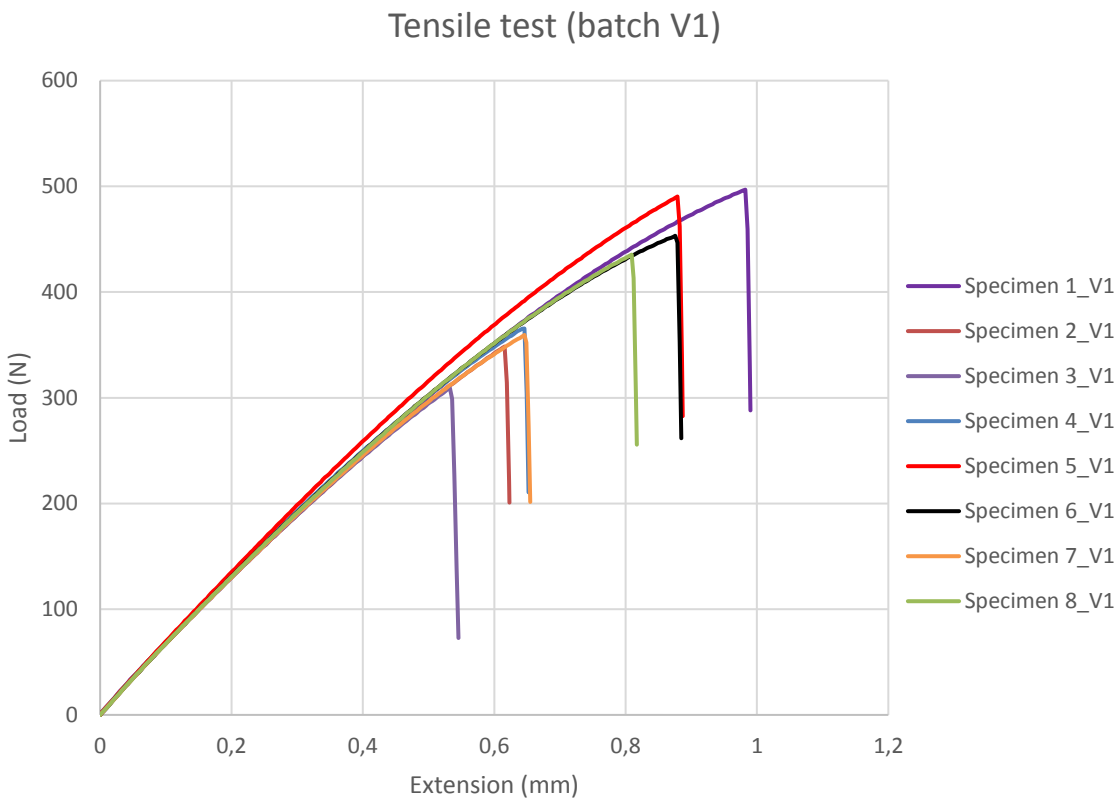

Values determined based on the tensile tests for batch V1.

Specimens	Modulus	Tensile stress at Break	Extension at Break
	(MPa)	(MPa)	(mm)
1	809.84055	12.319	0.98237
2	832.22489	8.63692	0.6157
3	823.06355	7.52425	0.53254
4	818.2128	8.7155	0.64592
5	828.22039	11.90444	0.87901
6	804.84698	11.01405	0.87578
7	800.50991	8.57745	0.6458
8	818.07166	10.7377	0.80912
Average	**816.873841**	**9.928664**	**0.74828**

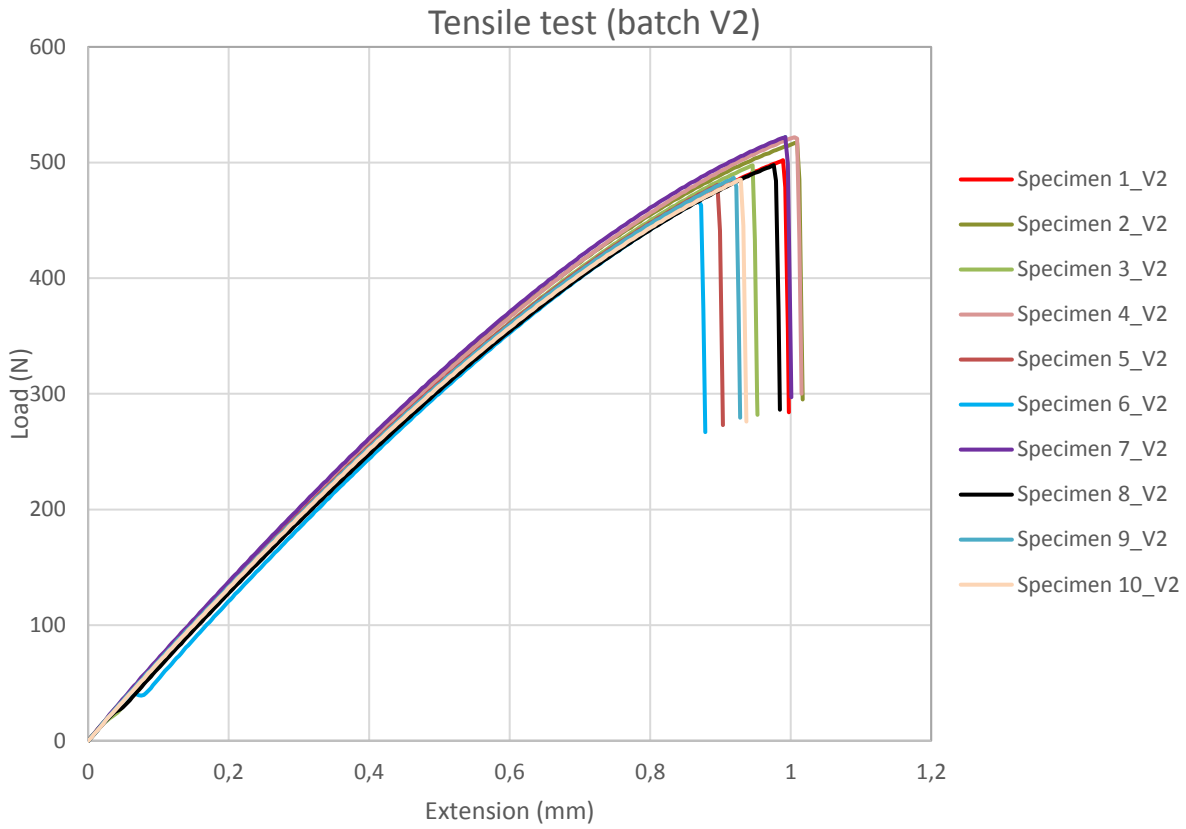

Values determined based on the tensile tests for batch V2.

Specimens	Modulus	Tensile stress at Break	Extension at Break
	(MPa)	(MPa)	(mm)
1	776.8023	11.74954	0.98911
2	787.07	11.92117	1.00908
3	771.8146	11.52207	0.94582
4	792.6294	12.20141	1.00577
5	780.8929	11.11814	0.89589
6	754.9622	10.92161	0.86904
7	794.3706	11.94878	0.99253
8	732.812	11.44997	0.97597
9	766.9946	11.11066	0.9191
10	773.9613	11.2883	0.92923
Average	**773.231**	**11.52317**	**0.953154**

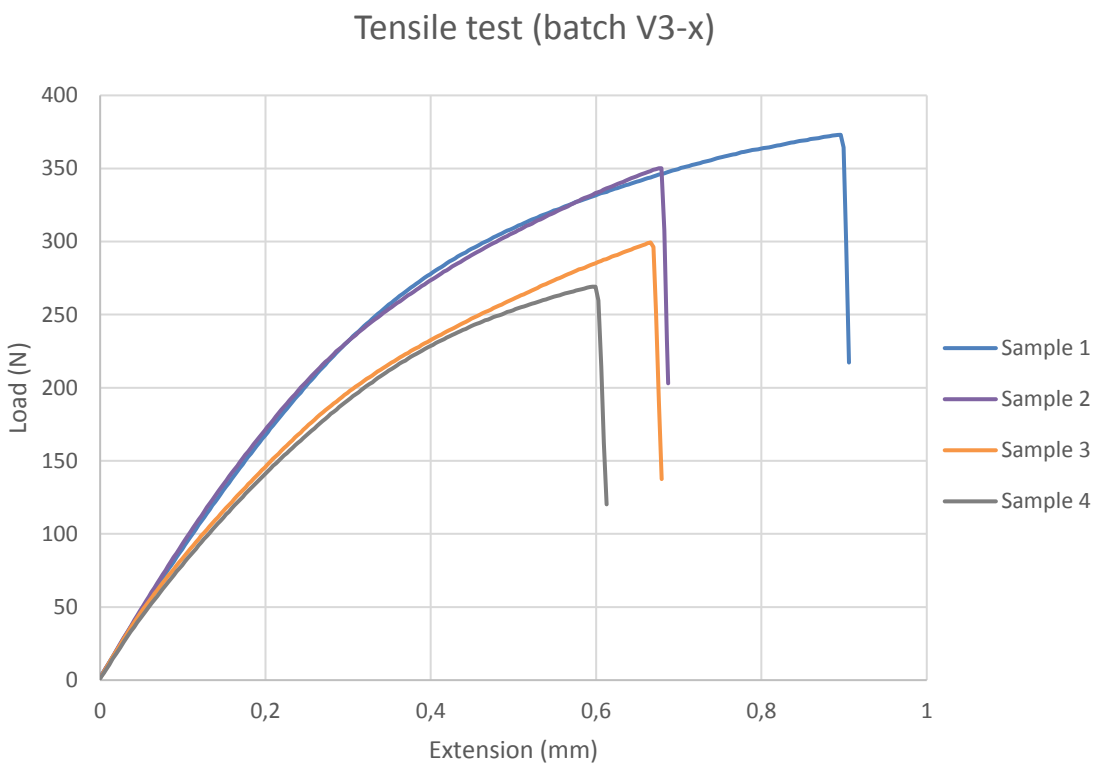

Values for modulus, tensile stress at break and extension at break determined based on the tensile tests for batch V3 specimens built in x-direction.

Sample	Modulus	Tensile stress at Break	Extension at Break
	(MPa)	(MPa)	(mm)
1	820.0334	6.83598	0.89588
2	852.3509	6.3703	0.67577
3	750.9711	5.106220495	0.66592
4	715.0638	4.64583406	0.59932
Average	**784.6048**	**5.739583639**	**0.709223**

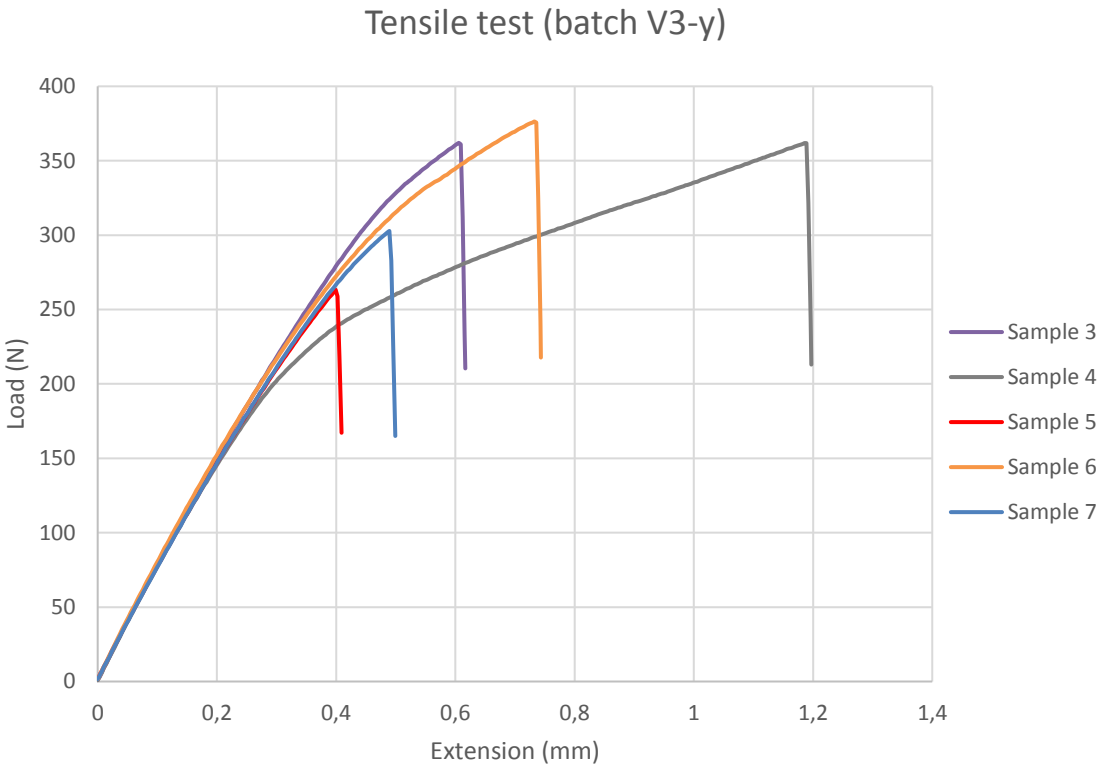

Values for modulus, tensile stress at break and extension at break determined based on the tensile tests for batch V3 specimens built in y-direction.

Sample	Modulus	Tensile stress at Break	Extension at Break
	(MPa)	(MPa)	(mm)
1	-	-	-
2	-	-	-
3	837.2121	7.72722	0.60573
4	799.1687	7.51484	1.18912
5	815.9095	5.54001195	0.3991
6	827.7007	7.88671	0.73258
7	821.4649	6.51837	0.48924
Average	**826.8241**	**7.03743039**	**0.683154**

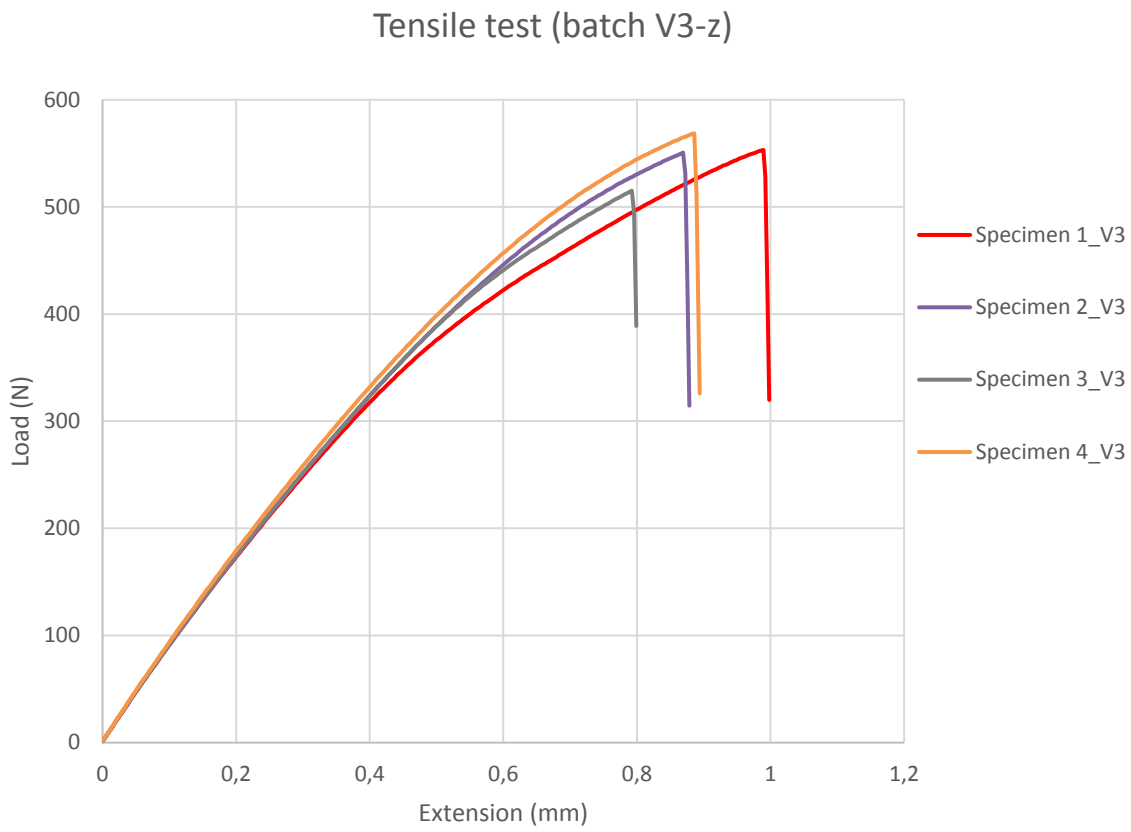

Values for modulus, tensile stress at break and extension at break determined based on the tensile tests for batch V3 specimens built in z-direction.

Specimens	Modulus	Tensile stress at Break	Extension at Break
	(MPa)	(MPa)	(mm)
1	850.38584	10.58131	0.98914
2	834.48950	10.35893	0.86913
3	859.00793	9.80034	0.79233
4	860.21845	10.72066	0.88602
Average	**851.0254**	**10.36531**	**0.884155**